Optimising CAR T cell manufacturing for solid cancers

by

NGA THI HONG TRUONG

Bachelor of Medical Science

A thesis submitted for the degree of

Masters by Research

Centre for Cancer Biology

School of Pharmacy and Medical Sciences

Division of Health Sciences



University of South Australia

7th November 2019

“That which does not kill us makes us stronger”

-Friedrich Nietzsche

Contents

Contents ..... **i**

List of figures ..... **v**

List of tables ..... **vii**

List of abbreviations ..... **viii**

Summary ..... **x**

Declaration ..... **xii**

Acknowledgments ..... **xiii**

Publication and presentation ..... **xiv**

Chapter 1: Introduction **1**

1.1 Overview 1

1.2 Solid cancers in need of new therapies 2

1.2.1 Glioblastoma 2

1.2.2 Pancreatic adenocarcinoma 3

1.2.3 Colorectal cancer 3

1.3 Chemotherapy and lymphocyte population 4

1.3.1 T cell subsets affected by chemotherapy 4

1.3.2 Depletion of circulating regulatory T cells 9

1.3.3 Decrease in circulating B lymphocytes 10

1.4 CAR T cell therapy in cancer 10

1.4.1 CAR T cell therapy is a passive immunotherapy 10

1.4.2 CAR T- cell design 12

1.4.3 Challenges in effective CAR T cell therapy for solid cancers 17

1.4.4 Enhancement of CAR T cell persistence and expansion 19

1.5 Early manufacturing of CAR T cells following chemotherapy could be beneficial 21

1.6 Hypothesis and aims 24
1.6.1 Hypothesis 24
1.6.2 Aims 24

Chapter 2: Materials and Methods 25

2.1 Overview 25
2.2 Materials 26
2.3 Methods 30
2.3.1 Study design and patient recruitment 30
2.3.1.1 Study design and overview 30
2.3.1.2 Patient recruitment and ethics 31
2.3.2 Sample collection and PBMCs isolation 33
2.3.2.1 Collecting blood from donors 33
2.3.2.2 Isolation of PBMCs 33
2.3.3 Manufacturing of CAR T cells 34
2.3.3.1 Preparation of Buffer and Media required for CAR T cell manufacturing 34
2.3.3.2 Activation of bulk PBMCs 35
2.3.3.3 Virus transduction 36
2.3.3.4 Expansion and cryo-preservation of CAR T cell products 36
2.3.4 CAR T cell activation 37
2.3.4.1 Coating sterile 96 well cell culture plates with antibodies 37
2.3.4.2 Activation of CAR T cells 37
2.3.5 Flow Cytometry 37
2.3.5.1 Preparation of buffers and solutions for cell staining 37
2.3.5.2 Preparation of full stained samples and controls 38
2.3.5.3 Flow cytometry data analysis 41
2.3.6 Real-time CAR T cell cytotoxicity analysis 41
2.3.6.1 Preparation of required media and cells for cytotoxicity assays 41
2.3.6.2 Setting up xCELLigence assays 42
2.3.6.3 Real time xCELLigence cytotoxicity assay 43

2.3.6.4 Calculation of percent cytotoxicity values 45
2.3.7 Statistical analysis 45
Chapter 3: Effects of chemotherapy on the cellular compartment of the immune system 47
3.1 Overview 47
3.2 Introduction 47
3.3 Results 50
3.3.1 Patient characteristic 50
3.3.2 Changes in the percentage and absolute number of leukocyte subsets post chemotherapy 53
3.3.3 Change in subsets of T cells post chemotherapy 59
3.4 Conclusion 68
Chapter 4: CAR T cell manufacturing 69
4.1 Overview 69
4.2 Introduction 69
4.3 Results 72
4.3.1 T cells from PBMCs collected at different timepoints of cancer treatment proliferated strongly during the manufacturing procedure 73
4.3.2 Efficiency of viral transduction and CAR expression 76
4.3.3 Immunophenotypes of CAR T cells 79
4.3.4 Changes in subset frequency between initial PBMC populations and final CAR T cell products 87
4.4 Conclusion 93
Chapter 5: Functions of CAR T cells manufactured from PBMCs collected at different time points 94
5.1 Overview 94
5.2 Introduction 95
5.3 Results 98
5.3.1 CAR T cells derived at different phases of cancer chemotherapy were competent at killing target cancer cells 98

5.3.2 CAR T cells manufactured from on-treatment blood samples are less sensitive to AICD 101
5.3.3 Change of exhausted markers on T cell and CAR T cells in the final transgenic products 104
5.3.4 Cytokine profile of CAR T cell products after activation 107
5.4 Conclusion 109
Chapter 6: Discussion and conclusion 112
5.1 Discussion 112
5.2 Conclusion 124
References 125

List of Figures

Figure 1.1: Chimeric antigen receptor structure....14
Figure 2.1: The layout of an E-plate used in xCELLigence assay....44
Figure 3.1: Key leukocyte populations maintain their cell number during treatment....56
Figure 3.2: Flow cytometric gating strategy for analysis of whole blood to identify leukocyte subsets....57
Figure 3.3: Main leukocyte populations and lymphocyte subsets show unchanged proportions after chemotherapy....58
Figure 3.4: Gating strategy for T cell subset analysis from patients' PBMCs....62
Figure 3.5: Comparison of proportions of four main $CD8^+$ T cell subsets between different time points (pre-treatment, on-treatment, relapse/progression)....63
Figure 3.6: Comparison of proportions of four main $CD4^+$ T cell subsets between different time points (pre-treatment, on-treatment, relapse/progression)....64
Figure 3.7: Young CD4 and CD8 T cells ($CD4^+$ $CD27^+$ or $CD8^+CD27^+$)....65
Figure 3.8: Terminal differentiated CD4 and CD8 T cells ($CD4^+$ $CD57^+$ or $CD8^+CD57^+$)....66
Figure 3.9: Memory T cells did not express stem cell- like marker CD95....67
Figure 4.1: Expansion of T cells during the CAR T cell manufacturing process....75
Figure 4.2: Transduction efficiency of CAR T cell products as determined by flow cytometry on day 6 post activation (4 days after transduction)....78
Figure 4.3: Gating strategy used for 12-colour flow cytometric analysis of CAR T cell products....83
Figure 4.4: The proportion of CD4 and CD8 in CAR T cell population....84
Figure 4.5: Major $CD8^+$ CAR T cell subsets do not change in proportion regardless of stages of chemotherapeutic treatment....85
Figure 4.6: Major $CD4^+$ CAR T cell subsets do not change in proportion regardless of stages of chemotherapeutic treatment....86
Figure 4.7: Gating strategy and representative plots of phenotypes of initial PBMCs and CAR T cell product....89

Figure 4.8: Alteration in $CD8^+$ and $CD4^+$ T cell frequencies in original PBMC population compared to final products 90
Figure 4.9: Alteration in major $CD8^+$ T cell subset frequencies in original PBMC population compare to final products 91
Figure 4.10: Alteration in major $CD4^+$ T cell subset frequencies in original PBMC population compare to final product 92
Figure 5.1: Percentage of cytolysis determined based on impedance measurement 100
Figure 5.2: Program cell death and activation induced cell death occurs spontaneously and after specific CAR stimulation, respectively 103
Figure 5.3: Expression of exhausted and senescent markers by Car T cells following stimulation 106
Figure 5.4: CAR T cells at different treatment time points exhibit similar cytokine release profiles upon activation 108
Supplementary figure S1: CD95 expression on $CD3^+CAR^+$ T cells following CAR stimulation or resting in supplemented medium 110
Supplementary figure S2: Concentration of GM-CSF and IL-6 in supernatant of resting/ specific stimulated CAR T cells/ universal stimulated CAR T cells 110
Supplementary figure S3.1: CD95 was detected in cell population positive for CD14 or CD56 or CD19 rather in naïve/memory T cells 67

List of Tables

Table 1.1: Markers expressed on different T cell subsets 6
Table 2.1: List of conjugated antibodies used for flow cytometry (12 colour panel) and their suppliers and catalogue numbers 26
Table 2.2: List of other primary and secondary antibodies, conjugated antibodies used for flow cytometry and their suppliers and catalogue numbers 27
Table 2.3: List of reagents used for flow cytometry and their suppliers and catalogue numbers 28
Table 2.4: List of reagents/ cytokines used for manufacturing CAR T cells and their suppliers and catalogue numbers 29
Table 2.5: List of reagents/ chemical compounds used for isolating of PBMCs and preparing buffers/media, and their suppliers and catalogue numbers 30
Table 3.1: Epidemiologico-clinical features of patients included in the study 52
Table 6.1: Cell yield of CAR T cell products did not meet the threshold value of 3 x107 cells after expansion 116
Table 6.2: Low transduction efficiency (≤ 5%) 118
Table 6.3: Entire population of on-treatment CAR T cells achieved the 30% of killing effect. 122
Table S1: 12 colour flow cytometry panel 46
Table S2: Mean concentration of cytokines released by CAR T cells at different treatment time points 111

List of Abbreviations

5-FU	5-fluorouracil
AICD	Activation-induced cell death
ALL	Acute lymphoblastic leukaemia
Anti-EGFR	Anti-epidermal growth factor receptor
Anti-VEGF	Anti–vascular endothelial growth factor
CAR	Chimeric antigen receptor
CLL	Chronic lymphoblastic leukaemia
E:T	Effector cell: target cell ratio
FCS	Fetal calf serum
FLEEOX	The combination of fluorouracil, leucovorin, epirubicin, epotoside, and oxaliplatin
FLAC	The combination of 5-fluoroural, 5-fluorouracil, leucovorin, doxorubicin, and cyclophosphamide
FOLFIRINOX	The combination of fluorouracil, irinotecan (topoisomerase I inhibitor), oxaliplatin, and leucovorin
GITR gene	Tumour necrosis factor receptor superfamily member 18 gene
HER2	Human epidermal growth factor receptor 2
ITAMs	Immunoreceptor tyrosine-based activation motif
MGMT	O6-methylguanine DNA methyltransferase
MHC	Major histocompatibility complex
PBMC	Peripheral blood mononuclear cell
RAH	Royal Adelaide Hospital
scFv	Single-chain variable fragment
TAAs	Tumour associated antigen
T_{CM}	Central memory T cells
TCR	T cell receptor
T_{EM}	Effector memory T cells
T_{EMRA}	Terminal effector T cells

TIL	Tumour-infiltrating T cells
TMZ	Temozolomide
T_{Naive}	Naïve T cells
TRAIL	TNF-related apoptosis-inducible ligand
T_{SCM}	Stem cell like memory T cells

Summary

The use of immunotherapy for treating advanced cancer has developed dramatically in recent years. Transferring T cells encoding tumour-specific chimeric antigen receptors (CAR) has shown great promise in treating haematological cancers but has been less successful in patients with solid tumours. Although partial remissions were observed in several clinical trials for solid cancers, most patients were stable or in disease progression at follow up. Furthermore, CAR T cells have been reported to expand less well and fail to persist after infusion in these patients. Therefore, the optimal production of long-lived and highly functional CAR T cells is clearly required for the successful application of this immunotherapy to solid tumours. Here, I investigate the ability of T cells derived from solid cancer patients receiving chemotherapy to generate satisfactory CAR T cell products. Previous studies have shown that certain chemotherapy agents can alter the proportion of T cell memory subsets. In accordance with this, I hypothesise that blood specimens of solid cancer patients undergoing chemotherapy may contain a high proportion of central memory T cells (T_{CM}) and thus represent the optimal starting population for manufacturing highly functional and effective CAR T cells. To test this hypothesis, CAR T cells were produced using leukocyte populations isolated from glioblastoma, advanced pancreatic cancer and metastatic colorectal cancer patients at three time points: before chemotherapy (pre-treatment), during chemotherapy (on-treatment) and at relapse/progression. Transduction efficiency, immune phenotypes and functionality of these three starting populations were compared. Our results have shown that CAR T cells can be successfully manufactured from patient blood at all time points, with no significant difference in transduction efficiency and T cell memory subset proportions for each product. This study has shown that T cells harvested from cancer patients at different stages of their disease can generate therapeutically useful yields of CAR T cells, and that the CAR T cell products generated from on-treatment samples may have a higher cytotoxic effect and improve viability *in vitro* compared to CAR T cells made at other study time points. Together, the findings support the feasibility of successfully generating functional CAR T cells from PBMCs even following exposure to anti-neoplastic drugs and at advanced stages of disease. This study thus

represents a critical validation for future clinical trials in these patient populations who would be the focus for CAR T cell therapy in the future.

Declaration

I declare that the work presented in this thesis is carried out by me and does not incorporate without acknowledgement any material previously submitted for a degree or diploma in any university. To the best of my knowledge, it does not contain any material previously published or written by another person except where due reference is made in the text; and all substantive contributions by others to the work presented, including jointly authored publications, is clearly acknowledged.



Nga TH Truong

November 2019

Acknowledgements

I wish to express my deepest appreciation to my supervisors Professor Michael Brown, Dr. Lisa Ebert and Dr. Tessa Gargett for their support, guidance and wisdom. Without your helps, I would not have made it this far. I have enormously learnt and improved myself from your insight and enthusiasm. Thank you for having patience with me and giving lots of advices during my study. I sincerely extend my gratitude to Professor Michael Brown who has provided me an opportunity to work on this project that has brought me to an exciting new area of research and reignited my passion for medicine and sciences. Dr. Lisa Ebert – thank you for your encouragement and suggestions on various aspects from study to life. Your positive attitude has been a great motivation for me for being more confident and open. You are truly a great advisor and mentor. Dr. Tessa Gargett –thank you for your precious friendliness and support which have guided me through and over many difficulties during study. Your persistence in life and in career has impressed me deeply. I have been grateful to have you as my supervisor and enjoyed working beside you. Again, it is a deepest gratitude for my supervisors whose inputs have been invaluable throughout this thesis and this phase of my life.

I extend my appreciation to all members of the Translational Oncology Laboratory: Dr. Stanley Yu who has assisted me with difficult lab techniques, Dr. Judy Li (former lab member) who I can shared every bit of moments in the group, Dr. Alex Staudacher, Dr. Vasilios (Bill) Liapis, Dr. Nicole Witter, Erica Yeo and Ruhi Polara who have made the lab more cheerful and joy. Words cannot express how gratitude I am for your energies.

Special thanks to the former and present clinical research fellows Dr. Anna Mislang and Dr. Gonzalo Tapia Rico who helped in recruiting patients and collecting patient clinical data for this project. Thanks to all patients and their family for their priceless contribution to this project.

I would like to acknowledge Miltenyi Biotec for the use of free antibodies.

And finally, I am greatly indebted my parents who always support me. Thank you for your patience, unconditional love and for making my life easier.

Publications and Conference presentations

Truong N, Gargett T, Ebert L, Brown MP. Optimising CAR T cell manufacturing for solid cancers. Eradicate Cancer 2018. Melbourne, March 2018 (Poster)

Truong N, Gargett T, Ebert L, Brown MP. Optimising CAR T cell manufacturing for solid cancers. Australian Society of Medical Research SA Branch Annual Meeting, Adelaide. June 2018 (Poster)

Truong N, Gargett T, Ebert L, Brown MP. Optimising CAR T cell manufacturing for solid cancers. Australian Society of Medical Research SA Branch Annual Meeting, Adelaide. June 2019 (Oral presentation)

Chapter 1

Introduction

1.1 Overview

Cancer is an often incurable disease and a serious global health issue. Although various cancer treatments are available such as surgery, chemotherapy, radiotherapy, chemo-radiation and targeted therapies, other treatment modalities are required for non-responsive patient groups. Immunotherapy, which includes checkpoint inhibitor therapy and chimeric antigen receptor (CAR) T cell therapy, is emerging as a new and promising cancer treatment modality. Checkpoint inhibitor therapy is successful in melanoma and lung cancer cancers that are resistant to other types of treatment. CAR T cell therapy has been approved for refractory/relapsed B cell malignancies. However, applying CAR T cell therapy to treat solid cancers faces challenges. Proposed methods to overcome constraints on CAR T cell therapy include selection of effective cancer-specific antigen receptors for T cells and improving the infiltration and persistence of CAR T cells in the circulation and in cancerous masses. In this chapter, a review is undertaken of the available chemotherapy for three types of cancer: glioblastoma, advanced pancreatic cancer and metastatic colorectal cancer, and a background to CAR T cell therapy is also provided, including its challenges and the ways it might be improved. The discussion also highlights alterations to the immune system that occur in response to antineoplastic drugs, and the significance of these alterations on CAR T cell manufacturing, which leads to the hypothesis and aims of this thesis.

1.2 Solid cancers in need of new therapies

Cancer is one of the leading causes of death worldwide. Cancer is responsible for an estimated 9.6 million deaths worldwide in 2018 (WHO 2019). The annual number of deaths from cancer (cancer mortality) is 163.5 per 100,000 people (NCI 2018). Interestingly, the overall cancer death rate has declined for some individual cancer types while the mortality rates for certain other cancers such as glioblastoma and pancreatic cancer have stabilized or even increased (NCI 2018). Likewise, advanced metastatic colorectal cancer has relatively poor 5-year survival rate.

1.2.1 Glioblastoma

Glioblastoma is the most common primary brain tumour and is classified as a grade IV or high-grade astrocytoma according to World Health Organisation criteria (Louis, DN et al. 2007). It is a fatal illness with limited therapeutic options and carries a poor prognosis with a 5-year survival rate of only 12% (AIHW 2019). In Australia, more than 1300 people died from primary brain tumours in 2014 and it is estimated that the mortality number for 2019 will increase to 1549 (AIHW 2019; Cancer-Australia 2019c). Standard therapy for newly diagnosed glioblastoma is surgical de-bulking of gross tumour mass if safe, then radiotherapy concurrent with temozolomide (TMZ) chemotherapy, followed by consolidation TMZ therapy (Stupp et al. 2014). Temozolomide is an alkylating agent that creates O6-methylguanine DNA adducts, which then induce unsuccessful DNA mismatch repair and cell apoptosis (Roos et al. 2006). Normal cells that strongly express O6-methylguanine DNA methyltransferase (MGMT) enzyme are capable of repairing O6-methylguanine back to guanine and so overcome the cytotoxic effect of TMZ (Roos et al. 2006). In contrast, tumour cells, which produce less MGMT because of methylation of MGMT gene promoter, are susceptible to TMZ cytotoxicity (Roos et al. 2006). Unfortunately, only 35% of glioblastoma lesions have epigenetic silencing of the MGMT gene promoter, demonstrating that TMZ treatment may not benefit the majority of high-grade brain tumour patients (Malmström et al. 2012; Stupp et al. 2014). TMZ is initially given at 75mg/m^2 intravenously one a day for up to 6 weeks, followed by a maintenance dose at 150mg/m^2 daily for 5 consecutive days in a 28-day cycle for up to 6 cycles (Stupp et

al. 2014). About 10% of TMZ-treated patients have been reported to have neutropenia, lymphopenia during TMZ treatment (Singhal, Selva-Nayagam & Brown 2007).

1.2.2 Pancreatic adenocarcinoma

Pancreatic adenocarcinoma is estimated to affect over 3200 people in Australia per year and more than 3051 people are expected to die from this cancer in 2019 (Cancer-Australia 2019b). Approximately 63% of people who are diagnosed with pancreatic cancer already have extensive metastatic disease (Iacobuzio-Donahue et al. 2009). With stage I-II pancreatic adenocarcinoma, only 25% of patients have tumours that are appropriate for tumour resection (Martin et al. 2009). With advanced unresectable tumours, there is on-going investigation of potential chemotherapeutic regimens in which the FOLFIRINOX regimen and the combination of gemcitabine (cytosine analogue) and nab-paclitaxel (albumin-bound-paclitaxel) have shown the most promising results, with 11.1 and 8.5 months median survival, respectively (Conroy et al. 2011; Von Hoff et al. 2013). The FOLFIRINOX regimen comprises the combination of 5-fluorouracil (5-FU), irinotecan (a topoisomerase I inhibitor), oxaliplatin, and leucovorin. However, 45% of patients treated with FOLFIRINOX were noted to have neutropenia and 5.4% suffered from febrile neutropenia (Conroy et al. 2011). Likewise, 38% of patients treated with and gemcitabine had neutropenia as an adverse effect (Von Hoff et al. 2013), indicating that treatment impairs production of the neutrophil subset of white blood cells and may affect the immune competency of patients.

1.2.3 Colorectal cancer

Colorectal cancer is the second most commonly diagnosed cancer in Australia with approximately 16398 new cases this year (Cancer-Australia 2019a). Data from 2004 to 2010 showed only 11% of stage IV colon cancer patients and 12% of advanced metastatic colorectal cancer patients survive at least 5 years (NCCI 2019). Advanced metastatic colorectal cancer thus has relatively poor 5-year survival rate and the mortality rate is the second highest after lung cancer in Australia, being estimated at more than 5500 deaths in 2019 (Cancer-Australia 2019a). Late stage colorectal cancer can be treated with surgery, radiotherapy and systemic chemotherapy (Hurwitz et al. 2004). The backbone of systemic

chemotherapy in metastatic colorectal cancer includes fluoropyrimidines (intravenous 5-FU/leucovorin or the oral 5-FU pro-drug, capecitabine) in combination with oxaliplatin or irinotecan (Hurwitz et al. 2004). Anti-vascular endothelial growth factor (VEGF) or anti-epidermal growth factor receptor (EGFR) monoclonal antibodies can also be combined with these cytotoxic agents and have shown an increase in progression-free survival from 6.2% (cytotoxic doublets + placebo) to 10.6% (cytotoxic doublets + bevacizumab) ($p<0.001$) (Hurwitz et al. 2004). Mild neutropenia was reported in about 39% of patients and 30% of patients suffered from severe neutropenia (Shitara et al. 2009; Verma et al. 2016).

In spite of the diversity of treatment strategies, glioblastoma, metastatic pancreatic carcinoma and advanced colorectal cancer are still considered incurable diseases. New therapeutic approaches to these types of cancer need to be urgently studied to improve survival and to decrease their burden on cancer patients, their families and the Australian health system. While CAR-T cell therapy is a potential therapeutic approach, consideration must be given to how CAR-T therapy would be integrated with the current standard chemotherapy treatments.

1.3 Chemotherapy and lymphocyte populations

Cells of the immune system can be affected by chemotherapy drugs in many ways. The numbers and intrinsic quality of immune cells are critical for the efficacy of subsequent immunotherapies (Wijayahadi et al. 2007). As discussed above, negative effects of chemotherapy drugs on the neutrophil subset are well known and can lead to an increased susceptibility to infections (Klastersky et al. 2016). Less well known, however, is that T cell populations, which are the main target of current immunotherapies, are also reported to alter in phenotype and to have their CD4/CD8 ratios reversed in response to chemotherapy treatment (Mackall, C et al. 1994). These effects are discussed in detail below.

1.3.1 T cell subsets affected by chemotherapy

1.3.1.1 Subsets of T cells

Thymic selection and maturation give rise to antigen-specific T cells with two separate lineages defined as $CD4^+$ T helper cells and $CD8^+$ cytotoxic T cells, based on cell surface expression of the co-receptor molecules, CD4 and CD8 (Broere et al. 2011). $CD4^+$ cells can be activated by antigens presented by major histocompatibility complex (MHC) class II molecules, which are expressed by professional antigen presenting cells. $CD8^+$ cytotoxic T cells can recognise antigens presented by MHC class I molecules, which are expressed on all nucleated cells (Broere et al. 2011). CD4 and CD8 T cells can be further distinguished based on their functional status as naïve, memory or effector cells (Broere et al. 2011). Cells released from the thymus are homogeneous naïve T cells (T_{Naive}) which have not been exposed to cognate antigen (Broere et al. 2011). T_{Naive} cells express high levels of lymph node homing receptors such as CC chemokine receptor 7 (CCR7), L-selectin (CD62L) and leukocyte function antigen-1 (LFA-1), facilitating their rolling, adhesion and extravasation through blood vessels. Naïve T cells continuously circulate through the secondary lymphoid organs where cognate antigen encounter occurs (Broere et al. 2011). . An isoform of common leukocyte antigen, CD45RA, and a costimulatory molecule CD27 are also expressed on T_{Naive} (Broere et al. 2011). Signals through CD27 support the antigen-specific expansion of T_{Naive} cells (Hendriks et al. 2000). Following encounter with cognate antigens within secondary lymphoid organs, naïve T cells become activated, proliferate and differentiate into effector or memory T cells (Broere et al. 2011; Sallusto et al. 1999). Additional subsets of memory cells can persist and reside in lymphoid organs, where they are called central memory T cells (T_{CM}), or in non-lymphoid organs, which are named effector memory T cells (T_{EM}) (Broere et al. 2011; Sallusto et al. 1999). Both memory subtypes express CD45RO, another isoform of the common leukocyte antigen, but only T_{CM} express the lymphoid-homing marker CCR7 and perhaps CD27 (Broere et al. 2011; Sallusto et al. 1999). T_{EM} cells can execute effector functions immediately after exposure to antigens, while T_{CM} have to proliferate and expand probably through CD27 signals, before acquiring effector functions (Broere et al. 2011). Terminal effector T cells (T_{EMRA}) lose their lymph node homing markers ($CCR7^-$), which allows them to migrate to peripheral tissues to exert their function (Hamann et al. 1997). T_{EMRA} cells re-express the CD45RA marker and may also express PD-1 and CD57 markers, which define their level of activation and exhaustion (Hamann et al. 1997). A rare subset of T cells with multiple stem cell-like

properties (T_{SCM}) share the functional capacity of T_{CM} and the ability to recirculate and distribute like-naïve T cells (Gattinoni et al. 2011). T_{SCM} bears all the markers that can be found on naïve T cells but differ from T_{Naive} by the overexpression of CD95 (Gattinoni et al. 2011).

Table 1.1: Markers expressed on different T cell subsets

	T_{Naive}	T_{SCM}	T_{CM}	T_{EM}	T_{EMRA}
CD45RA	+	+	−	−	+
CD45RO	−	−	+	+	−
CCR7	+	+	+	−	−
CD27	+	+	+	+/−	−
CD57	−	−	+	+/−	+
CD95	−	+	−	+	+

1.3.1.2 The survival and enhanced activity of CD8⁺ T lymphocytes following chemotherapy

The number and function of $CD8^+$ T cells is well preserved after exposure to various chemotherapy drugs, both *in vitro* and *in vivo.* Several studies have revealed that the mean absolute number of $CD8^+$ T lymphocytes is maintained, and in fact, T cell function is even enhanced, after chemotherapy (Fadul et al. 2011; Scurr et al. 2017; Suzuki et al. 2005).

In an analysis of absolute number of $CD8^+$ T cells , researchers found that the mean absolute number of $CD8^+$ T cells in pre-treatment blood samples collected from glioblastoma patients did not reduce 4 weeks after beginning treatment with radiation therapy and concomitant temozolomide (Fadul et al. 2011). Similar findings were cited in other studies in which patients with brain tumours and breast cancers received high doses of either cyclophosphamide (ranging from 1.2 g/m^2/cycle to 7 g/m^2/cycle) or epirubicin (90mg/m^2) plus paclitaxel (175 mg/m^2), respectively (Fagnoni et al. 2002; Mackall, CL et al. 1997b). These latter studies have shown $CD8^+$ T lymphocytes recovered rapidly after intensive chemotherapy regimens with a median doubling time of 12.6 days. Looking at the subpopulations of $CD8^+$ T cells that accounted for the rapid expansion, researchers

reported that effector cells ($CD8^+CD28^-$ or $CD8^+$ $CD62L^-$) were expanded during and after doxorubicin, carboplatin, paclitaxel and cyclophosphamide (Coleman et al. 2005a; Fagnoni et al. 2002; Mackall, CL et al. 1997a). Fadul et al. further differentiated effector cells into $CD8^+$ T_{EM} cells, which are negative for both CD45RA and CCR7 markers, and $CD8^+$ T_{EMRA} cells, which also lack CCR7 but have regained expression of CD45RA (Fadul et al. 2011). His group found that $CD8^+$ T_{EM} cells were significantly increased whereas $CD8^+$ T_{EMRA} cells were remarkably decreased after temozolomide (Fadul et al. 2011). Interestingly, most studies have reported both the proportion and absolute number of naïve T cells and $CD8^+$ T_{CM} cells are neither decreased nor increased post alkylating agent-based as well as anti-microtubule-based chemo therapeutic treatment (Coleman et al. 2005b; Fadul et al. 2011; Fagnoni et al. 2002; Mackall, CL et al. 1997a). This may suggest that $CD8^+$ T_{EM} cells are the main source for the re-expansion of the $CD8^+$ population after chemotherapy.

Corresponding with these findings, Turtle et al. have identified a mechanism underlying the strong resistance of memory $CD8^+$ T cells to cytotoxic treatment (Turtle et al. 2009). A distinct proportion of central memory and effector memory $CD8^+$ T cell over-express ATP-binding cassette (ABC)-superfamily multidrug efflux proteins which protect cells from toxic agents, and these subpopulations were strongly resistant to daunorubicin-induced apoptosis (Turtle et al. 2009). Importantly, $CD8^+$ memory T cells with high efflux capacity were shown to proliferate strongly with IL-7/IL-15 supplements *in vitro* and after lymphodepletion *in vivo* (Turtle et al. 2009). This again supports the contribution of these cells to reforming the T cell memory subpopulation after chemotherapy (Turtle et al. 2009).

Interestingly, chemotherapy agents not only enhance effector memory $CD8^+$ cell numbers but can also induce anti-cancer T cell responses. A phase I/II clinical trial in metastatic colorectal cancer measuring the effects of cyclophosphamide (50mg twice a day) on T cell subsets showed a remarkable increase in the percentage of granzyme B and IFN-γ producing T cells after treatment (Scurr et al. 2017). Similar results were also reported in a study on a metastatic ovarian cancer cohort with carboplatin and paclitaxel chemotherapy (Coleman et al. 2005b). These data suggest that, in addition to a direct

cytotoxic effect on cancer cells, antineoplastic drugs also strengthen the cytotoxic effect of $CD8^+$ T cells, which may contribute to their anti-cancer activity.

1.3.1.3 Inconsistent changes in $CD4^+$ T cells

The effects of various chemotherapeutic agents on $CD4^+$ T cells were not uniform among studies. Blood samples collected from glioblastoma patients after temozolomide treatment, or from breast cancer patients who had received docetaxel, doxorubicin and cyclophosphamide, had a remarkable drop, approximately by half, in the absolute number of $CD4^+$ T cells (Fadul et al. 2011; Verma et al. 2016). Similarly, Hakim et al. showed a prolonged reduction in $CD4^+$ T cell number in another breast cancer patient cohort up to 12 months after high dose chemotherapy with FLAC (a combination of 5-FU, leucovorin, Adriamycin (doxorubicin), and Cytoxan (cyclophosphamide)). There was a particularly severe depletion of $CD4^+$ T cells in groups of patients who had docetaxel in the treatment plan and they did not recover after cessation of chemotherapy (Verma et al. 2016). In contrast, the percentage of peripheral $CD4^+$ T cells was shown to steadily increase every week for a 6-week treatment period in pancreatic carcinoma patients receiving a combination of cisplatin, gemcitabine, and fluorouracil (Bellone 2009). Another cohort of gastric cancer patients treated with a regimen of 5 different cytotoxic drugs (FLEEOX) had no change in $CD4^+$ T cell proportion (He et al. 2017). These findings show unexpected and inconsistent changes in the $CD4^+$ T cell population post chemotherapy, probably due to different types of chemotherapy drugs used, differences between patients and types of cancers. In a further analysis of $CD4^+$ subsets, Fagnoni et al. and Verma et al. found cyclophosphamide, doxorubicin, and docetaxel caused a significant drop in both the mean absolute number and the percentage of naïve $CD4^+$ T cells, defined as $CD45RA^+$ $CD45RO^-$ $CD62L^+$ (Fagnoni et al. 2002; Verma et al. 2016). Similarly, Hakim et al. revealed a greater than 50% loss of $CD45RA^+CD4^+$ cells, and this subset was still not fully replenished up to 9 months post FLAC (Hakim et al. 1997). Conversely, memory $CD4^+$ T cells ($CD45RO^+$) remained stable during treatment with cyclophosphamide, docetaxel and doxorubicin and then progressively increased by 20% in their proportion for 9 months follow up (Fagnoni et al. 2002; Verma et al. 2016).

Importantly, $CD4^+$ and $CD8^+$ T cells use different pathways to regenerate, which may contribute to the differences seen in response to chemotherapy. The thymus plays a central role in the regeneration of $CD4^+$ T cells but not $CD8^+$ T cells (Hakim et al. 1997; Mackall, CL et al. 1997a). The thymus undergoes atrophy with age and is disorganised by chemotherapy drugs which could explain deficiencies in $CD4^+$ T cells, especially the $CD4^+$ $CD45RA^+$ subset, in most studies with aged patient cohorts (Gui et al. 2012; Talmadge JE 1993). Conversely, $CD8^+$ T cells demonstrate thymic-independent restoration, with high proliferative capacity from the $CD8^+$ $CD28^-$ repertoire (Mackall, CL et al. 1997a). These findings should be carefully noted because the pool of regenerated $CD8^+$ T cells could determine the effectiveness of engineered cytotoxic T cells.

1.3.2 Depletion of circulating regulatory T cells

Regulatory T cells (Tregs; characterized as $FoxP3^+$ $CD25^+$ $CD4^+$) are potent suppressive cells in the immune system and considered to constrain anti-tumour immune responses (Kondelkova et al. 2010). Interestingly chemotherapy can induce changes to this population that are beneficial to the immune system (Galsky et al. 2018; MAEDA et al. 2011; Wang, L et al. 2018). Two studies in gastric cancer and colorectal cancer using FOLFOX 6 (folinic acid/fluorouracil/oxaliplatin) and FOLINIC regimens identified a significant decrease in the frequency of Tregs in PBMCs after at least three cycles of treatment, especially in a group of patients that exhibited a high proportion of Treg before treatment ($p<0.001$) (MAEDA et al. 2011; Wang, L et al. 2018). The suppression of Treg numbers in circulation was also seen in non-small-cell lung carcinoma (NSCLC) and urothelial cancer patients after two to four cycles of treatment with cisplatin-based chemotherapy (Galsky et al. 2018; Li et al. 2014). Similarly, cyclophosphamide was reported to induce apoptosis of Tregs ($CD4^+CD25^+$) and eliminate the homeostatic maintenance of this population in a mouse model (Brode et al. 2006; Lutsiak et al. 2005). Studies showed that the genes for FoxP3 and GITR, which relate to Treg cell function (proliferation and resistance to TCR-mediated cell death) were significant downregulated in mice treated with cyclophosphamide (Fontenot, Gavin & Rudensky 2003; Lutsiak et al. 2005). Cyclophosphamide-induced depletion of Tregs and loss of suppressive function were shown to rescue immune dysfunction in animal models of cancer (Ghiringhelli et al.

2004; Shimizu, Yamazaki & Sakaguchi 1999). Thus, chemotherapy significantly depletes regulatory T cells, which leads to reversal of immune dysfunction and therefore facilitates anti-tumour immunity, at least in animal models.

1.3.3 Decrease in circulating B lymphocytes

In the context of cancer, B cells present tumour antigens to T cells and produce tumour antigen-specific antibodies (Reuschenbach, von Knebel Doeberitz & Wentzensen 2009; Rodríguez-Pinto 2005). B cells are also categorized into naïve, memory, immature, regulatory B cells (Breg) and plasma cells. Both the absolute number and the frequency of all B cell subsets were significantly diminished post treatment with cyclophosphamide, epirubicin/doxorubicin, and cisplatin (Ziebart et al. 2017; Zirakzadeh et al. 2017). Although absolute cell count was decreased, studies have shown that B cells treated with anthracycline (doxorubicin) and platinum-based chemotherapy drugs *in vitro* have an enhanced ability to activate T cells, facilitated by the upregulation of co-stimulatory molecules CD86 and a decrease in suppressive factor (IL-10, adenosine) secretion (Ziebart et al. 2017; Zirakzadeh et al. 2017). In contrast, methotrexate had an opposing effect on Breg cell population. The proportion of Breg cells was increased and the production of exogenous adenosine was also enhanced (Ziebart et al. 2017). This negative effect further protects tumour cells from anti-tumour T cells (Ohta et al. 2006; Ziebart et al. 2017). In short, selected antineoplastic drugs enhance B cell function which overcomes the remarkable decrease in circulating B cell number.

In summary, chemotherapy gives rise to a repopulation of circulating lymphocytes, skewing towards enhancing the immune response. Cell number and cytotoxicity of $CD8^+$ T cells were increased while the frequency and functions of both regulatory T cells and regulatory B cells were significantly suppressed post treatment with antineoplastic drugs. $CD4^+$ T cells have showed inconsistent alteration in their physiological proportion in response to different types of chemotherapy drugs.

1.4 CAR T cell therapy in cancer

1.4.1 CAR T cell therapy is a passive immunotherapy

The use of immunotherapy for treating advanced cancer has developed dramatically in recent years (Yu et al. 2017). Immunotherapy can be categorized as active immunization e.g. using cancer vaccines to enhance natural immune effects, and passive immunotherapy e.g. infusing monoclonal antibodies or tumour-targeted T cells. Passive immunotherapies such as adoptive cell transfer, which exploit the patients' own immune system and transfer effector cells to attack tumour cells through their surface markers, have emerged as a powerful cancer treatment. Early trials investigated *in vitro* expanded tumour-infiltrating T cells (TIL) whereas more recent studies have focused on adoptive cell therapy with genetically engineered T cells (Rosenberg & Dudley 2004). One method for producing gene-modified T cells involves selecting T cells from autologous peripheral lymphocytes, which are then transduced *ex vivo* with retrovirus encoding a specific CAR (Kershaw et al. 2006). This procedure produces CAR T cells, which are then expanded *in vitro* and infused into patients at a concentration expected to be sufficient for cancer therapy (Gargett et al. 2016). Adoptively transferred CAR T cells track down and kill malignant cells by attaching to a specific surface marker, then triggering apoptotic signalling (Yu et al. 2017).

Transferring T cells encoding tumour-specific CAR molecules has shown great promise in treating haematological cancers but has been less successful in patients with solid tumours (Porter et al. 2011). In a phase I/II clinical trial, modified T cells (CTL019) that target CD19 expressed on B cells in acute lymphoblastic leukaemia (ALL), resulted in stable complete remission in 65% of patients without further therapy up to 7 months (Maude et al. 2014). A phase II trial has been conducted to determine the efficacy and safety of CTL019 in relapsed/refractory ALL paediatric patients and has led to US FDA approval of the first CAR T cell product, tisagenlecleucel (Kymriah™). With this milestone approval, researchers are aiming to apply CAR T cell therapy to other cancer types (NCI 2017). Nonetheless, CAR T cell therapy has been less effective when applied to solid cancer treatment (Kershaw et al. 2006; Louis, CU et al. 2011). A lack of specific and homogenously expressed tumour-associated antigens in solid cancer, an immune-suppressive microenvironment within the tumour, and the loss of function or depletion of CAR T cells after infusion are outstanding problems for CAR T cell therapy (Gargett et al. 2016). Several different solid tumour antigens have been selected as targets for the T cell chimeric

receptor structure, such as GD2, HER 2 (human epidermal growth factor receptor 2) and IL13Rα2 (overexpressed by majority of brain tumours)(Ahmed et al. 2017; Brown et al. 2016b; Gargett et al. 2016). The GD2 tumour antigen, which is a sialic acid-containing glycosphingolipid, is a research focus of my laboratory, and is expressed in a variety of solid tumours, such as neuroblastoma, melanoma, small cell lung cancer, breast cancer, some sarcomas, peripheral neuroectodermal tumours (PNET), glioblastoma, and metastatic pancreatic carcinoma (Battula et al. 2012; Bilchik et al. 2000; Künkele et al. 2015; Maude et al. 2014; Wu et al. 1986; Yu et al. 2017). Recent *in vivo* data indicate that GD2-expressing breast cancer cells may have greater generative potential than non-expressing cells because $GD2^+$ cells exhibited larger tumours compared to GD2-negative cells from the same source (Battula et al. 2012). CAR T cells targeting these antigens were used in different phase I clinical trials to test their efficacy/safety on the treatment of melanoma (ACTRN12613000198729) and glioblastoma (Ahmed et al. 2017; Brown et al. 2016b). Although partial remissions were observed in some of these trials, most patients were stable or in disease progression at follow up (Ahmed et al. 2017; Brown et al. 2016b). Furthermore, CAR T cells have been reported to expand less well and fail to persist after infusion to these patients (Gargett et al. 2016). Therefore, the optimal production of long-lived and highly functional CAR T cells is clearly required for the successful application of this immunotherapy to solid tumours.

1.4.2 CAR T cell design

CAR design is based on understanding T cell receptor (TCR) signalling mechanisms that direct the cytotoxic effect of T cells toward tumour cells (Konig 2010). TCR activation leads to signalling cascades that ultimately drives cytokine production, T cell survival, differentiation, and proliferation. A TCR is a heterodimer including one α chain and one β chain that together recognize a specific peptide antigen bound in the context of a major histocompatibility complex (MHC) (Srivastava & Riddell 2015). The TCR includes a CD3-ζζ complex which provides an activation signal in T cells (Srivastava & Riddell 2015). Physiologically, CD3-ζζ is a homodimer transmembrane protein and is associated with CD3-γε and CD3-δε expressed at the T cell surface (Srivastava & Riddell 2015). CD3-ζζ is comprised of a small extracellular part, a transmembrane region, and a long cytoplasmic

tail that contains three immunoreceptor tyrosine-based activation motifs (ITAMs), which are phosphorylated when TCR- αβ binds to antigen (Ashe et al. 1999). ITAMS are phosphorylated by the Lck tyrosine kinase, which is bound to the cytoplasmic tails of CD4 or CD8 co-receptors. Phosphorylated ITAMS can then recruit ZAP-70/Syk tyrosine kinase molecules which phosphorylate other downstream signalling molecules and lead to activation of a number of transcription factors such as NK-κB , AP1, and NFAT (Ca^{2+} flux) (Mócsai, Ruland & Tybulewicz 2010; Steinberg et al. 2004).

This first signal emanating from the TCR complex and its CD4 or CD8 co-receptors are antigen-specific but not sufficient for full T cell activation (Konig 2010). T cells that are only activated by signalling from the CD3-ζζ complex without co-stimulation can become anergic, in which case T cell proliferation is inhibited (Schwartz 2003). Additional signals are required to increase the amplitude of the CD3 transcriptional response and for full activation of T cells. Such co-stimulatory signalling can be induced following the ligation of CD28 molecules on the T cell membrane by its B7 ligands (CD80/CD86) on antigen-presenting cells (Konig 2010). When a co-stimulatory CD28 receptor binds to CD80/CD86, it recruits phosphoinositide -3 -kinase (PI3K)/Akt that block NFAT nuclear export, resulting in upregulation/enhancement of transcription factor NFAT and consequently T cell differentiation and activation (Boomer & Green 2010; Diehn et al. 2002). Co-stimulatory signals can also come from receptors of tumour necrosis factor (TNF) receptor superfamily such as 4-1BB, OX40 or CD27 (Croft 2003). These receptors are upregulated hours or days post activation and allow T cells to continue dividing (Croft 2003). Hence, co-stimulation is important for effective T cell activation and helps to maintain the immune response (Oren et al. 2014).

Applying insights from studies of TCR recognition and activation mechanisms, antigen-specific chimeric receptors are constructed to induce a potent immune response when they recognise tumour cells (Konig 2010). T cells are genetically engineered to express CARs that combine an extracellular domain derived from a single chain variable fragment (scFv), a transmembrane domain, and intracytoplasmic T cell-derived signalling domains as shown in **Figure 1.1**

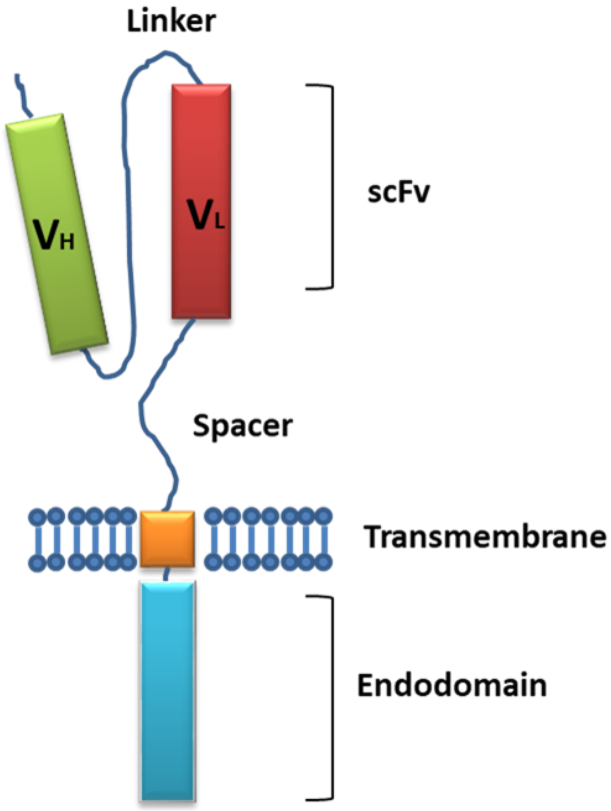


Figure 1.1: Chimeric antigen receptor structure. scFv: single chain variable fragment, V_H: Heavy chain of a variable domain, V_L: Light chain of a variable domain

The scFv recognition domains (ectodomains) are designed from antibody V_H (heavy chain of a variable domain) and V_L (light chain of a variable domain) sequences specific for tumour-associated molecules (Srivastava & Riddell 2015). The major advantage of a chimeric receptor is that it does not require the MHC-dependent antigen recognition which is normally required for initial native T cell priming (Srivastava & Riddell 2015). The antibody-derived scFv allows a CAR to specifically identify native rather than processed antigen (Srivastava & Riddell 2015). This permits CAR T cell killing of malignant cells which down-regulate MHC expression to bypass the immune system. The only downside of this non- MHC-restricted characteristic is that CAR T cells can only recognize cell surface markers, not intracellular antigens (Srivastava & Riddell 2015). Another advantage of CARs is the antibody region can recognize not only protein antigens but also glycolipid or carbohydrate antigens (Sadelain, Rivière & Brentjens 2003). Therefore, CAR T cells can be structured with different antibody domains to target a wide range of tumour antigens (Sadelain, Rivière & Brentjens 2003). However, the scFv is usually of nonhuman origin (often from a mouse antibody) and may prompt anti-CAR immune responses which can speed up CAR T- cell clearance *in vivo* and even cause anaphylaxis in patients (Abate-Daga & Davila 2016). In the future, humanized scFv structures may be required to reduce immunogenicity and, therefore, increase the safety and efficacy of adoptive CAR T cell therapy (Abate-Daga & Davila 2016).

The extracellular domain of a CAR is fused to its intracellular domains via the hinge (spacer) and a transmembrane domain (Schwartz 2003). These domains, especially the length of the spacer, can have significant impact on CAR T cell function as they determine a CAR's ability to bind target epitopes (Srivastava & Riddell 2015). Physiologically, during immune synapse formation, there is a space of about 15nm between the T cell and the antigen presenting cell. This small distance helps in excluding the large ectodomains of inhibitory CD45 and CD148 molecules from the synapse, allowing T cell activation (Cordoba et al. 2013). Several studies have found that CAR T cells with short spacer domains are efficiently activated by membrane-distal epitopes and vice versa (Guest et al. 2005; James et al. 2008). The short spacer may facilitate the exclusion of inhibitory CD45 and CD148 from the CAR T cell: target cell interactions (Srivastava & Riddell 2015).

Therefore, the spacer length of a CAR needs to be designed for each specific target to increase antigen sensitivity and produce optimal T cell signalling (Srivastava & Riddell 2015). Moreover, the spacer sequence of a CAR structure is usually from the immunoglobulin Fc (CH_2-CH_3) which can undergo a nonspecific interaction with Fc gamma receptor (FcγR) expressed on immune cells (Jonnalagadda et al. 2015). This could lead to AICD and thus limiting CAR T- cell functions and persistence *in vivo* (Srivastava & Riddell 2015). Modifications such as point mutations, single CH3 domain spacers or using CD8α which lacks FcγR binding activity as the spacer have been applied in CAR construction and shown improvement of CAR T cell persistence (Jonnalagadda et al. 2015; Milone et al. 2009; Watanabe et al. 2016).

The transmembrane domain anchors the CAR in the T cell membrane and stabilizes the expression of the CAR on the cell surface (Srivastava & Riddell 2015). In the first generation of CAR T cells, this region was derived from the CD4 or CD8 transmembrane domain (Fitzer-Attas et al. 1998) Later generations of CAR T cells adopt either the CD3ζ transmembrane domain, which show an increase in anti-tumour responses but less stability, or a more stable CD28 transmembrane domain (Bridgeman et al. 2010). The CD3ζ transmembrane domain also facilitates the interaction between CARs and endogenous CD3 as well as the heterodimerization of CAR and native TCR, leading to potent immune responses (Bridgeman et al. 2010).

The intracellular domain of a CAR consists of stimulatory and co-stimulatory components *in cis* and plays an important role in T cell activation and proliferation. The CD3-ζ cytoplasmic domain (stimulatory signal 1) recruits tyrosine kinase molecules which in turn produce activating signalling cascades (Steinberg et al. 2004). Co-stimulatory signals (signal 2) can be derived either from a single element such as CD28, 4-1BB or OX40 receptor, or from a complex of two co-stimulatory domains, for example CD28 and OX-40 or CD28 and 4-1BB (van der Stegen, Hamieh & Sadelain 2015).

The first generation of engineered T cells was initially developed in 1989. Its endodomain consists of only CD3-ζ or Fcγ (van der Stegen, Hamieh & Sadelain 2015). These artificial receptors were sufficient to initiate T cell activation but were not successful in

stimulating cytokine secretion and resulted in rapid T cell anergy (Thistlethwaite et al. 2017). Second-generation CAR T cells have co-stimulatory domains such as CD28, OX40 or 4-1BB that link to the CD3-ζ in their CAR structure, in an attempt to mimic the co-stimulation during T cell activation (van der Stegen, Hamieh & Sadelain 2015). Furthermore, third-generation CAR T cells combine CD28 together with either OX-40 or 4-1BB as co-stimulatory domains in the structure of their receptor, and this has further increased the ability of CAR T cells to proliferate and produce cytokines (Konig 2010). Knowledge of CAR T cell design has now progressed to the extent that effective and functional CAR T cells have been engineered and manufactured for clinical trials and approved CAR T cell therapy.

1.4.3 Challenges in effective CAR T cell therapy for solid cancers

The first CAR T cell immunotherapy clinical trials were conducted in the setting of relapsed and refractive acute lymphoblastic leukaemia (ALL) using autologous CD19-specific CAR T cells. These trials showed a great promise, with 89% of patients achieving a complete response (Kalos et al. 2011). Other CD19 specific CAR T cell phase I trials in ALL and chronic lymphoblastic leukaemia (CLL) patients were also very successful (Maude et al. 2014; Porter et al. 2011). These CAR T cells are specific for the CD19 marker which is uniquely expressed on B cells and their malignant counterparts, and contain a CD3-ζ activation domain and 4-1BB costimulatory domain (Maude et al. 2014). They were reported to proliferate strongly *in vivo*, limit the expansion of malignant cells, and maintain functional activity and were long-lived beyond 3 years post-infusion (Kochenderfer & Rosenberg 2013).

Despite convincing evidence from the therapeutic use of CD19 specific CAR T cell therapy, the adoptive transfer of engineered T cells has not been as successful for the treatment of solid cancers (Brown et al. 2016b; Kershaw et al. 2006). A case report from a phase I study has shown a transient complete response in a glioblastoma patient who was treated with intracavitary infusion of autologous CAR T cells against IL13Rα2 (Brown et al. 2016b). However, another brain tumour was detected after 7.5 months in that patient although the treated site had no evidence of tumour progression (Brown et al. 2016b). In

another phase I study using CAR T cells specific for the ovarian cancer-associated antigen α folate receptor, no evidence of reduction of tumour burden was detected in any patient (Kershaw et al. 2006). Similarly, no clinical responses were recorded in a clinical trial in which metastatic renal cell carcinoma was targeted with carboxy anhydrase IX-specific CAR T cells (Fesnak, June & Levine 2016).

Among the challenges in the development of effective CAR T cell therapy for solid cancers are the safety of CAR T cells (Gargett et al. 2016). CAR T cell toxicity includes on-target but off-tumour reactions, tumour lysis syndrome and cytokine release syndrome (Brentjens, R et al. 2010). Unlike CD19, which is only expressed on normal B cells and malignancies derived from these cells, most of the antigens targeted by CAR T cells on solid cancers are tumour-associated antigens (TAAs) which are found mostly in tumour but also to some degree in healthy tissues. Some examples include the differentiation antigen HER2 and the tumour-associated stroma antigen FAP (Morello, Sadelain & Adusumilli 2016). The on target/off -tumour side effects can occur due to the high sensitivity of CARs for the low-level expression of TAAs on normal healthy tissue such as lung epithelial and cardiovascular cells (Morello, Sadelain & Adusumilli 2016; Morgan et al. 2010). A case report has revealed a fatal adverse event related to ERBB2 -CAR T cell therapy with high cell doses (Morgan et al. 2010). Hence, identification of better tumour specific antigens is required for safe CAR T cell therapy. Another toxicity related to adoptively transferred CAR T cells is cytokine release syndrome (CRS) (Gargett et al. 2016). Potent cytokine production was observed in ALL patients treated with CD19-CAR T cells, with high levels of interleukin (IL)-2, IL-6, and interferon γ (IFN-γ) released (Brentjens, R et al. 2010; Kalos et al. 2011; Kochenderfer et al. 2012; Porter et al. 2011). Although these cytokines are produced as a consequence of T cell activation and are necessary for effective therapy, the CRS can lead to life-threatening adverse effects (Lamers et al. 2013). However, these can be countered by administration of anti-cytokine antibodies or corticosteroids, although steroids may limit the efficacy of CAR T cell therapy (Gargett et al. 2016; Lamers et al. 2013).

Another concern about the effectiveness of CAR T cell therapy in solid cancers is the persistence of CAR T cells (Gargett et al. 2016). The engineered T cells in patient peripheral

blood were only detectable for a short period of time and they were hardly detected in circulation four to six weeks after infusion (Gargett et al. 2016; Louis, CU et al. 2011). Notably, better clinical outcomes were observed with long term CAR T cell persistence (Louis, CU et al. 2011). These findings indicate that CAR T cell persistence is important for successful cancer treatment. The mechanisms proposed to underlie the short-term persistence of CAR T cells are AICD and functional exhaustion (Gargett et al. 2016). T cell activation can lead to increased death ligand (FasL) expression on the T cell surface (Brunner et al. 1995). When FasL on activated T cells binds to death receptors (Fas) on tumour cells, apoptotic signalling cascades are triggered inside T cells, (Brunner et al. 1995). AICD also occurs when TNF-related apoptosis-inducible ligand (TRAIL) on activated mature T cells binds to its receptors (DR4, DR5) on tumour cells (Mariani SM 1998; Wang, S & El-Deiry 2003). Effector and memory T cells are found to be susceptible to cell death stimuli while naïve T cells do not have sufficient expression of the death receptor pathway (Brunner et al. 1995). Notably, AICD was found to occur in CAR T cells when the chimeric receptor encounters cognate antigen or when the CAR-spacer domain was bound non-specifically by FcyR-bearing cells (Hudecek et al. 2015; Künkele et al. 2015).

A study from our research group has shown that GD2-specific CAR T cells undergo AICD after repeated stimulation *in vitro*, and that the level of CAR T cell death is correlated with the level of antigen expression on target cells (Gargett et al. 2016). This finding indicates that the more potent the activation signal that CAR T cells experience, the more they undergo AICD. Similarly, endogenous T cells can be exhausted after they persistently encounter antigens (Wherry & Kurachi 2015). During chronic antigen exposure, integration of signals from prolonged TCR ligation, suppressive cytokines such as IL-10 and TGF-β, cell surface inhibitory receptor PD-1, and alterations from tissue environment such as hypoxia give rise to a deterioration in T cell proliferation and, hence, exhaustion (Wherry & Kurachi 2015). Altogether, AICD and T cell exhaustion phenomena are essential for T cell homeostasis, but can limit the effectiveness of CAR T cell therapy in which T cells are strongly and continually activated via multiple signalling domains (Gargett et al. 2016).

1.4.4 Enhancement of CAR T cell persistence and expansion

The positive correlation between clinical efficacy and the persistence/expansion of CAR T cells after infusion was systematically reviewed (Xu, X-J, Zhao & Tang 2013). Studies from four phase I clinical trials using CD19-CAR T cells have shown that CAR T cells that persisted longer than 4 weeks *in vivo* and had a high copy number of the CAR transgene (>1 copy per ng DNA) were related to better patient outcomes (Brentjens, RJ et al. 2011; Kalos et al. 2011; Kochenderfer et al. 2012; Porter et al. 2011; Xu, X-J, Zhao & Tang 2013). Another paper observed that the persistence of GD2-CAR T cells beyond 6 weeks was associated with disease remission in neuroblastoma (Louis, CU et al. 2011). Therefore, manufacturing long-lived and self-renewing CAR T cells represents an important goal in this field to improve clinical efficacy.

As mentioned above, effector memory T cells are more susceptible to AICD (Brunner et al. 1995). Therefore, I hypothesise that effector memory CAR T cells will also be vulnerable to AICD. In fact, CAR T cells produced from effector memory T cell subsets might be short-lived *in vivo* after encountering target tumour antigens (Sallusto, Geginat & Lanzavecchia 2004). A higher frequency of central memory CAR T cells in the infused product increases resistance to cell death after repeated activation by antigen *in vivo* (Mackall, C et al. 1994). Other studies also demonstrated that the duration of persistence of CAR T cells is highly concordant with the proportion of central memory phenotype T cells ($CD45RO^+$ $CD62L^+$or $CD62L^+$) (Brentjens, RJ et al. 2011; Louis, CU et al. 2011) in the infused products and the establishment of functional memory T cells ($CCR7^+$ $CD27^+$ $CD28^+$ $CD57^-$) *in vivo* (Kalos et al. 2011). In our Royal Adelaide hospital (RAH)-sponsored CARPETS phase I clinical trial of GD2-specific CAR T cells for the treatment of metastatic melanoma, CAR T cells in the infused product were mainly of effector memory phenotype and, when recovered from the peripheral blood of treated patients, were found to switch to a terminal effector phenotype as well as significantly express the PD1 exhaustion marker (Gargett et al. 2016). Consequently, our *in vitro* data suggest that the adoptively transferred CAR T cells might lose cytotoxic function and not proliferate in patients (Gargett et al. 2016). Hence, *ex vivo* manufacture of CAR T cells clearly demands an optimal method to increase the proportion of central memory-derived CAR T cells in the infused product for an effective treatment.

The efficacy of CAR T cell treatment is associated of the expansion of CAR T cells after infusion which may relate to the senescence stage of infused cells. T cells that express CD57, a marker of late stage differentiation, accumulate at a higher proportion in chronic immune activation, normal aging and cancer (Brenchley et al. 2003b; Iida et al. 2014; Kared et al. 2016). $CD57^+$ T cells lose the CCR7 marker, reduce the expression of CD27 and CD28 and re-express CD45RA (Palmer et al. 2005). Senescent T cells are susceptible to AICD and unable to replicate (Brenchley et al. 2003a). $CD8^+CD57^+$ T cells lack proliferative capability in response to T cell receptor activation even in the presence of IL-2, IL-7 and IL-15, but still can secrete inflammatory cytokines such as IFN-γ and TNF (Brenchley et al. 2003a; Le Priol et al. 2006a, 2006b). Therefore, CAR T cell products that have high proportion of senescent T cells may still preserve cytotoxic effect but unable to expand *in vivo*, giving rise to low treatment efficacy. In cancer context, the increase in frequency of senescent T cells may affect the quality of PBMCs for CAR T cell manufacturing, which may lead to the slow expansion of T cells during manufacturing process, and an increased proportion of senescent CAR T cells in final products. Interestingly, one paper has shown that the proportion of $CD8^+$ $CD57^+$ T cells (either $CD28^+$ or $CD28^-$) did not significantly increase following DNA damaging chemotherapy (Onyema et al. 2015). This leads to the hope that PBMCs exposed to anti-neoplastic drugs are able to efficiently generate CAR T cells with high cell yield which is a key factor of successful CAR T cell manufacturing.

1.5 Early manufacturing of CAR T cells following chemotherapy could be beneficial

As discussed above, cytotoxic chemotherapy is able to change the profile of a cancer patient's immune system. A transient reduction of all subtypes of circulating T cells has been demonstrated. However, as mentioned in part 1.3.1, treatment with selected antineoplastic drugs such as gemcitabine, 5-FU, paclitaxel, doxorubicin, temozolomide and cyclophosphamide were found to enhance T cell responses *in vitro* and in murine models, and in patients (Coleman et al. 2005b; Scurr et al. 2017; Turtle et al. 2009). More interesting, repopulating T cells were described as having an increased proportion of memory cells but a decreased proportion of terminal effector cells (Coleman et al. 2005b;

Fadul et al. 2011; Mackall, C et al. 1994). These findings suggest that, after cancer chemotherapy, circulating lymphocytes, which may be enriched in central memory $CD8^+$ T cells, could be an appropriate input material for CAR T cell production. However, the reduction in overall leukocyte and/or lymphocyte numbers may hamper the generation of sufficient numbers of CAR T cells for an effective therapeutic product.

CAR T cell therapies have shown remarkable success in B-cell malignancies. **Tisagenlecleucel (Kymriah™)** and **Axicabtagene ciloleucel (Yescarta™)** have been approved by the US FDA for refractory or relapsed cases of acute B-lymphoblastic leukaemia (B-ALL) and diffuse large B cell lymphoma (Jacobson, Farooq & Ghobadi 2019; LLS 2009). Interestingly, the process of manufacturing these CAR T cells routinely commences following the failure of second-line therapy (either systemic immunochemotherapy or salvage chemotherapy) (Jacobson, Farooq & Ghobadi 2019). A clinical report described successful application of anti-CD19 CAR T cells in an advanced follicular lymphoma patient who had received extensive systemic treatments, ranging from PACE (prednisone, doxorubicin, cyclophosphamide, and etoposide) to the anti–CTLA-4 monoclonal antibody, ipilimumab, and EPOCH-R (etoposide, prednisone, vincristine, cyclophosphamide, doxorubicin, and rituximab) one year before (Kochenderfer et al. 2010). Earlier, Kochenderfer had showed PBMCs from chronic lymphoblastic leukaemia and myeloma patients who underwent chemotherapy can generate highly functional CAR T cells *in vitro*, with a high proliferation rate and transduction efficiency (Kochenderfer et al. 2009). It is not clear from this report the time between the last treatment with chemotherapy drugs and PBMC collection for CAR T cell manufacturing, but some patients had evident lymphopenia before blood collection (Kochenderfer et al. 2009).

Successful outcomes from the two approved CAR T cell products for relapsed and/or refractory B-cell malignancies imply that the generation of functional CAR T cells with a good yield is feasible using PBMCs exposed to chemotherapy agents as starting populations. It is still a question whether this observation also holds true for other cancer patients treated with different chemotherapy regimens. In fact, recent clinical trials for CAR T cell therapy in brain tumours, mesothelin-expressing tumours (metastatic pancreatic and other types cancer), and ovarian cancers have been recruiting patients with recurrent or

progressive disease (Clinical trials NCT01454596, NCT01583686, NCT03799913). They must receive at least first-line standard treatment and have not received any cytotoxic drugs for 2-4 weeks before entering these trials (NCT01454596). In other trials, patients are eligible who were previously treated with two or more lines of standard treatments (NCT03799913, NCT01583686). Preclinical data from these trials showed the feasibility of manufacturing functional CAR T cells with high cytotoxicity *in vitro,* which indicates that previous chemotherapy can preserve T cell function and not harm the immune system (Morgan et al. 2012). Interestingly, one group of researchers indicated that T cell metabolic pathways are similar between pre-treatment T cells and those collected after the second cycle of chemotherapy (Rose 2018). These results was observed in a wide range of solid cancers (Rose 2018). These researchers also hypothesised that T cells collected at the sixth cycle of chemotherapy would have little potential of success as CAR T cell therapy (Rose 2018). However, they did not generate CAR T cells from these cells to check and compare functions of all products. From their perspective, it is presumed that blood cells collected before and within eight weeks after the first dose of chemotherapy drugs are healthy and able to generate functional CAR T cells.

Here, I investigate the ability of T cells derived from solid cancer patients receiving chemotherapy to result in the generation of satisfactory CAR T cell products. Adopting the techniques used for CAR T cell manufacturing in the CARPETS clinical trial, CAR T cells were produced from patient peripheral blood samples to compare the suitability of different starting immune populations for engineering transgenic T cells. A retroviral vector encoding a GD2-specific, third-generation CAR (Cell and Gene Therapy, Baylor College of Medicine, Houston, Texas), which is being used in the CARPETS study, was also used in this project for efficient transduction of autologous T cells during the manufacture of the CAR T cell products.

In this study, blood specimens from patients with primary glioblastoma, metastatic pancreatic cancer and metastatic colorectal cancer were collected at three time points: at baseline (pre-treatment), during their chemotherapy (on-treatment) and at relapse/progression. PBMCs from these blood specimens were isolated for CAR T cell production. $CD4^+$ and $CD8^+$ T cells bearing a GD2-CAR were then examined for their

function by testing cytokine production and tumour killing ability *in vitro*, and their phenotype for markers associated with memory and persistence. The detailed phenotype of the source PBMCs was also examined. Together, this information could be used to optimise the production of CAR T cells that have the potential to persist in a patient's circulation in the long term and retain effective cytotoxic activity against solid cancer cells.

1.6 Hypothesis and aims

1.6.1 Hypothesis

On-treatment blood specimens from solid cancer patients contain a high proportion of central memory T cells and thus represent the optimal starting population for manufacturing highly functional and effective CAR T cells**.**

1.6.2 Aims

In this study, my overall aim was to determine which time point of patient blood collection provides the optimal starting population for engineering CAR T cells.

Aim 1: To immunophenotype leukocyte populations isolated from peripheral blood of glioblastoma, colorectal cancer and pancreatic cancer patients at different time points: pre-treatment, on-treatment, and at relapse. The CD4/CD8 ratio, the individual proportions of T_{CM}, T_{EM} and T_{Naive} within PBMCs, and the proportion of exhausted T cells longitudinally within individuals, were analysed by multi-colour flow cytometry.

Aim 2: To manufacture CAR T cells from peripheral blood samples collected from cancer patients. Changes in T cell immunophenotype during CAR T cell generation were observed. Transduced CAR T cells were immunophenotyped using multi-colour flow cytometry on days 6 and after a cryopreservation- thawing cycle.

Aim 3: To assess the functional characteristics of CAR T cells *in vitro* by measuring their ability to proliferate, produce cytokines and directly kill tumour cells, and their susceptibility to AICD. The final CAR T cell product from each treatment time point was tested in a range of functional assays to compare their ability to survive and exert an anti-tumour effect.

Chapter 2

Materials and Methods

2.1 Overview

The three main approaches adopted in this study were multiparameter flow cytometry, CAR T cell manufacturing, and real-time cytotoxicity assay (xCELLigence). This chapter summarises the materials and methods used in this study, including the patient recruitment procedure.

2.2 Materials

The specific concentration (specific volume) of conjugated antibodies (**Table 2.1**) used for immunophenotyping T cell subsets and detecting exhausted markers.

Table 2.1: List of conjugated antibodies used for flow cytometry (included in the 12 colour panel for immunophenotyping T cell susbsets) and their suppliers and catalogue numbers

Antibody	Working concentration	Supplier	Catalogue number
CD3-BV510	1 µl/test	BD Horizon	564713
CD4-PE-Cy7	0.5 µl/test	BD Pharmingen	557852
CD8-APC-H7	0.5 µl/test	BD Pharmingen	560179
CD45RA-BUV395	0.5 µl/test	BD OptiBuild	740298
CCR7-AF647	5 µl/test	BD Pharmingen	560816
PD-1-BV786	3 µl/test	BD Horizon	563789
CD27-BB515	0.5 µl/test	BD Horizon	564642
CD57-BV421	0.5 µl/test	BD Horizon	563896
CD95-BUV737	0.5 µl/test	BD Horizon	564710
CD14-PerCP-Cy5.5	0.5 µl/test	BD Pharmingen	550787
CD19-PerCP-Cy5.5	0.5 µl/test	BD Pharmingen	561295
CD56-PerCP-Cy5.5	0.5 µl/test	BD Pharmingen	560842
Fixable Viability Stain 700	0.1 µl/test	BD Horizon	564997

Table 2.2 shows the list of other conjugated antibodies (small panel CD3/CD4/CD8/CD14), primary antibodies, secondary antibodies, and staining kit used for determining transduction efficiency of CAR T cell products, immunophenotyping main leukocyte subsets in fresh whole blood, and cytokine concentrations of activated CAR T cells.

Table 2.2: List of other primary and secondary antibodies, conjugated antibodies used for flow cytometry and their suppliers and catalogue numbers

Antibody	Working concentration	Supplier	Catalogue number
CD3-FITC	2 µg/ml (1µl/test)	Tonbo Biosciences	35-0036
CD4-PE	0.12 µg/ml (1µl/test)	Tonbo Biosciences	50-0048
CD8-PE-Cy7	0.125 µg/ml (0.5µl/test)	Tonbo Biosciences	60-0088
CD14-AF647	0.5µl/test	BD Biosciences	562690
7 colour immunophenotyping kit human	5µl/test	Miltenyi Biotec	130-098-456
MACSPlex Cytokine 12 kit	As suggested in the product data sheet	Miltenyi Biotec	130-099-169
1A7	200µg/ml	Home made	
Rat anti-mouse IgG1-PE	2µg/ml	BD Pharmingen	550083

Table 2.3 lists reagents required for flow staining.

Table 2.3: List of reagents used for flow cytometry and their suppliers and catalogue numbers

Antibody	Working concentration	Supplier	Catalogue number
Brilliant Stain Buffer	As recommended by manufacturer	BD Horizon	566385
Bovine Serum Albumin	0.5%	Sigma Aldrich	A7906
Normal mouse serum	1uL/tube	Life Technologies	10410
PBS	1X	Sigma Life Science	D8537
Sodium Azide	0.01%	Sigma Aldrich	S2002

Table 2.4 details the reagents and cytokines required for manufacturing of CAR T cells (transduction and expansion of T cells).

Table 2.4: List of reagents/ cytokines used for manufacturing CAR T cells and their suppliers and catalogue numbers

Reagents/Cytokines	Working concentration	Supplier	Catalogue number
CD4 MicroBeads	As suggested in data sheets	Miltenyi Biotec	130-045-101
CD8 MicroBeads	As suggested in data sheets	Miltenyi Biotec	130-045-201
T Cell TransAct™	As suggested in data sheets	Miltenyi Biotec	130-111-160
TexMACS™	1X	Miltenyi Biotec	130-097-196
Retronectin	7 µg/ml	Takara	T100B
IL-7	10 ng/ml	Miltenyi Biotec	130-095-362
IL-15	5 ng/ml	Miltenyi Biotec	130-095-764
Penicillin/Gentamycin	1X	Sigma	P4333
Virus	GD2-SFG.iCasp9.2A.14g2a.CD28.OX40.ζ	Baylor College of Medicine, Texas	RV1202

Reagents and chemical compounds required for isolating PBMCs, preparing FACs fix and other media for cell cryopreservation and culture are listed in **Table 2.5**

Table 2.5: List of reagents/ chemical compounds used for isolating of PBMCs and preparing buffers/media, and their suppliers and catalogue numbers

Reagents/Compounds	Supplier	Catalogue number
Lymphoprep	Stemcell technology	07801
Phosphate buffer saline (PBS)	Sigma	D8537
Fetal calf serum (FCS)	Thermo Fisher	SH30071.03
DMSO	Sigma	D2650
Advanced RPMI 1640	Gibco	12633-012
Glucose	Sigma	G7021

2.3 Methods

2.3.1 Study design and patient recruitment

2.3.1.1 Study design and overview

The aim of this study was to investigate how chemotherapy affects circulating immune cells and the feasibility of CAR T cell generation from patients undergoing chemotherapy. To do that, the phenotype of patients' PBMC and of their PBMC-derived CAR T cells was investigated. I compared immunophenotypes of PBMCs collected at different stages of treatment and determined the phenotype and function of CAR T cells manufactured from those PBMCs. The three different time-points included in this study are pre-treatment, on-treatment, and relapse/progression. Pre-treatment refers to samples collected prior to patients receiving the first dose of chemotherapy. On-treatment refers to samples collected after the first dose but before the second dose of chemotherapy.

Relapse/progression refers to samples collected once the patients are no longer responding to the current therapeutic regimen. Pre-treatment and on-treatment blood samples were collected just before chemo drugs were infused. The timeframe between pre-treatment and on-treatment sample collection is not restricted because some patients might have suffered from neutropenia or leukopenia which halts the second cycle of treatment. However, the on-treatment blood sample was always collected before the infusion of the second dose of chemotherapy. For the relapse/progression samples, blood was taken at any time since hospital admission. Approximately 80 ml of whole blood was collected at each time point. Blood samples were transferred to the Translational Oncology (TO) Laboratory, Centre for Cancer Biology, for PBMC isolation on the same day. Isolated PBMCs from each time point were cryopreserved in liquid nitrogen. When a full set of three samples (pre-treatment, on-treatment, relapse/progression) of one patient was obtained, CAR T cell manufacturing was started using the optimal protocol of my laboratory. All CAR T cell products were transferred to the SA Pathology Central Liquid Nitrogen Facility for cryopreservation prior to functional testing. CAR T cells from three time points were compared with each other. Results from a comparison of cytotoxicity, immune phenotype and viability between different CAR T cell groups were used to answer the study questions. Simultaneously, the immunophenotype of CAR T cells before and after activation, the change in immunophenotype from PBMCs to CAR T cells, and exhausted makers expressed on CAR T cells post activation were also investigated to understand the differentiation of CAR T cells during manufacturing and activation. CAR T cells from healthy PBMCs (obtained either from buffy coat (Red Cross Australia) or healthy donors at middle age) were also produced for as controls for the CAR T cell manufacturing process. This project was supported by Miltenyi Biotec as part of a research collaboration, and reagents for manufacturing and immunophenotyping were provided for free or at a discounted rate.

2.3.1.2 Patient recruitment and ethics

Subjects included in this study were confined to metastatic colorectal cancer, advanced pancreatic cancer, and primary glioblastoma. These represent some of the most malignant tumours, with the lowest overall survival rate and few choices for effective treatment. CAR T cell therapy, therefore, could be a valuable alternative therapeutic

modality for these types of cancers. I aimed to enrol as least five participants for each type of cancer (15 subjects in total). However, I knew that the number of patients able to stay until the end of the study and to donate all three blood specimens could be significantly less than the number of recruited ones. Therefore, I planned to engage as many eligible participants as possible in the beginning to ensure a complete dataset despite dropouts. The time frame for sample collection was estimated over 18 months, which covers disease-free survival time of these types of cancers, allowing for collection of the relapse/progression sample (AIHW 2019). Therefore, I stopped enrolling new patients for this project one year before the anticipated project completion date, which was the thesis submission date, to ensure that the last relapse sample could be collected with time for subsequent CAR T cell manufacturing, functional assays, and data analysis.

Eligibility criteria were male and female patients diagnosed with one of the three types of cancers mentioned in part 3.1.1. The study does not have an upper limit on the age range, but enrolled patients must be over 16 years old. Eligible patients were mainly identified from Royal Adelaide Hospital (RAH) cancer outpatient clinics' database and could be from any hospitals belonging to the Central Adelaide Local Health Network (CALHN; the approved study site). Patients must be willing to donate a minimum of 80 ml of whole blood each time for three times. They understood participating in this study was not a guarantee for better outcomes, blood donation was voluntary, and donors did not receive any reimbursements. Ethics approval for this Low/Negligible risk study was granted by CALHN HREC (HREC reference number: HREC/16/RAH/341; CALHN Reference number: R20160823) and by UniSA HREC (Protocol no. 201919).

Our clinical research fellows who are based at Oncology department in RAH were responsible for patient recruitment. They flagged potential patients who satisfied eligible criteria beforehand and met them in their first interview. These patients and their family (if needed) were consulted about the CAR T cell study and given an information hand-out which includes a consent form. Patients willing to donate blood for the study must give their consent before blood extraction which was organised for another time. Patients were able to withdraw from the study at any time as a result of their disease's stage or their willingness to participate.

Other information about patients such as URN, day of birth, total blood cell counts, and chemotherapeutic regimens were also recorded for study purposes. Personal information was kept confidentially in files that were password protected. Only study investigators were able to access these data.

2.3.2 Sample collection and PBMC isolation

2.3.2.1 Collecting blood from donors

If signed consent was given, blood sample collection would be organised with the help of clinical nurses from the day centre at the site treatment. Buffy coat was collected from Red Cross Australia. Healthy donors gave consents and had blood extraction at SA Pathology.

2.3.2.1.1 Preparing heparinised tubes

Heparinised tubes were prepared beforehand under aseptic conditions by the addition of 200 µl of heparin (Heparin Sodium 1mg/ml) per tube. Tubes containing heparin were stored at the hospital at room temperature, ready to use.

2.3.2.1.2 Blood collection

Two heparinised tubes were given to clinical nurses who took care of participants on the treatment day. Approximately 80 ml of blood was extracted just before chemotherapy drug infusion, and immediately transferred from the collection syringe to heparinised tubes. Blood tubes needed to be immediately inverted gently 4-5 times to make sure fresh blood is well mixed with heparin. These blood tubes were passed to the Translational Oncology lab for processing on the same day where possible. If samples were collected after hours, they were left at room temperature overnight with gentle mixing for processing the next day.

2.3.2.2 Isolation of PBMCs

PBMCs were isolated using Lymphoprep density gradient centrifugation. The following procedures were performed under sterile conditions in a class 2 biosafety cabinet. Eighty ml of fresh whole blood was diluted in 80 ml of PBS at room temperature

(1:1 dilution) and set aside. Fifteen ml of Lymphoprep was aliquoted per tube in a 50ml Falcon tube. Approximately 35 ml of fresh whole blood was layered over Lymphoprep by allowing the blood/buffer mixture to run slowly along the side of the tubes. Capped tubes were centrifuged for 20 minutes at 700g using 0 for acceleration and no brake. After centrifugation, a transfer pipette was used to collect the second layer which contained PBMCs into another 50 ml tube. Tubes containing PBMC were toped up with room temperature PBS to 45ml in total. Tubes were centrifuged at 270g for 5 mins. The slow speed centrifugation will keep platelets in suspension so that they can be discarded after that. After centrifugation, supernatant was discarded, and the wash repeated for a second time. Cell pellets after the second wash were resuspended in 10ml of PBS. Viable cell counts were performed using Trypan Blue and a haemocytometer. Cells were cryopreserved in fetal calf serum (FCS) with 10% DMSO at a concentration of 5 x 10^6 cells/ml/cryovial. Cryovials were put into a freezing chamber (Mr. Frosty), and then placed in a -80^{o}C freezer for 24 hours. Cryopreserved PBMCs were transferred to liquid nitrogen storage on the next day where possible, and always within a week of freezing.

2.3.3 Manufacturing of CAR T cells

PBMCs from patients and healthy donors were simultaneously activated and transduced for CAR T cell generation.

2.3.3.1 Preparation of buffer and media required for CAR T cell manufacturing

2.3.3.1.1 <u>Reconstitution of IL-7 and IL-15 in appropriate concentration</u>

Lyophilised recombinant human IL-7 and IL-15 were obtained from Miltenyi Biotec. Both were first reconstituted with 100 µl of deionised water and then with enough PBS containing 0.1% BSA to give a final concentration of 10 µg/ml and 5 µg/ml, respectively. IL-7 and IL-15 stocks were divided into 100 µl aliquots and stored at -20^{0}C.

2.3.3.1.2 <u>Supplemented TexMACs medium</u>

TexMACS medium (research grade) was obtained from Miltenyi Biotec. It was supplemented with Human IL-7 and Human IL-15 to a final working concentration of 10ng/ml and 5ng/ml respectively. Penicillin and Streptomycin antibiotics were added into

TexMACS at 1% concentration. Neither serum nor Glutamax was included in TexMACs medium. Supplemented TexMACS is a full and final medium for CAR T cell culture.

2.3.3.1.3 Cryopreserved medium for CAR T cells

Cryopreserved medium consisted of 90% FCS and 10% DMSO. It was freshly made on the day CAR T cells were harvested and kept cold at 4^0C.

2.3.3.2 Activation of bulk PBMCs (day -1, 0)

All steps were performed under sterile conditions in a class 2 biosafety cabinet, within an OGTR-certified PC2 laboratory.

2.3.3.2.1 Thawing and resting PBMC (day -1)

Cryopreserved PBMCs from all three time points of one patient and from one healthy donor were retrieved from the central of liquid nitrogen facility (CLNF) and rested in supplemented TexMACS medium overnight before starting CAR T cell manufacturing. Approximately 1 x 10^7 cells were required to generate 3 x 10^7 CAR T cells at the end of manufacturing. Cryopreserved PBMCs were thawed in a 37^oC water bath and then quickly diluted 1:10 in cold PBS with 5% FCS. Cell suspensions were centrifuged at 300g for 5 mins. Supernatants were discarded and cell pellets were resuspended in 10 ml of supplemented TexMACS medium for counting. Approximately 2x10^6 cells were placed in one well of a 24-well plate. Cells were rested in the 37^0C incubator for overnight.

2.3.3.2.2 Activation of bulk PBMCs (day 0)

Overnight rested PBMCs were activated using T cell TransAct which is polymeric nanomatrix conjugated to humanized CD3 and CD28 agonists. A 48-well plate was used for activation with an optimal surface density of 2 x10^6 PBMCs per well (1cm^2 surface area). A minimum of 1 x 10^7 PBMCs were required for stimulation. Cell suspensions were centrifuged at 300g for 5 minutes and supernatants discarded. Cell pellets were resuspended in 990 µl of supplemented TexMACS medium and 10 µl of T cell TransAct for every 2 x 10^6 PBMCs. Cells were aliquoted at 1 ml of stimulated cell suspension per well of a 48-well plate. Cells were incubated at 37^0C, 5% CO_2 for two days.

2.3.3.3 Virus transduction (day 2)

2.3.3.3.1 Coating plates with RetroNectin

Tissue culture 24 well plates were coated with RetroNectin on the day prior to transduction (day 1). A solution of 7µg/ml RetroNectin was made by diluting RetroNectin stock (1mg/ml) with sterile PBS. One ml of sterile RetroNectin solution was dispensed per well. RetroNectin coated plates were sealed with Parafilm and kept at 4^0C overnight. On the day of transduction, RetroNectin solution was removed and plates were briefly washed with PBS kept at room temperature. After discarding the wash solution, plates were ready for use.

2.3.3.3.2 Transduction

Virus supernatant was removed from -80^{o}C storage and slowly thawed at room temperature and kept on ice when it was half-thawed. Five hundred µl of virus supernatant was added to each well of the RetroNectin-coated plate. Plates were left at room temperature for 30 minutes, allowing virus to attach to the RetroNectin layer. Then virus supernatant was aspirated, and plates were re-coated with 500 µl of fresh virus supernatant for a second time, also at room temperature and for 30 minutes. In the meantime, activated T cells were collected and counted. A suspension of 1.2 x 10^6 cells/ml was prepared in supplemented TexMACs medium and kept inside the class 2 biosafety cabinet. A mixture of activated T cells and virus was made by diluting 500 µl of cell suspension into 1.5 ml of virus supernatant. After discarding the second virus supernatant coating, 2 ml of T cells and virus mixture were dispensed into each well. Plates were then centrifuged at 1000g for 5 minutes before putting in the 37^0C incubator, facilitating the co-localisation of virus and T cells.

2.3.3.4 Expansion and cryo-preservation of CAR T cell products (day 4-10)

Transduced cells were split one in two every two days and re-cultured in fresh cytokine supplemented TexMACs medium. Cells were collected, washed, and resuspended in new medium. The number of cells was recorded every two days for expansion results. Viability of CAR T cell product was determined by Trypan Blue count. On day 10, all cells

were collected and resuspended in cryopreserved media (part 3.3.1.4). Cells were dispensed at $1x10^7$ cells per cryovial and quickly transferred in a freezing chamber to a -80^0C freezer. Cryopreserved CAR T cell products were transferred to the CLNF on dry ice and stored in liquid nitrogen until needed.

2.3.4 CAR T cell activation

2.3.4.1 Coating sterile 96 well cell culture plates with antibodies

Pure anti-human CD3 antibody and pure anti-human CD28 antibody (both at 100 µg/ml; Miltenyi) were diluted with sterile distilled water to make a 1 µg/ml solution of each antibody. Fifty µl of antibody solution were added to each well of a flat bottom 96 well plate. Likewise, 1A7 antibody (stock 200 µg/ml) was diluted with distilled water to a concentration of 200 ng/ml (1:1000) and 50 µl of antibody solution was dispensed into each well of the 96-well plate. The plate was tightly covered by Parafilm and kept at 4^0C overnight. Just before adding cells (on the next day), the antibody solution was removed, and wells rinsed with 100 µl of PBS*.*

2.3.4.2 Activation of CAR T cells

Single cell suspensions were prepared under sterile conditions for activation. Each CAR T cell product was thawed in the 37^0C water bath for less than 2 minutes then diluted in 9 ml of cold 1xPBS with 10% FCS. Cell suspensions were centrifuged at 300g for 5 minutes, and the supernatants discarded. Cell pellets were resuspended at 1 x 10^6 cells/ml in TexMACs medium. CAR T cells were activated using either anti-CD28/anit-CD3 or anti-CAR (1A7) coated plate at a density of 2 $x10^5$ cells/well. The plate was placed in a humidified 37^0C, 5% CO_2 incubator for 3 days. After activation cells were harvested to check viability and expression of exhaustion markers by flow cytometry. Supernatants were collected into a fresh 96 well plate and frozen at -20^0C for later cytokine detection.

2.3.5 Flow Cytometry

2.3.5.1 Preparation of buffers and solutions for cell staining

2.3.5.1.1 <u>FACS buffer</u>

FACS buffer was used for cell and antibody dilution, surface marker staining, and washing. It contained 1xPBS and 0.5% BSA to prevent non-specific bindings of antibodies. 0.01% NaAzide was also added into the buffer as preservative. The FACS buffer was kept at 4^0C for preservation.

The recipe to make 1000ml of FACS buffer:

1. 1000ml of 1xPBS
2. 5g of BSA
3. 1ml of 10% NaAzide solution

2.3.5.1.2 FACS fix

The homemade FACS fix was used to fix cells after extracellular staining for preservation.

The recipe to make 1000ml of FACS fix:

1. 20g of Glucose
2. 2ml of 10% NaAzide
3. 40ml of formalin 10% (Perrrigo Australia)
4. 1xPBS to 1 L

2.3.5.2 Preparation of full stained samples and controls

2.3.5.2.1 Staining fresh whole blood with 7 colour immunophenotyping kit from Miltenyi

Fifty µl of fresh whole blood was used to evaluate the main leukocyte populations. Firstly, 5 µl of pre-prepared cocktail of antibodies from the kit was added to the staining tube. Then, 50 µl of fresh and well-mixed anticoagulated whole blood was pipetted onto the antibodies cocktail. The tube was capped and gently vortexed to mix antibody and blood. Tubes were incubated in the dark for 15 minutes at room temperature. After incubation, 1 ml of 1X red cell blood lysis solution which included in the kit (Miltenyi) was added, and the tube was vortexed for 15 seconds and then incubated for 15 minutes in the dark at room temperature, allowing red blood cells to be lysed. Stained cells were immediately analysed by BD LSRFortessa (BD/ model 647800L6).

2.3.5.2.2 *Phenotyping thawed PBMCs using the 12-colour panel*

Cryopreserved PBMCs were thawed in the 37^0C water bath for less than 2 minutes then diluted in 9 ml of cold FACS buffer for washing. Cell suspensions were centrifuged at 300g for 5 minutes and supernatants discarded. Cell pellets were then resuspended in 1ml of FACS buffer for counting. Additional FACS buffer was added into each tube to dilute cell suspensions to 2 x 10^7 cells/ml. About 2 x 10^6 cells (100 µl) per sample (pre-treatment, on-treatment, and relapse/progression) were taken for staining (in duplicate) using the designed 12 colour panel (**Table S1**). Three fluorescence minus one (FMO) control tubes (FMO BUV395, FMO AF647, and FMO BV786) and 12 single stained tubes were also included for compensation and gating. Cells from patient samples were used for compensation staining. Fifty µl of cells from each group were dispensed into duplicate FACS tubes and Fc receptors were blocked by incubating with 5 µl of Fc block reagent (Invitrogen) at 4^0C for 5 minutes. Without washing, cells were stained with 5 µl of AF647 conjugated anti-CCR7 antibody in the dark at room temperature for 15 minutes, as this antibody requires a longer incubation time than others. Subsequently, a cocktail of the remaining 11 antibodies (9 fluorochromes as 3 antibodies-anti-CD14/CD19/CD56- are conjugated with PerCP-Cy5.5): BUV395-CD45RA, BV737-CD95, BV510-CD3, BV421-CD57, BV786-PD-1, BB515-CD27, APC-H7-CD8, PE-Cy7-CD4, PerCP-Cy5.5-CD14, PerCP-Cy5.5-CD19, PerCP-Cy5.5-CD56 together with the viability dye FVD-AF700 prepared in Brilliant Stain Buffer (BSB) (BD) was added to tubes and incubated for another 15 minutes. After that, cells were washed with 1ml of FACS buffer and cell pellets were resuspended in 250 µl of FACS fix. Stained PBMCs were covered using foil paper and stored in the fridge for flow cytometry analysis on the following day.

2.3.5.2.3 *CAR detection on transduced T cells*

Approximately 1 x 10^5 transduced T cells were taken from culture wells for detection of transduction efficiency at day 6. T cells were washed in FACS buffer and incubated in 5 µl of Fc block for 10 minutes at 4^0C. Each transduced cell sample was analysed in duplicate, and one tube of non-transduced T cells was included as a negative control. CAR structure was stained with 1A7 primary antibody at 4^0C for 20 minutes and

washed once. Cells were resuspended in FACS buffer and stained with a secondary antibody conjugated with a PE fluorochrome (BD) also at 4^0C for 20 minutes. After washing, free binding sites on the secondary antibody were blocked by incubation with 5µl of normal mouse serum for 5 minutes at room temperature and then stained with a mixture of 3 antibodies: FITC-labelled CD3 (Tonbo), PE-Cy7-labelled CD8 (Tonbo) and Alexa Fluor 647-labelled CD14 (BD Biosciences) for 15 minutes at room temperature. For this small panel, samples were acquired on a BD Accuri™ C6 flow cytometer.

2.3.5.2.4 *Flow cytometric analysis of thawed CAR T cell products and activated CAR T cells*

CAR T cell products were thawed in the 37^0C water bath for less than 2 minutes then diluted in 9 ml of FACs buffer. Activated CAR T cells were collected from the 96-well plate (part 2.3.4.2). Cell suspensions were centrifuged at 300 g for 5 minutes and supernatants discarded. Cell pellets were resuspended in enough FACS buffer to achieve 1 x 10^7 cells/ml. Approximately 4 x 10^5 cells from each CAR T cell sample were taken for staining in duplicate tubes (2 x 10^5 cells/staining tube) using the 12-colour panel together with detection of the CAR using the 1A7 antibody. CAR structures were first stained with 1A7 primary antibody at 4^0C for 20 minutes and followed by a secondary antibody conjugated with a PE fluorochrome also at 4^0C for 20 minutes. Washing was done between these two steps and after staining with the secondary antibody. Normal mouse serum was used to block the free site of the secondary antibody. Following the blocking, cells were stained with conjugated CCR7 antibody first and then with a cocktail of the remaining antibodies plus the viability dye diluted in BSB, as described in part 3.4.3.3. After the last wash, cells were also fixed using FACS fix and stored in the fridge until flow cytometric analysis the following day. FMO control tubes (FMO-BUV395, FMO-AF647, FMO-BV786) and IgG control for CAR staining were also included for each condition.

2.3.5.2.5 *Cytokine profile analysis using the MACSPlex Cytokine Kit*

Frozen supernatants were completely thawed at room temperature. Supernatant plates were centrifuged at 1000g for 5 minutes to remove particles. Five µl of supernatant was transferred from each sample to a new 96 well plate, then 40 µl of supplied MACSPlex

Buffer was added to each well to achieve a 1:9 dilution. Fifty µl of standard samples, prepared according to the manufacturer's instructions, were also added to the staining plate. Twenty µl of Capture Beads were added to each well and incubated in the dark for 2 hours on an orbital shaker. After incubation, the plate was washed: 150 µl of MACSPlex buffer was added to each well and the plate was centrifuged at 1000 g for 5 minutes, and then 150 µl of supernatant was aspirated from each well using a multichannel pipette and discarded. Twenty µl of Detection Reagent was added to each well and incubated for 1 hour, protected from light, and on an orbital shaker. Samples were washed as above and contents of each well resuspended and transferred to a FACS tube, and then analysed using the Fortessa flow cytometer.

2.3.5.3 Flow cytometry data analysis

FlowJo (BD) version 10.6.1 software was used for flow cytometry analysis.

2.3.6 Real-time cytotoxicity assay

2.3.6.1 Preparation of required media and cells for cytotoxicity assays

2.3.6.1.1 <u>LAN-1 culture media</u>

LAN-1 media was prepared as a 1:1 mix of advance RPMI 1640 and Ham's F12 (Gibco), supplemented with 20% FCS, 1% Glutamax and 1% P/S. This media was used for the culture of thawed LAN-1 cells which is sensitive. The media for continuous passages can be supplemented with only 10% FCS.

2.3.6.1.2 <u>Preparation of LAN-1 cells as target cells</u>

LAN-1 is a human neuroblastoma cell line which expresses high level of GD2 (Hettmer, Ladisch & Kaucic 2005) . These cells were used as target cells in assays to test the cytotoxic activity of CAR-T cells. They have a tear-drop shape and grow as semi-adherent cell aggregates. LAN-1 cells were thawed and allowed to slowly grow in their "favourite" media (part 2.3.6.1.1) one week before the start of the cytotoxicity assay. The first seeding density was 8 x 10^5 live cells per a T-75 flask (1 x 10^4 cells/cm^2) and cells were gently

detached by TrypLE and split at a 1:15 or 1:20 ratio for subsequent passages after cells achieved 90% confluency.

2.3.6.1.3 Preparation of CAR T cells as effector cells

A complete set of CAR T cell products (pre-treatment, on-treatment, relapse/progression) from each patient was analysed together using the xCELLIgence system to measure and compare cytotoxic activity. CAR T cells were thawed, washed and resuspended in advance RPMI 1640 supplemented with IL-7/IL-15 (10ng/ml and 5 ng/ml) at a concentration of 2 x 10^6 cells/ml. CAR T cells were rested in a 37^0C incubator overnight.

2.3.6.2 Setting up xCELLigence assays

2.3.6.2.1 Software and equipment

Cytotoxicity assays were conducted using xCELLigence real time cell analysis (RTCA) instrument to measure the kinetic of target cell's responses (Cerignoli et al. 2018). The xCELLigence® RTCA DP instrument include the Real-time Cell Analysis (RTCA) software run from a laptop which is the control unit of a DP instrument (plate station) (ACEA Biosciences). The DP instrument was housed in a 37^oC incubator with 5% CO_2. The principle of this assays is measuring the impedance through gold electrodes embbed at the bottom of an E-plate. Adherent target cells act as insulators and impede the alternating flow (considered as a sweep in this assay) of electric current between electrodes. The impedance value is called cell index which is a unitless parameter and increase when cell number increases. In contrast, non-adherent effector cells do not affect the impedance signals, but their cytotoxic activity can reduce target cell number which decreases impedance value. The continuous measuring impedance value allows the generation of a real time killing curve of effector cells.

2.3.6.2.2 Plate layout

One PET E-Plate 16 (16 wells) (ACEA Biosciences) was used for all three CAR T cell products (pre-treatment, on-treatment, relapse/progression) from one patient. Each group of CAR T cells was tested for their killing effect at two different effector:target (E:T) cell

ratios: 5:1 and 2:1. Each condition was examined in duplicate. Non-transduced T cells and no effector cell condition (media only) were utilised as negative controls for this assay.

The layout for each E-Plate (PBMC or sorted T cell) was designed as below

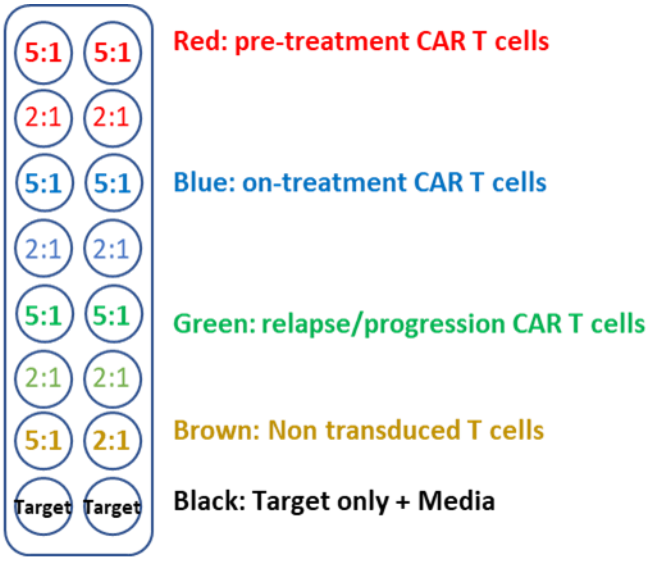


Figure 2.1: **The layout of an E-plate used in xCELLigence assay**. Effector cell: target cell ratio was assigned (as shown) for each well and each condition was run in duplicate. Target cells were GD-2 expressed LAN-1 cells. Media was LAN-1 media

2.3.6.2.3 *xCelligence analysis schedule*

Three analysis steps were run for the xCELLigence cytotoxicity assay. Step 1 was used for background measurement and was set for 3 sweeps with 1 min interval between sweeps. Step 2 was set to 15 mins interval per sweep, to determine the baseline cell-index of the LAN-1 target tumour cell line. Step 3 was also set at 15 min interval between sweeps and was initiated after adding CAR T cells to the plate.

2.3.6.3 *Real time xCELLigence cytotoxicity assay*

2.3.6.3.1 *Day 1*

Fifty µl of pre-warmed LAN-1 cell media was transferred to each well of the E-plates, avoiding touching pipette tips on the surface of wells. E-Plates were placed into the RTCA instrument within the 37^0C incubator and Step 1 of the experiment was initiated for

background measurement. After that, E-Plates were left in the 37^0C incubator for 30 minutes for pH buffering.

Meanwhile, LAN-1 cells were harvested from their culture flask. The culture media was fully aspirated followed by a brief wash with PBS. All PBS from the wash step was collected into a 50 ml tube because LAN-1 are semi-adherent cells and they are easy to detach with just PBS. Then, about 1 ml of pre-warmed TrypLE was transferred to the flask (T-75) and the flask inverted to allow TrypLE to cover the whole surface of cell layer. Subsequently, cells were quickly detached with additional taps on the side of the flask. About 9 ml of full media was added to the flask to stop trypsin activity and cells were transferred to the 50 ml Falcon tube which also contained cells from the PBS wash. Cells were centrifuged at 300g for 5 mins and supernatant discarded. The cell pellet was resuspended in 10 ml of LAN-1 media and cells counted. Cells were diluted to 1 x 10^5 cells/ml and 100 µl was then added to each well of the E-Plate 16 PET. E-Plates were then returned to the RTCA instrument. After 5 mins, the second step was initiated with scanning at 15-minute intervals. This step required overnight scanning (at least 20 hours).

2.3.6.3.2 *Day 2*

After 20-24 hours, cell index should achieve 0.5 -1 which indicated target cells were healthy and attached on the well surface. A cell index lower than this suggests poor quality of target cells, and the experiment must be discarded.

CAR T cell products were collected after overnight resting. Cells were washed and resuspended in LAN-1 media. For the 5:1 E:T ratio, I needed 5 x 10^4 effector cells/50 µl/well while the 2:1 ratio required 2 x 10^4 T cells/50 µl/well. These dilutions were prepared in LAN-1 medium.

E-Plates were carefully taken out of the RTCA instrument to the class 2 biosafety cabinet and 50 µl of appropriately diluted CAR-T cells were carefully added to the corresponding E-Plate wells, avoiding disrupting target cell layer which could cause inaccuracies in the cell index. E-Plates were returned to the RTCA instrument and Step 3 of the experiment was initiated, monitoring every 15 mins for at least 72 hours (288 sweeps), although in some instances the experiment was left for longer (up to 120 hours).

2.3.6.4 Calculation of percent cytotoxicity values

Raw and normalised cell index data and the experiment's information were exported to Excel spreadsheets. Normalised cell index data are manipulated data represented as proportions of cell index set as 1.0 by the software at the time effector cell added. The cytotoxicity effect was calculated using the following formula

$$\% \text{ Cytotoxicity} = \left(1 - \frac{\boldsymbol{CI}ti/\boldsymbol{CI}nml_ti}{\boldsymbol{CI}\,TargetOnly-ti/\boldsymbol{CI}\,TargetOnly-nml_ti}\right) \times 100$$

With:

CI_{ti} *:* The average of cell index between replicate wells at the time *ti*

$CI_{nml\text{-}ti}$*:* The average of cell index between replicate wells at normalisation time

$CI_{TargetOnly\text{-}ti}$: The average cell index between replicate target only well at the time *ti*

$CI_{TagrgetOnly\text{-}nml\text{-}ti}$*:* The average cell index between replicate target only well at normalisation time (Cerignoli et al. 2018)

2.3.7 Statistical analysis

Data analysis was performed with GraphPad Prism 7 (GraphPad Software, La Jolla, CA). An ANOVA one-way analysis was used for analysing the difference in the mean of three groups of samples (pre-treatment, on-treatment, relapse/progression). ANOVA two-way test was used to analyse the difference in the mean of three groups of samples which were treated in distinct conditions. P values < 0.05 were considered statistically significant. Summary data on plots represent mean +/- SD.

Table S1: 12 colour flow cytometry panel

CD3	BV510
CD4	PE-Cy7
CD8	APC-H7
CD45RA	BUV395
CCR7	AF647
PD-1	BV786
CD27	BB515
CD57	BV421
CD95	BUV737
CD14	PerCP-Cy5.5
CD19	PerCP-Cy5.5
CD56	PerCP-Cy5.5
CAR	PE
Fixable Viability Stain 700	FVS700

Chapter 3

Effects of chemotherapy on the cellular compartment of the immune system

3.1 Overview

This chapter describes the clinico-epidemiological characteristics of the patient cohort and compares the leukocyte populations and detailed lymphocyte subsets present in peripheral blood taken from patients at three different time points: (i) before starting the first cycle of chemotherapy (pre-treatment), (ii) before the second cycle of chemotherapy (on-treatment) and (iii) when admitted to hospital due to relapse or disease progression. Flow cytometry with two different antibody panels was used to analyse populations of interest in PBMCs.

3.2 Introduction

Chemotherapeutic drugs widely used in cancers as standard treatments have been assessed for their roles in modulating the immune system (Eriksson et al. 2016). Antineoplastic drugs that have been studied in this context include gemcitabine, capecitabine, 5-FU, and oxaliplatin. These drugs include alkylating agents (oxaliplatin) and antimetabolites (gemcitabine, capecitabine, 5-FU) which are mainly used as first line

chemotherapeutic regimens in colorectal and pancreatic cancers (*ESMO clinical practice guidelines news*). Numerous articles have reported the positive immunomodulatory effects of these regimens in cancers, especially following the first cycle of treatment (Plate et al. 2005). They give rise to an increase in the proportion of young cells and sustained depletion of suppressive cells (Galluzzi et al. 2015; Plate et al. 2005; Verma et al. 2016). Changes of the immune system in the early phase post chemotherapy may facilitate subsequent immunotherapies.

The changes in of leukocyte compartments post chemotherapy are correlated with the estimation of overall survival rate in cancer (Walsh et al. 2005). Neutrophil granulocytes are sensitive to cytotoxic drugs, as manifested by a significant deficiency in peripheral cell numbers in patients undergoing chemotherapy (ACS 2016). Neutropenia (absolute neutrophil count of less than 1500/ µl) is a common side effect of chemotherapy in cancer (ACS 2016). Although the decrease in the number of neutrophils affects the body's ability to fight infections, retrospective analyses have reported that the depletion of systemic neutrophils in response to chemotherapy is correlated with improved overall survival (Walsh et al. 2005). The neutrophil: lymphocyte ratio (NLR) at baseline (pre-treatment) or post chemotherapy (pre-cycle 2) is used as a prognostic biomarker of therapeutic outcomes in a variety of solid cancers (Giakoustidis et al. 2018; Luo et al. 2015). Results from these studies showed that NLR >3 prior to chemotherapy and increased NLR post chemotherapy are significantly corelated with distant metastasis and a decrease in overall survival rate of cancer patients. On the other hand, a post chemotherapy decrease in NLR may result if chemotherapy depletes myeloid-derived suppressor cells while the absolute lymphocyte count is preserved, and may reflect enhanced anti-cancer effects of immune system function (Eriksson et al. 2016; Koinis et al. 2016; Vincent et al. 2010). The question of whether or not the NLR ratio can predict the capability of lymphocytes, especially engineered T lymphocytes to efficiently destroy cancer cells, has not been reviewed. This issue will therefore be discussed later in the thesis.

T cells are important for the adaptive immune system and adoptive cell therapy in the context of cancer. Re-populated proportions of $CD4^+$ and $CD8^+$ T lymphocytes and other subsets such as $T_{Naïve}$, T_{CM}, T_{EM}, T_{EMRA}, terminally differentiated T cells ($CD57^+$) have been

deeply investigated to understand how chemotherapy affects their frequencies and functions. The $CD4^+$ and $CD8^+$ T cell compartments in peripheral blood are depleted during anti-cancer chemotherapy treatment but have distinct recovery patterns post chemotherapy, leading to a significant change in T cell subset ratio in repopulated T cell pools (Coleman et al. 2005b; Plate et al. 2005; Verma et al. 2016). Numerous articles have reported that gemcitabine alone or in combination with 5-FU decreases circulating T cell number but not their relative proportion after the first cycle of treatment (Plate et al. 2005). Most studies found that the $CD4^+$ T cell proportion is significantly decreased after initiating chemotherapeutic doses and does not return to the pre-treatment level (Plate et al. 2005; Verma et al. 2016). In contrast, statistical analyses of data from various studies revealed that the proportion of $CD8^+$ T cells recovers to baseline following the initial decline in the first week of cytotoxic treatment (Plate et al. 2005). Other subsets of T cells such as terminally differentiated ($CD57^+$) and memory ($CD45RO^+$) lymphocytes were significantly reduced in their proportions in circulation after treatment with antimetabolites (Plate et al. 2005). Remarkably, pyrimidine antagonists (gemcitabine, capecitabine, 5-florouracil) and taxane (paclitaxel) have been shown to increase T cell activation manifested by increasing levels of IL-6, IL-2 and IFN-γ 4-7 weeks following the initial dose (Middleton et al. 2016; Plate et al. 2005). From these studies, the first cycle of antineoplastic treatment chemotherapy has been revealed to facilitate cell-mediated cytotoxicity by increasing immunological functions of T cells, especially cytotoxic lymphocytes.

Here, I have analysed blood specimens collected from patients diagnosed with three different types of solid cancers to investigate the proportion of repopulated immune populations following chemotherapy at an early time point (post treatment 28-56 days) and a late time point (relapse or progression of the disease). This comparison provides information about the differences in immunophenotypes between PBMCs collected at different time points in our samples, which were subsequently used for CAR T cell manufacturing (see Chapter 4).

3.3 Results

3.3.1 Patient characteristics

From 18 May 2017 to 4 June 2018, 16 patients (8 females and 8 males) at the Royal Adelaide Hospital, who were diagnosed with metastatic colorectal cancer (n=10), advanced pancreatic cancer (n=4) and primary glioblastoma (n=2), consented to this study. No participant received anti-cancer treatment within one year before entering this study. Patients' performance status scores were based on the Eastern Cooperative Oncology Group (ECOG) scale and were grade 0-2. Patients consented to have blood collected at three time points: before starting chemotherapy, before the second cycle of chemotherapy, and at relapse or disease progression (Oken M 1982). However, not all participants completed the study and had all three blood samples collected. Five participants (31%) were unable to donate blood at the second time point because the location at which treatment was given was changed (n=1), they entered palliative care (n=3), or the patient's family declined (n=1). Of the remaining 11 patients, eight patients (72%) donated blood for the third time point (relapse/progression). The other three patients either died or entered palliative care after the second blood donation. Of note, patient #05 with pancreatic cancer died after the second blood donation, but I included pre-treatment and on-treatment samples from this patient into the study because of the low number of pancreatic cancer patients recruited. Thus, the final patient cohort used for further analyses included nine participants.

Characteristics of the nine patients are shown in **Table 3.1**. There was only one patient with glioblastoma (patient #09) and two patients with advanced pancreatic adenocarcinoma (patients #04 and #05). Patient #05 did not have a relapse/progression sample collected, as mentioned above. The remaining six patients were diagnosed with metastatic colorectal cancer. The median age at diagnosis was 68 years (range 31 to 88 years). Eight out of nine patients (88 %) were older than 50 years of age at the time of diagnosis, and one (patient #01) was 31 years of age.

Patient #09 (glioblastoma) had undergone surgery to remove the brain tumour and received radiation therapy combined with temozolomide. Both patients diagnosed with

pancreatic cancer were treated with gemcitabine and nab-paclitaxel as first-line chemotherapy. Three out of six colorectal cancer patients (patients #10, #12, and #16) were given the combination of capecitabine, oxaliplatin and bevacizumab. Two other patients (patients #01 and #13) in the colorectal cancer group received only capecitabine and bevacizumab. Patient #07 was the only participant treated with 5-FU in combination with bevacizumab. The average time interval between on-treatment and relapse/progression blood donation was 25 weeks (range from 8 to 67 weeks).

Table 3.1 Epidemiologico-clinical features of patients included in the study

	Number of patients
n	9
Mean age	68 (32-89)
Male: female	4:5
Diagnosis	
Metastatic colorectal cancer	6
Glioblastoma	1
Advanced pancreatic cancer	2
First line of treatment	
Capecitabine + Oxaliplatin + Bevacizumab	3
Capecitabine + Bevacizumab	2
Gemcitabine + Nab Paclitaxel	2
5-FU + Bevacizumab	1
Temozolomide + Chemoradiation	1
Interval of blood collection	
Pre-treatment – On-treatment	
3 weeks	2
5 weeks	5
8 weeks	2
On-treatment –Relapse/Progression	
< 8 weeks	4
> 40 weeks	4

3.3.2 Changes in the percentage and absolute number of leukocyte subsets post chemotherapy

Differential white blood cell counts (total leukocytes, neutrophils, eosinophils, lymphocytes, and monocytes) were performed by SA Pathology using routine diagnostic methods and were also collected and retrospectively analysed (**Figure 3.1**). Six leukocyte populations (neutrophils, eosinophils, monocytes, B cells, T cells, and NK cells) and two T cell subpopulations ($CD8^+$ and $CD4^+$) were detected and quantified using 7 colour flow cytometry. The gating strategy to differentiate these populations is shown in **Figure 3.2**.

The proportions of six leukocyte populations (neutrophils, eosinophils, monocytes, NK cells, B cells, T cells) analysed by flow cytometry are shown for each patient at each time point in **Figure 3.3**. Neutrophils are fragile and have a short lifespan, and as a result this population needs to be analysed immediately after collection. Therefore, I used fresh whole blood as the material input for leukocyte staining. Red blood cells were lysed using lysis solution before proceeding to flow cytometric analysis. As a result of this staining procedure, stained samples needed to be run without fixation for later analysis. Five blood specimens (either pre-treatment, on-treatment or relapse/progression) taken from patients #01, #07 and #13 were not included in this analysis because the flow cytometer was not available when these samples were collected.

Flow cytometry data revealed that the mean percentages of neutrophils, eosinophils, monocytes, and NK cells were not significantly different between the three time points (pre-treatment, on-treatment, and relapse/progression). Similarly, the mean absolute numbers of these cell types, as determined by diagnostic laboratory testing by SA Pathology, were not significantly altered between time points (**Figure 3.1** and **Figure 3.3**). In contrast, flow cytometry data revealed that the proportions of B lymphocytes were affected by chemotherapy (**Figure 3.3**). The mean percentage of B lymphocytes significantly reduced at the relapse/progression time point compared to pre-treatment time point (mean = 2.1; SD = 1.5 *vs* mean = 3.6; SD = 1.7, respectively) (**Figure 3.3**). The reduction in B cell frequency was observed for all patients. This result was similar to findings from a previous study (Verma et al. 2016).

Results from our patient cohort did not show a statistically significant difference in the mean proportion of T cells among the three time points, although T cell frequencies from different time points within many individuals were highly variable. Fifty percent of patients (n=4) showed a significant decrease (by more than 40%) in the percentage of T cells at the second time point compared to baseline (**Figure 3.3a**). The other four patients had higher proportions of T cells on-treatment (patient #09 and #10) or showed no change (patients #12 and #13). Absolute lymphocyte count values, which do not differentiate B and T cells, showed no significant change in the mean number of lymphocytes during treatment (**Figure 3.1**). Lymphopenia (<1000 cells/μL) was observed in samples #05 pre-treatment and on-treatment (pancreatic cancer) and in sample #09 at relapse (glioblastoma).

Similar to the bulk T cells, analysis of $CD8^+$ and $CD4^+$ T cell subsets also revealed no significant alteration in response to antineoplastic drugs. The proportions of $CD8^+$ T cells were slightly increased or decreased in post-treatment samples, ranging from 17% to 37% (mean = 26%; SD = 5.7) of T cells, compared to pre-treatment. No difference in the mean percentage of this subset was observed between times of treatment. $CD4^+$ T cells, which constituted 45% to 73% (mean = 64%; SD = 8.5) of T lymphocytes, showed more fluctuation in their proportions after treatment, but the mean percentages of $CD4^+$ T cells were not significantly different between pre-treatment, on-treatment, and relapse/progression time points. Interestingly, most CD4/CD8 ratios at all treatment phases were higher than 2, which is similar to that of healthy donors (Bofill et al. 1992). This result may indicate homeostatic preservation of CD4 and CD8 proportions in order to maintain immune system function after chemotherapy. **Figure 3.3b** displays the mean fraction of $CD4^+$ and $CD8^+$ T cells in pie chart format, showing that $CD4^+$ T cells made up ~70 % of the T cell population and $CD8^+$ T cells accounted for ~30% of T lymphocytes at all time points.

Neutrophil-lymphocyte ratio (NLR) is an inflammation-based score, which conveys prognostic information for patients diagnosed with cancer (Coussens & Werb 2002; Motomura et al. 2013), such that high NLR indicates worse overall survival and progression free survival (Giakoustidis et al. 2018; Lee et al. 2018; Luo et al. 2015). In this study, NLRs

were calculated and matched with outcomes of patients. Four patients (patients #01, #05, #09 and #12) had high NLR values at baseline (5, 6, 4 and 4, respectively). The NLR of patient #05 increased from 6 to 8 after the first cycle of treatment suggesting a worsened prognosis. This patient entered palliative care soon after the second blood donation, resulting in no blood sample being collected at the relapse/progression time point. Patient #12 had a drop in NLR at relapse/progression and responded well to second-line chemotherapy. NLR of patients #01 and #09 remained high after treatment suggesting ultimately poor outcomes. Patient #09 was lost to follow up after the third sample collected because of the changed location of treatment. However, patient #01 has shown a good response to second-line chemotherapy until data collection cut-off date. Notably, patient #07 had low NLR at baseline (2.3) but this increased post chemotherapy (4.7). Records showed this patient entered palliative care after I obtained the relapse/progression sample. Thus, results from our patient cohort support previous findings that a high NLR is a negative prognostic factor (Lee et al. 2018).

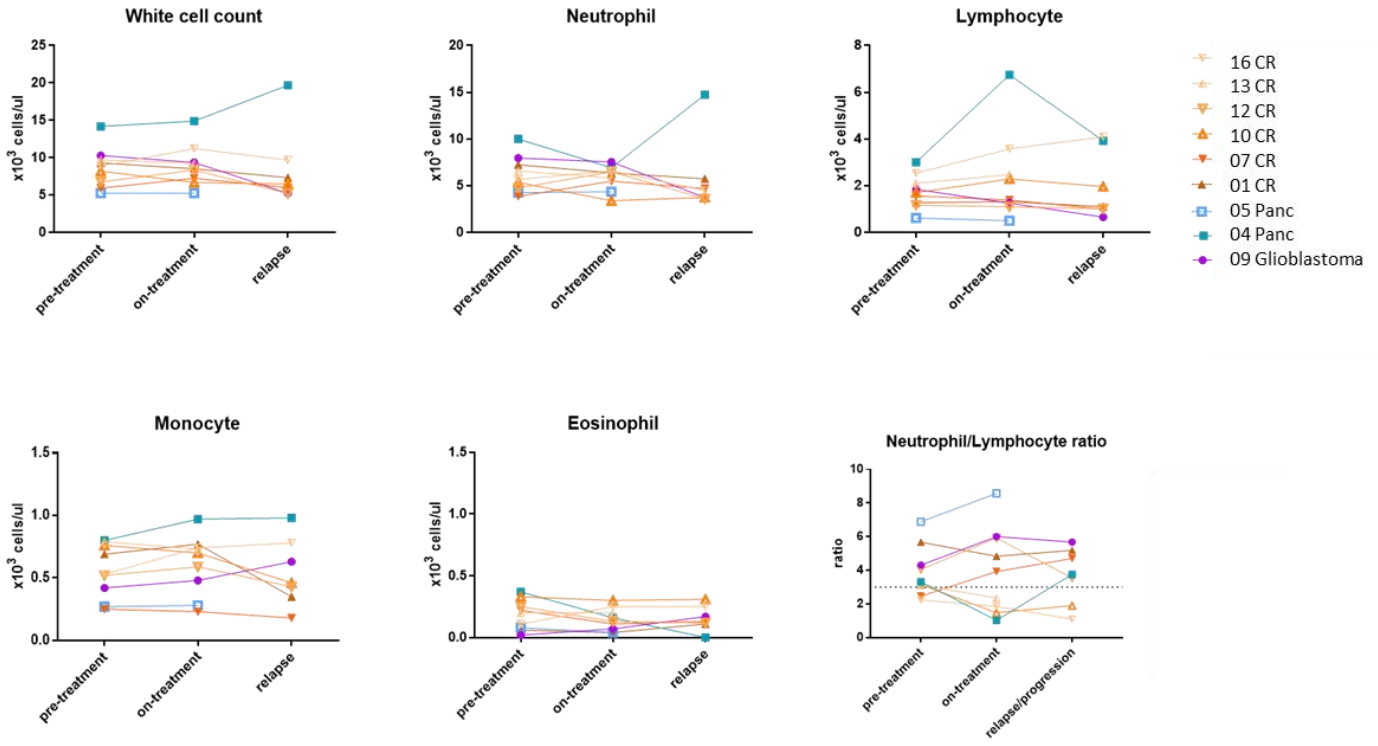


Figure 3.1: Key leukocyte populations maintain their cell number during treatment. Absolute cell count of different leukocyte populations performed by SA Pathology using Coulter Counter. Data was retrieved from patient database. Neutrophil/Lymphocyte ratio (NLR) at different timepoints of each subject was calculated manually and the dotted line shows the low NLR cut-off (<3) (Luo, Guo et al. 2015). **CR**: colorectal cancer, **Panc**: pancreatic cancer. No significant difference by ANOVA one-way was detected in all tests, n=9

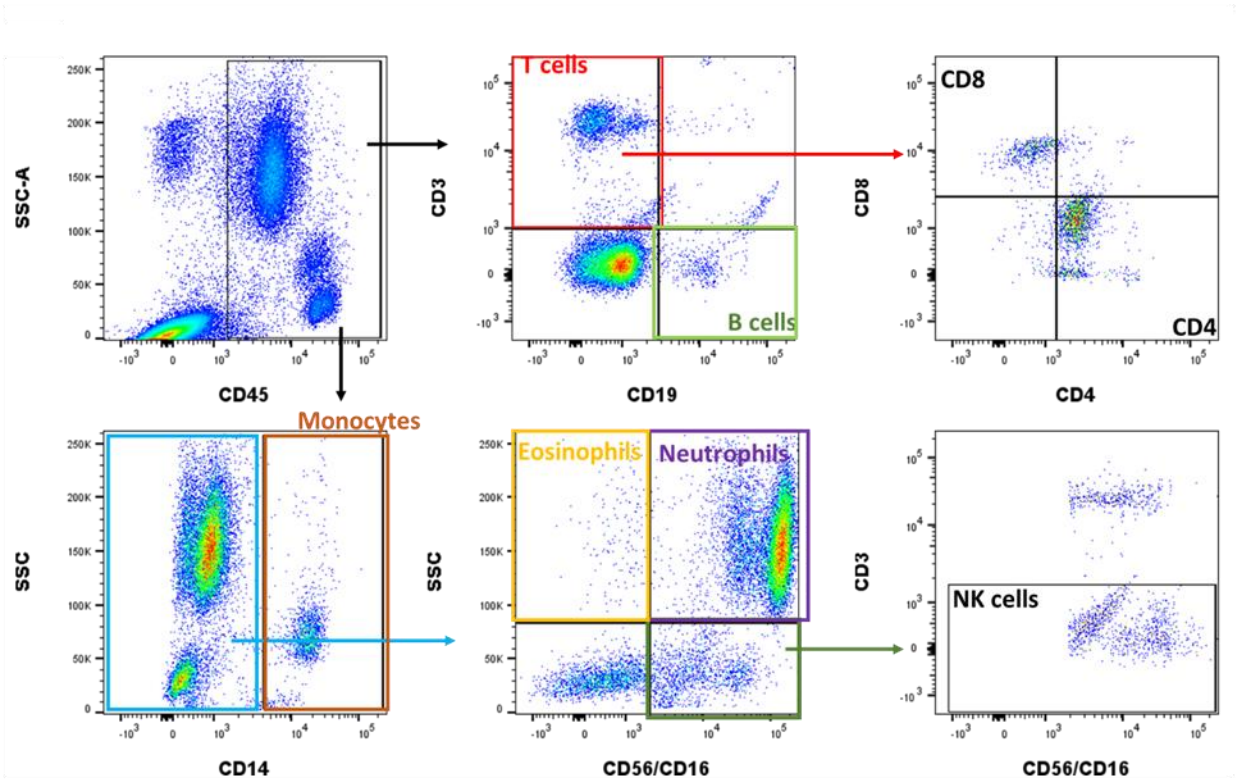


Figure 3.2: Flow cytometric gating strategy for analysis of whole blood to identify leukocyte subsets. Blood samples were obtained from patients and 50 ul of fresh whole blood was stained using a 7 colour immunophenotyping kit (Miltenyi). CD45-positive cells were gated. B cells and T cells and monocytes were defined within the overall leukocyte population by staining for CD19, CD3 or CD14, respectively. $CD3^+$ T cells were further separated into $CD4^+$ and $CD8^+$ subsets. CD14 negative cells were gated using CD16/CD56 and SSC parameters to identify mature neutrophils (CD16 and SSC-high) and eosinophils (CD16 positive and SSC-low). Cells that were SSC-low and CD56 positive were further gated on CD3 to determine NK cells which are CD3 negative.

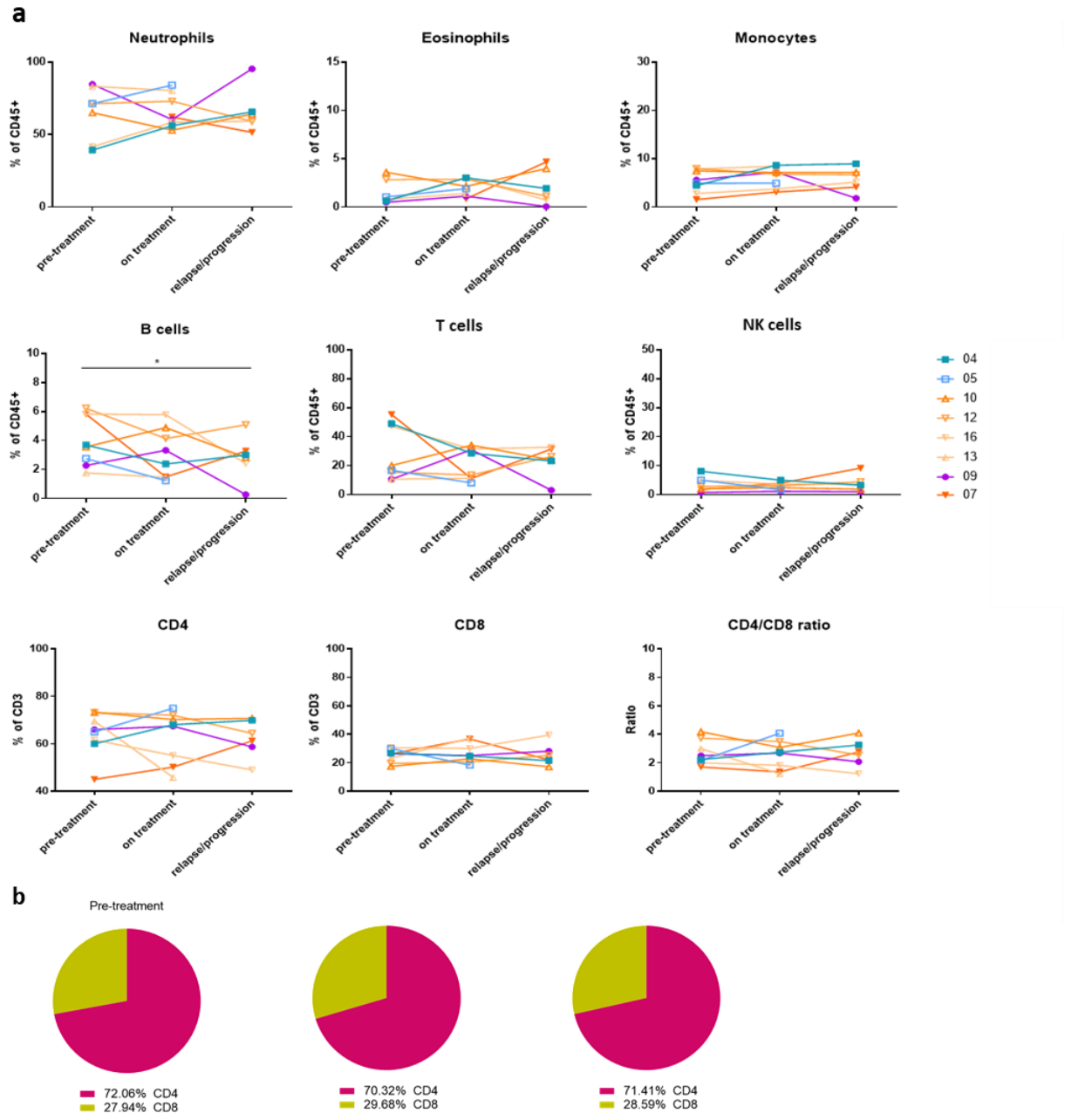


Figure 3.3 : Main leukocyte populations and lymphocyte subsets show mostly unchanged proportions after chemotherapy. The percentage of each population within total CD45 positive cells was determined by 7-colour flow cytometry on fresh whole blood samples taken from 8 patients either pre- cycle 1 of chemotherapy (pre-treatment), or pre-cycle 2 of chemotherapy (on-treatment), or at disease relapse/progression (relapse/progression). **(a)** Percentage of Neutrophils, Eosinophils, Monocytes, B cells, T cells, NK cells, $CD8^+$ T cells, $CD4^+$ T cells, and CD4/CD8 ratios at different time points. **(b)** Pie charts summarising the mean proportion of CD4 and CD8 T cells at different time points of treatment. (n= 8, ANOVA one-way test, *$p<0.05$)

3.3.3 Change in subsets of T cells post-chemotherapy

Thawed PBMCs were stained with a multi-colour flow cytometry panel for detailed T cell subset analysis. The gating strategy is shown in **Figure 3.4**. $CD4^+$ and $CD8^+$ subsets were gated from the $CD3^+CD14^-CD19^-CD56^-$ (T cell) population and then further gated based on the CD45RA isoform and the chemokine receptor CCR7 to determine sub-immunophenotypes: naïve T cells ($CD45RA^+$ $CCR7^+$), central memory (CM) T cells ($CD45RA^-$ $CCR7^+$), effector memory (EM) T cells ($CD45RA^-$ $CCR7^-$) and terminal effector (EMRA) T cells ($CD45RA^+$ $CCR7^-$) (Broere et al. 2011).

In keeping with the results of the whole blood analysis shown in **Figure 3.3**, analysis of $CD8^+$ and $CD4^+$ subpopulations within PBMC confirmed that there was no significant impact of chemotherapy on either $CD4^+$ or $CD8^+$ T cells. Thus, the proportion of $CD8^+$ T cells showed limited variation between time points within individuals. The proportion of $CD8^+$ T cells at baseline was 17% to 37% of $CD3^+$ lymphocytes (mean = 25.9%; SD= 6) and this proportion changed only slightly in samples collected post-treatment (both on-treatment and at relapse/progression). Similarly, the proportion of $CD4^+$ T cells at the first time point (mean = 62.3%; SD = 12.4) neither increased nor decreased following chemotherapy (both the second and the third time points) (data not shown).

Figure 3.5a shows the proportion of each subset in the $CD8^+$ T cell population. The mean percentage of $CD8^+$ T cells with a naïve phenotype was 23% (SD = 22.4) for pre-treatment, 20% (SD = 23.6) for on-treatment and 19.6% (SD = 20) for relapse/progression samples. Compared to other patients, patient #09 (glioblastoma) had a strikingly high proportion of naïve $CD8^+$ T cells in all three samples. Central memory phenotype T cells only contributed a small proportion of $CD8^+$ T cells. The proportion of this subset was 1% to 10% in pre-treatment, on-treatment and relapse/progression samples. The mean percentages of $CD8^+$ T cells double negative for CD45RA and CCR7 (EM) were 25% (SD = 11), 25% (SD = 12) and 20% (SD = 11) for pre-treatment, on-treatment and relapse/progression samples, respectively. The $CD45RA^+$ $CCR7^-$ cell (EMRA) subset is considered a terminal effector phenotype and accounted for approximately 50% of $CD8^+$ T

cells. The mean percentage of $CD8^+$ T_{EMRA} cells was 45% (SD = 20) for pre-treatment samples, 50% (SD = 21) for on-treatment sample and 55% (SD = 24) for relapse/progression samples. There was no significant difference in the mean percentages of naïve, CM, EM and EMRA subsets among pre-treatment, on-treatment and relapse/progression samples. Again, the results suggest that the chemotherapeutic agents used in the treatment of patients included in this study, did not significantly affect the CD8 compartment of T cells. Pie charts in **Figure 3.5b** represent the mean proportion of each subset of the $CD8^+$ population at three different timepoints and showed no significant differences.

Figure 3.6a displays the proportion of $CD4^+$ T cells with naïve, CM, EM and EMRA phenotypes. Most on-treatment and relapse/progression samples had proportions of all four subsets similar to samples at baseline. The mean proportion of T_{naive} was approximately 32% of total $CD4^+$ T cells at all three time points (SD = 19 for pre-treatment and on-treatment, SD = 14 for relapse/progression). Similarly, the mean proportions of $CD4^+$ T cells with a central memory phenotype were 33% (SD = 16) for pre-treatment and on-treatment samples, and 29% (SD = 10) for relapse/progression samples. Samples collected from patient #09 (glioblastoma) showed a large change in naïve and central memory $CD4^+$ T cell proportions between different time points and could be the result of long-term chemo-radiation. No significant difference was observed in mean proportions of $CD4^+$ T_{EM} cells and $CD4^+$ T_{EMRA} among the three time points. In short, the proportions of each $CD4^+$ T cell subset did not significantly alter during treatment. In support of this conclusion**, Figure 3.6b** shows the mean proportions of four main subsets of $CD4^+$ T cells in pie chart format.

CD27 and CD57 are alternative markers, which are associated with the differentiation stage of lymphocytes. They are constitutively expressed on naïve/central memory and senescent T cells, respectively (Brenchley et al. 2003a; Gravestein et al. 1998). To gain better understanding of the differentiation stage of T cells within patient PBMC samples, the expression of CD27 and CD57 on $CD4^+$ and $CD8^+$ T cells was investigated.

$CD27^+$ and $CD57^+$ cells were gated from $CD8^+$ and $CD4^+$ populations, as shown in **Figure 3.4**. **Figure 3.7** shows the proportions of $CD27^+$ cells among either $CD4^+$ or $CD8^+$ lymphocytes and **Figure 3.8** illustrates the proportion of $CD57^+$ cells among either $CD4^+$ or $CD8^+$ lymphocytes. Among samples collected at the three different time points, although proportions varied substantially within individuals, there was no difference in the mean proportion of either $CD27^+$ cells or $CD57^+$ cells in the $CD8^+$ population. The patterns of CD57 expression on $CD8^+$ T cells contrasted with CD27 expression patterns. Patients who had a low proportion of $CD27^+$ $CD8^+$ T cells showed a high proportion of CD57-expressing $CD8^+$ T cells and vice versa. This phenomenon was observed for all participants, showing the dominance of senescent ($CD57^+$) T cells and the relative lack of $CD27^+$ T cells with higher proliferative capacity and effector function.

Within the $CD4^+$ T cell subset, CD27 and CD57 expression was mostly stable after chemotherapy. Seventy seven percent of patients (n=7) had more than 70% of $CD4^+$ T cells expressing CD27 and the proportion of this subset was preserved post-chemotherapy. The "true" exhaustion marker of CD57, on the other hand, was expressed on less than 50% of $CD4^+$ T cells in eight out of nine patients and also remained unchanged following chemotherapy. It seems that chemotherapy agents did not significantly affect the proportions of CD27 and CD57-expressing $CD4^+$ T cells.

In summary, $CD8^+$ T cells expressed CD27 and CD57 to varying degrees. The expression of the costimulatory molecule, CD27, was consistently high in the $CD4^+$ T cell population whereas the proportion of $CD57^+$ $CD4^+$ T cells was consistently below 50% in most samples at all time points. The reciprocal relationship between CD27 and CD57 expression was detected in both $CD8^+$ and $CD4^+$ populations.

To determine the proportion of T cells with a stem cell-like phenotype, naïve T cells ($CD45RA^+$ $CCR7^+$) and central memory T cells ($CD45RA^-$ $CCR7^+$) were examined for the expression of the CD95 marker (Gattinoni et al. 2011) . Consistently, all $CD4^+$ and $CD8^+$ T cells did not express this stem/memory cell marker, suggesting that they are "true" naïve T cells/central memory T cells. **Figure 3.9** shows a representative analysis from patient #10

in whom T cell expression of CD95 was not detected. **Figure S3.1** shows the expression of CD95 markers on monocytes/B cells/NK cells, indicating that CD95 antibody worked well.

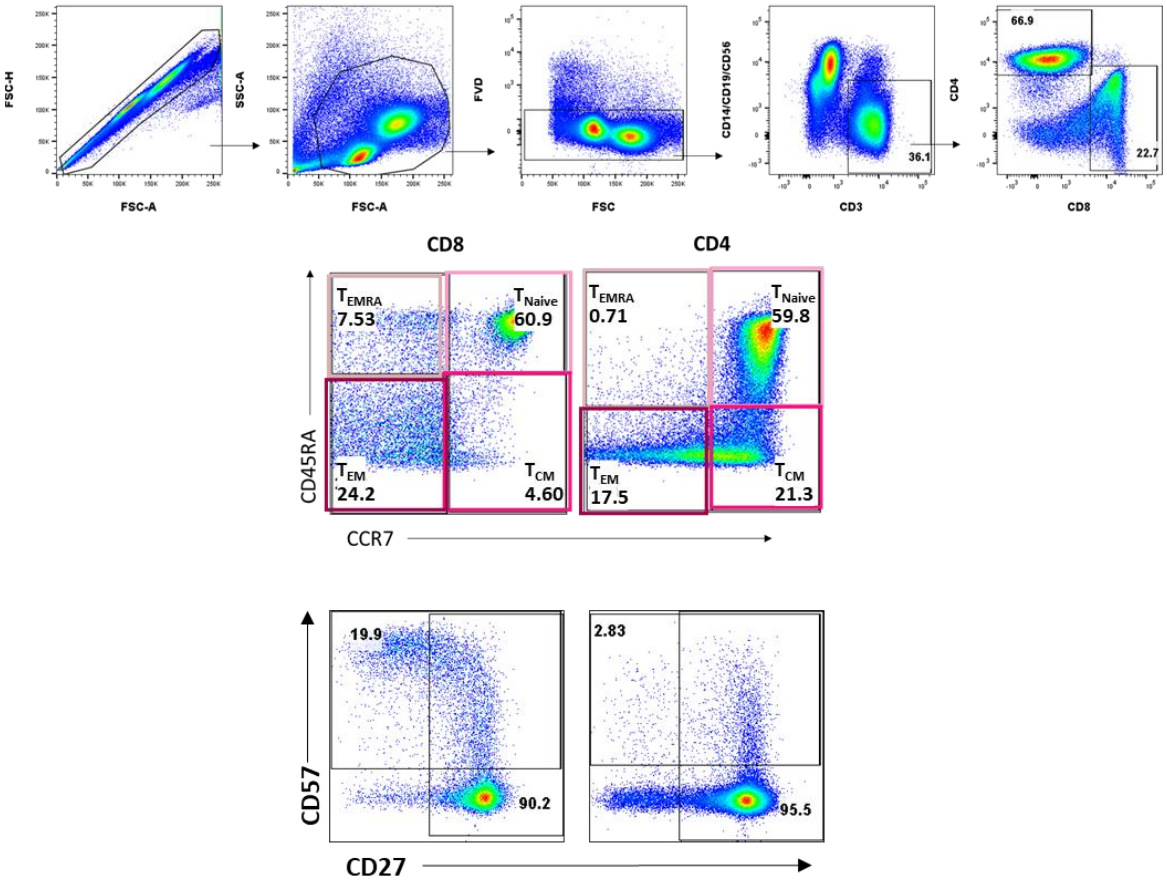


Figure 3.4: Gating strategy for T cell subset analysis from patients' PBMCs. Thawed PBMCs were stained with multi-colour panel for flow cytometry (see chapter 2). Forward scatter area (FSC-A) vs forward scatter-height (FSC-H) was used to select singlets. From the singlet population, debris was excluded by gating on FSC-A and side scatter-area (SSC-A). Dead cells were removed from total events by selecting the FVD negative population. Then, T cells were selected using the CD3 marker vs a dump channel including CD14/CD19/CD56. From CD3 positive T cells, CD4 and CD8 subsets were split as shown in the above figure. CD45RA and CCR7 were utilised as markers to differentiate the four main subsets of either CD4 or CD8 population. $T_{naïve}$:$CD45RA^{+}CCR7^{+}$, T_{CM} $CD45RA^{-}CCR7^{+}$, T_{EM} $CD45RA^{-}CCR7^{-}$, T_{EMRA} $CD45RA^{+}CCR7^{-}$. Finally, young cells ($CD27^{+}$) and terminally exhausted cells ($CD57^{+}$) were defined within CD4 and CD8 T cells.

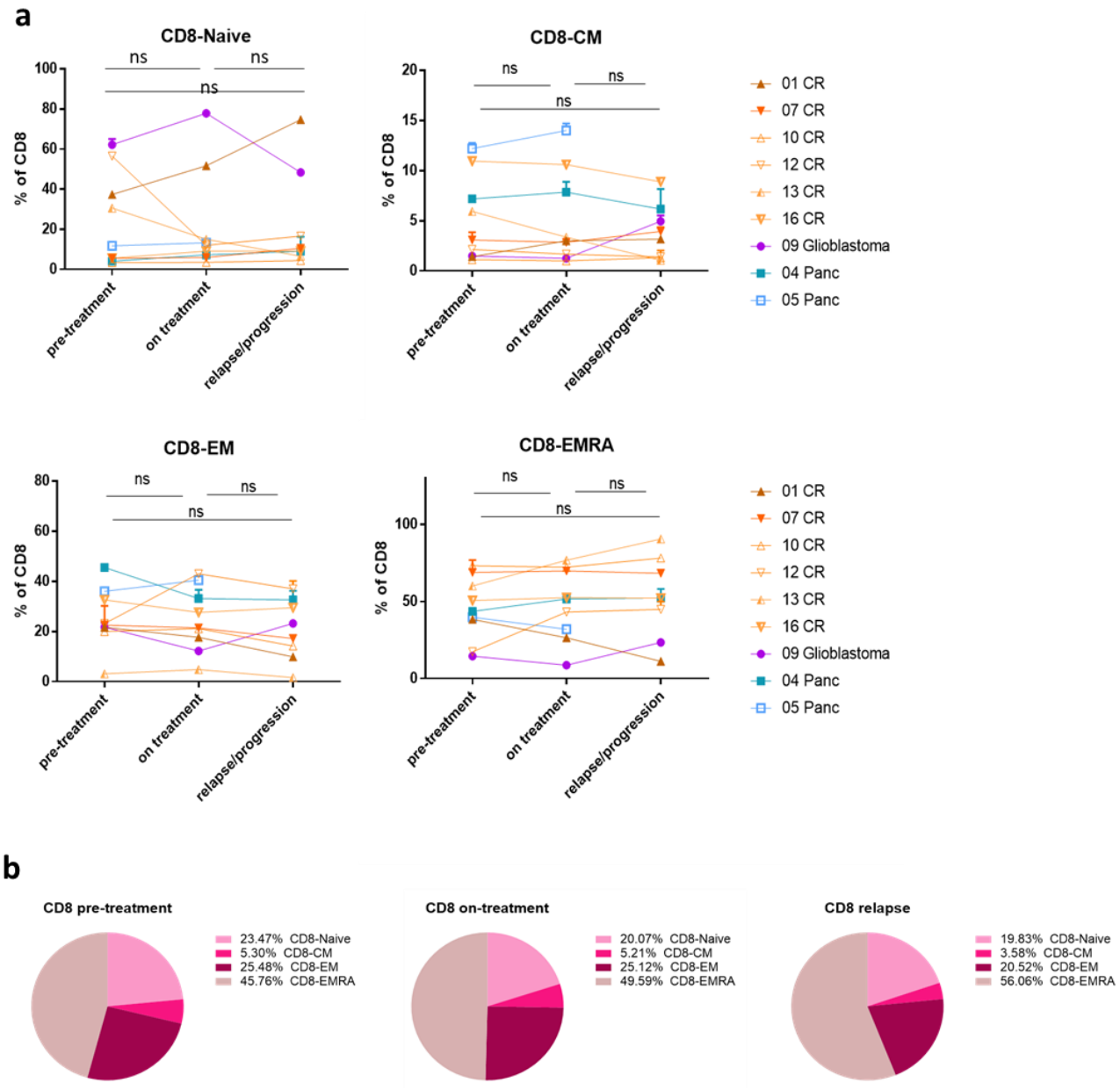


Figure 3.5: Comparison of proportions of four main CD8⁺ T cell subsets between different time points (pre-treatment, on-treatment, relapse/progression). The proportion of CD8+ T cells with various phenotypes ($T_{naïve}$:CD45RA⁺CCR7⁺, T_{CM} CD45RA⁻CCR7⁺, T_{EM} CD45RA⁻CCR7⁻, T_{EMRA} CD45RA⁺CCR7⁻) was determined by 12 colour flow cytometry on PBMCs taken from each individual at pre-treatment, on-treatment or relapse/progression time points. **(a)** Data for each patient over time. **(b)** Pie charts summarising the mean proportion of four main subsets of CD8⁺ T cells at different time points of treatment. (n = 9, one-way ANOVA test, ns: not significant, CM: central memory, EM: effector memory, EMRA: terminal memory, CR: colorectal cancer, Panc: pancreatic cancer)

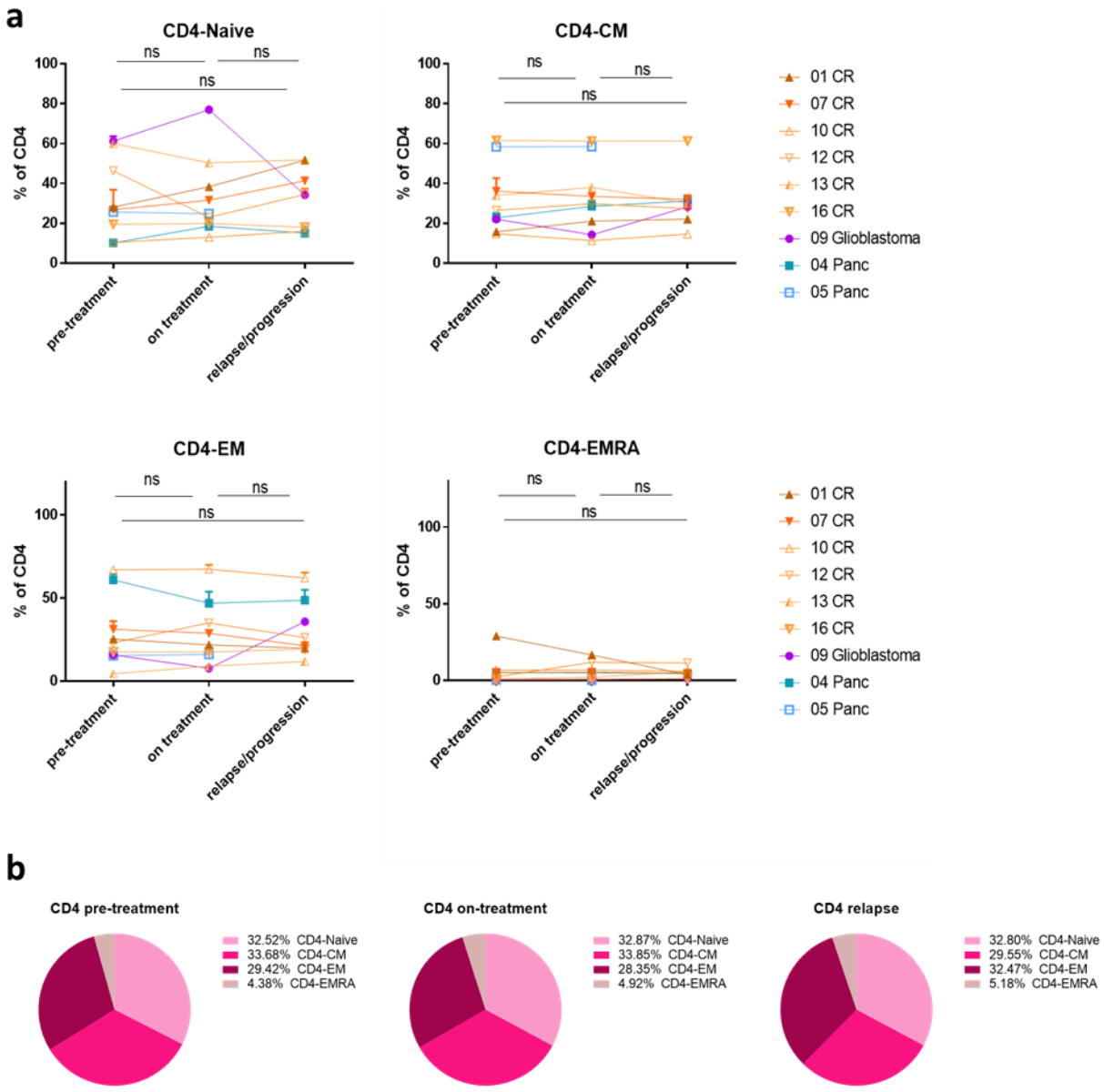


Figure 3.6: Comparison of proportions of four main CD4⁺ T cell subsets between different time points (pre-treatment, on-treatment, relapse/progression). The proportion of CD4⁺ T cells with various phenotypes ($T_{naïve}$:CD45RA⁺CCR7⁺, T_{CM} CD45RA⁻CCR7⁺, T_{EM} CD45RA⁻CCR7⁻, T_{EMRA} CD45RA⁺CCR7⁻) was determined by 12 colour flow cytometry on PBMCs taken from each individual at pre-treatment, on-treatment or relapse/progression time points. **(a)** Data for each patient over time. **(b)** Pie charts summarising the mean proportion of four main subsets of CD4⁺ T cells at different time points of treatment. (n = 9, one-way ANOVA test, ns: not significant, CM: central memory, EM: effector memory, EMRA: terminal memory, CR: colorectal cancer, Panc: pancreatic cancer)

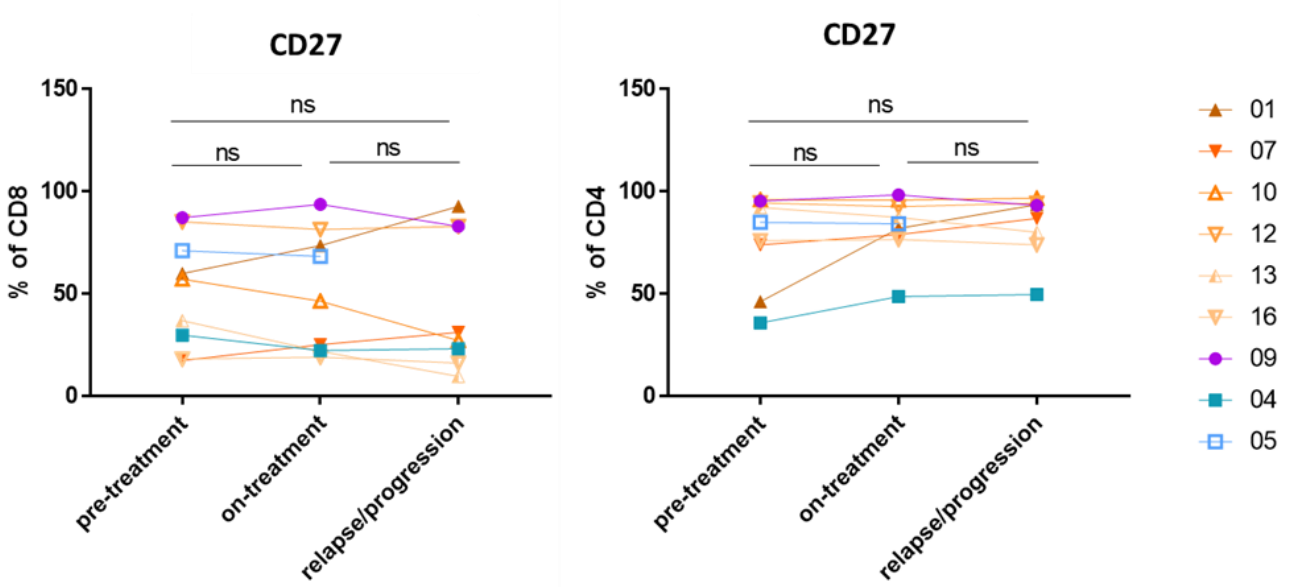


Figure 3.7: Young CD4⁺ and CD8⁺ T cells (CD4⁺ CD27⁺ or CD8⁺CD27⁺). Proportion of CD27 positive cells in CD4 and CD8 population was determined by 12 colour flow cytometry on PBMCs taken from each individual at pre-treatment, on-treatment or relapse/progression time points. (n=9, one-way ANOVA test, ns: not significant)

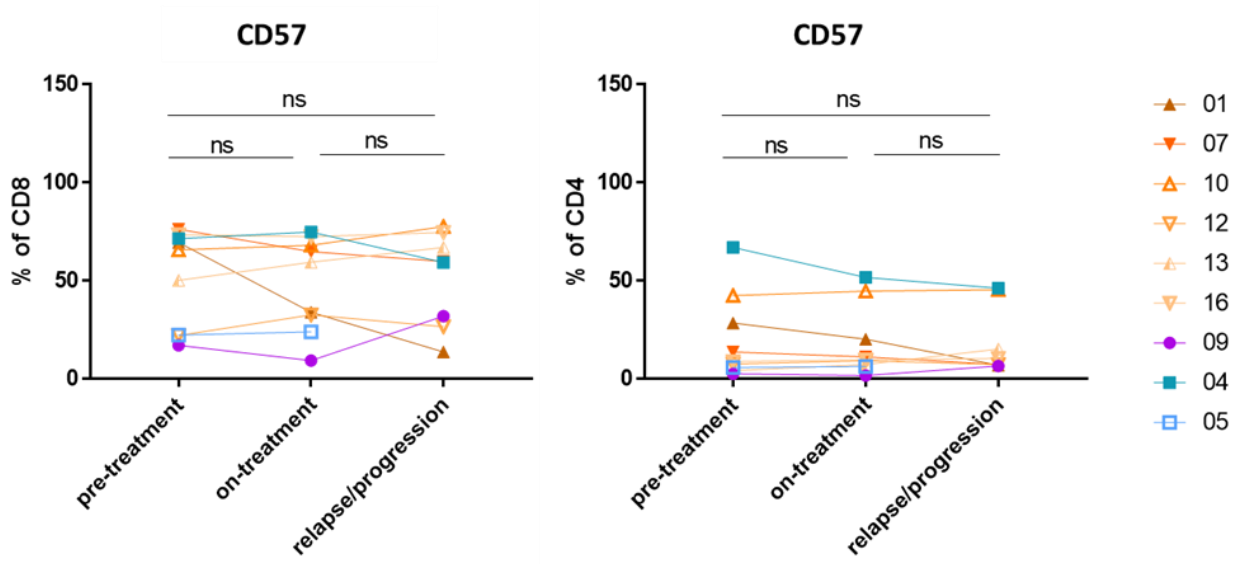


Figure 3.8: Terminally differentiated $CD4^+$ and $CD8^+$ T cells ($CD4^+$ $CD57^+$ or $CD8^+CD57^+$). Proportion of CD57 positive cells in CD4 and CD8 population was determined by 12 colour flow cytometry on PBMCs taken from each individual at pre-treatment, on-treatment or relapse/progression time points. (n=9, one-way ANOVA test, ns: not significant)

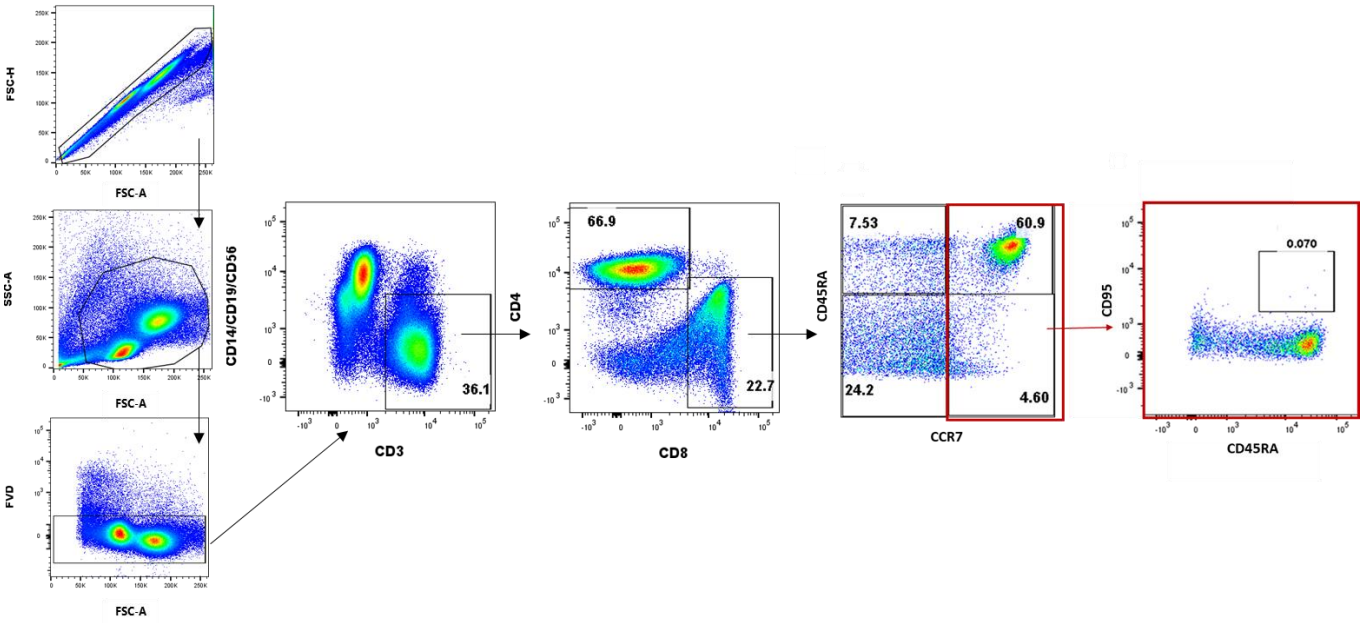
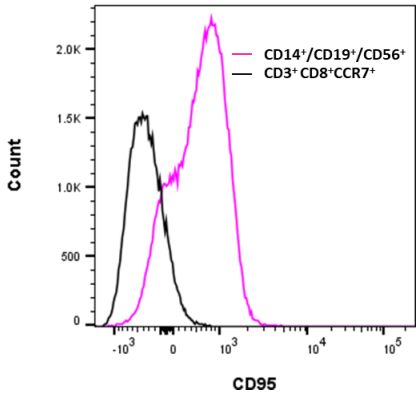


Figure 3.9: Memory T cells did not express stem cell- like marker CD95. Representative image from one patient shows no CD95 expression was detected in $CD8^+$ T cells positive for CCR7

S3.1



Supplementary figure S3.1: CD95 was detected in cell population positive for CD14 or CD56 or CD19 rather in naïve/memory T cells.

3.4 Conclusions

Eight out of sixteen participants, who were diagnosed with metastatic colorectal cancer (n=6), advanced pancreatic adenocarcinoma (n=1) and glioblastoma (n=1), were able to donate a whole set of three blood samples (pre-treatment, on-treatment and relapse/progression). Two patients, #05 and #09, demonstrated lymphopenia: #05 at the pre-treatment/on-treatment time point and #09 at the relapse/progression time point. Despite differences in cancer type, disease stage and chemotherapy received, most patients had a CD4/CD8 ratio in the normal range. While there was variability in how each individual responded to treatment, the mean proportions of the main leukocyte populations and T cell subsets did not significantly change following treatment, at either early or late time points. The apparent preservation of the T cell compartment post-chemotherapy suggests that CAR T cell manufacturing initiated from PBMCs collected during different phases of chemotherapy is feasible.

Chapter 4

CAR T cell manufacturing

4.1 Overview

In this chapter, I describe the feasibility of generating CAR T cells from PBMCs obtained at different phases of chemotherapy for solid cancer: pre-treatment, on-treatment, and at relapse/progression. Transduction efficiency, which is the percentage of T cells expressing CAR molecules, was compared between different CAR T cell products. The proportions of T cell subsets at four stages of differentiation were also compared as well as the proportions of young and senescent $CD4^+$ and $CD8^+$ T cells. Finally, the frequency of each T cell subset was compared between the final CAR T cell product and the PBMC starting population.

4.2 Introduction

Adoptive immunotherapy using CAR T cells has been remarkably successful in cases of relapsed/refractory B-cell malignancies but has faced many obstacles when applied in the solid tumour setting (Gargett et al. 2016; Kochenderfer & Rosenberg 2013; Morello, Sadelain & Adusumilli 2016) . Several parameters, that may contribute to treatment success have been identified, and include those related to the tumour microenvironment

and the CAR T cells themselves (Blaeschke, Franziska et al. 2016; Srivastava & Riddell 2015). These parameters include target antigen, CAR structure, tumour homing efficiency, long term survival of CAR-T cells in the circulation and in the tumour microenvironment, and pre-conditioning of a patient's immune system before adoptive cell therapy (Abate-Daga & Davila 2016; Abken 2017; Benmebarek et al. 2019). In this project, I used unselected PBMCs, which were isolated from the blood of solid cancer patients at different phases of chemotherapy, as inputs for the successful manufacture of CAR T cell products.

The differentiation and expansion of CAR T cells in patients after infusion appear to be critical for achieving clinical efficacy (Xu, X-J, Zhao & Tang 2013). In haematological malignancies, FDA approved CD19-CAR T cells induce a sustained anti-cancer response with persistence of circulating CAR T cells (Kochenderfer & Rosenberg 2013). In contrast, CAR T cells have had less positive outcomes for the treatment of solid cancers, with reports of short-term persistence, and a lack of expansion, of engineered T cells in the patient's circulation and in tumours (Ahmed et al. 2017; Gargett et al. 2016; O'Rourke et al. 2017). Therefore, improving the amplification of engrafted CAR T cells in solid cancer patients is an urgent requirement for successfully implementing this form of therapy.

Naïve (T_{Naive}) and central memory (T_{CM}) subsets of T cells have the capacity for self-renewal and differentiation into effector T cells after encountering cognate antigens (Boyman, O, Le´tourneau, S., Krieg, C., & Sprent, J. 2009). Several studies have indicated the potential for expansion of CAR T cells with naïve and central memory phenotypes *in vitro* and *in vivo* (Hinrichs et al. 2011; Xu, Y et al. 2014). The link between naïve/stem cell like memory/central memory subsets of CAR T cells and superior anti-tumour efficacy has also been revealed in pre-clinical models (Klebanoff et al. 2011; Sommermeyer et al. 2015). Therefore, predominance of these defined subsets of CAR T cells in the final product for infusion could contribute to persistence of infused CAR T cells in the patient, which in turn could contribute to positive outcomes for the patient.

A number of approaches have been developed for generating CAR T cell products with a high proportion of naïve/stem cell like memory/central memory T cells (Gargett et al. 2019; Turtle et al. 2016a; Wang, X et al. 2012). In one study, $CD4^+$ T_{CM} and $CD8^+$ T_{CM}

subsets were selected using an immunomagnetic approach and used as a starting population for CAR T cell manufacturing, resulting in persistent and highly functional central memory CAR T cell products (Wang, X et al. 2012). For two other studies, CAR-T cells were generated from slowly activated bulk PBMCs or bulk $CD4^+$ and $CD8^+$ T cells and cultured in special media supplemented with interleukin (IL)-7 and IL-15 (Gargett et al. 2019; Turtle et al. 2016b). Results from the latter studies also revealed final CAR T cell products with a high fraction of central memory cells. Hence, manufacturing CAR T cells with enhanced central memory subsets is feasible by employing either pre-selected lymphocyte populations as starting materials and/or special reagents during CAR T cell culturing.

In recent years, chemotherapy has been shown to modulate the immune system in ways that promote anti-tumour effects (Galluzzi et al. 2015). Rapid recovery of the $CD8^+$ T cell population, a reversal of the CD4/CD8 ratio, and an enhancement of cytolytic function after cytotoxic drug administration were reported in a number of studies (Ferrari et al. 2006; Mackall, CL et al. 1997a; Turtle et al. 2009; Wijayahadi et al. 2007). Survival of central memory T cells after chemotherapy and the strong proliferation of this subtype in response to the homeostatic cytokines IL-7 and IL-15 have also been described (Turtle et al. 2009). Interestingly, chemotherapy drugs can sustainably deplete regulatory T cells and other suppressor cells such as MDSCs (Ghiringhelli et al. 2004; Scurr et al. 2017). These favourable changes in T cell number and function are proposed to benefit CAR T cell manufacturing.

The feasibility of manufacturing potentially long-lived CAR T cells using PBMCs obtained from patients at different phases of chemotherapy has been considered. CD19-CAR T cells applied to haematological cancers are routinely generated using PBMCs from patients in the setting of relapsed/refractory disease (Neelapu et al. 2017; Porter et al. 2011). Until now, no studies have investigated the feasibility of producing functional CAR T cells using PBMCs collected before, during and after chemotherapy given to solid tumour patients. Here, CAR T cell products were manufactured from PBMCs collected at different treatment time points, and analysed as to their immunophenotype, cytotoxic activity and states of exhaustion or senescence. Results derived from this project may illustrate the

feasibility of generating CAR T cell products from PBMC populations at different phases of chemotherapy.

For my project, the protocol for CAR T cell manufacturing was adopted from work previously published by our group (Gargett et al. 2019) in which altering the *ex vivo* manufacturing conditions led to different phenotypes of CAR T cells in the final product (Gargett et al. 2019). A polymeric nanomatrix conjugated to recombinant humanised CD3 and CD28 agonists (MACS TransAct, Miltenyi) was used for 'slow and gentle' T cell activation, in combination with TexMACS medium and IL-7/IL-15 for cell expansion. This combination was determined to promote CAR T cell products which stem cell-like and central memory phenotypes predominated. In contrast, the original culture condition in which T cells were strongly activated by anti-CD28 and anti-CD3 (Miltenyi Biotec) and expanded in advanced RPMI supplemented with IL-7/IL-15, resulted in only minor populations of stem cell-like and central memory phenotypes. Our study is consistent with another report (Blaeschke, F. et al. 2018) in which the investigators also used TexMACs medium supplemented with IL-7 and IL-15 for T cell expansion, giving rise to CAR T cell products with similar phenotypes. Interestingly, the type of gene transfer vector used in these studies (retroviral vector used by our group (Gargett et al. 2019) or lentiviral vector used by Blaeschke et al.), seems not to play a role in defining T cell phenotypes in the end product (Blaeschke, Franziska et al. 2016; Gargett et al. 2019). Therefore, I employed our optimised protocol for engineering transgenic T cells (Gargett et al. 2019) to address the feasibility of manufacturing from peripheral blood samples CAR T cell products with high proportions of stem cell-like/central memory phenotypes irrespective of phase of chemotherapy.

4.3 Results

In this project, CAR T cell products generated from PBMCs collected at three different time points during cancer treatment were compared. PBMCs were cryopreserved after isolation from whole blood at the time of collection. When a full set of PBMCs from each individual was collected, I generated CAR T cell products from that set of samples. The

different CAR T cell products are referred to as pre-treatment, on-treatment and relapse/progression CAR T cells in the text.

4.3.1 T cells from PBMCs collected at different time points of cancer treatment proliferated strongly during the manufacturing procedure.

Thawed PBMCs were rested overnight in TexMACs medium supplemented with IL-7 and IL-15. Approximately 1x 10^7 to 1.5 x 10^7 cells were activated using TransAct on day 0. Activated T cells were counted on day 2 and approximately 3 x10^6 cells were transduced with retrovirus encoding the GD2-specific CAR. Transduced T cells were expanded in culture for another 8 days and harvested on day 10 post activation. Cells were counted using a haemocytometer and Trypan Blue dye every second day to check cell proliferation during the manufacturing process. Fold expansion was calculated by dividing the cell number on each day by the respective cell count on day 2. **Figure 4.1a** shows fold expansion of the three groups of products. Cell proliferation was quite distinct between individuals and between groups. Samples in the pre-treatment group showed a trend toward better cell expansion compared to the on-treatment and relapse/progression groups. After 10 days, transduced T cells in the pre-treatment group demonstrated a mean expansion of 19-fold (SD = 15). In contrast, cells from the on-treatment and relapse/progression groups showed a mean expansion of 14-fold (SD = 13) and 11-fold (SD= 10), respectively **(Figure 4.1b).** However, these differences were not statistically significant.

There was no significant difference in the mean fold expansion of any of the patient samples compared to healthy control samples processed in the same manner (including cryopreservation and thawing), with a mean expansion of 13-fold (SD= 2) observed for the healthy controls **(Figure 4.1b).** Although all T cells from patient samples showed a diverse range of expansion capacity, there was a more consistent fold change in the expansion of healthy cells **(Figure 4.1b).** Patient #01 (aged 31) had T cells that proliferated strongly in culture. Older age may affect the ability of T cells to proliferate**.** This feature will be discussed further in details in chapter 6. Slower expansion did affect the number of cells at the end of manufacturing. In this study, the critical number of 3 x10^7 cells is the quantity of

cells above which the production of CAR-engineered T cells should be considered successful to yield adequate cells for later functional assays *in vitro.* As seen in **Figure 4.1c**, the yield of T cells from several patients' PBMCs did not achieve a threshold of 3 x10^7 cells, indicating that although CAR T cell manufacture was feasible for every patient, the yield was not always adequate at every time point, especially at the relapse/progression time point. These findings suggest that the number of chemotherapy courses experienced by the patient, which accumulate by the relapse/progression time point, may contribute to a critically low cell yield. Otherwise, high cell yields were achieved in the majority of samples pre-treatment and on-treatment. A summary table of common features of patients whose T cell number did not reach the CAR T cell production threshold will be mentioned in the discussion chapter.

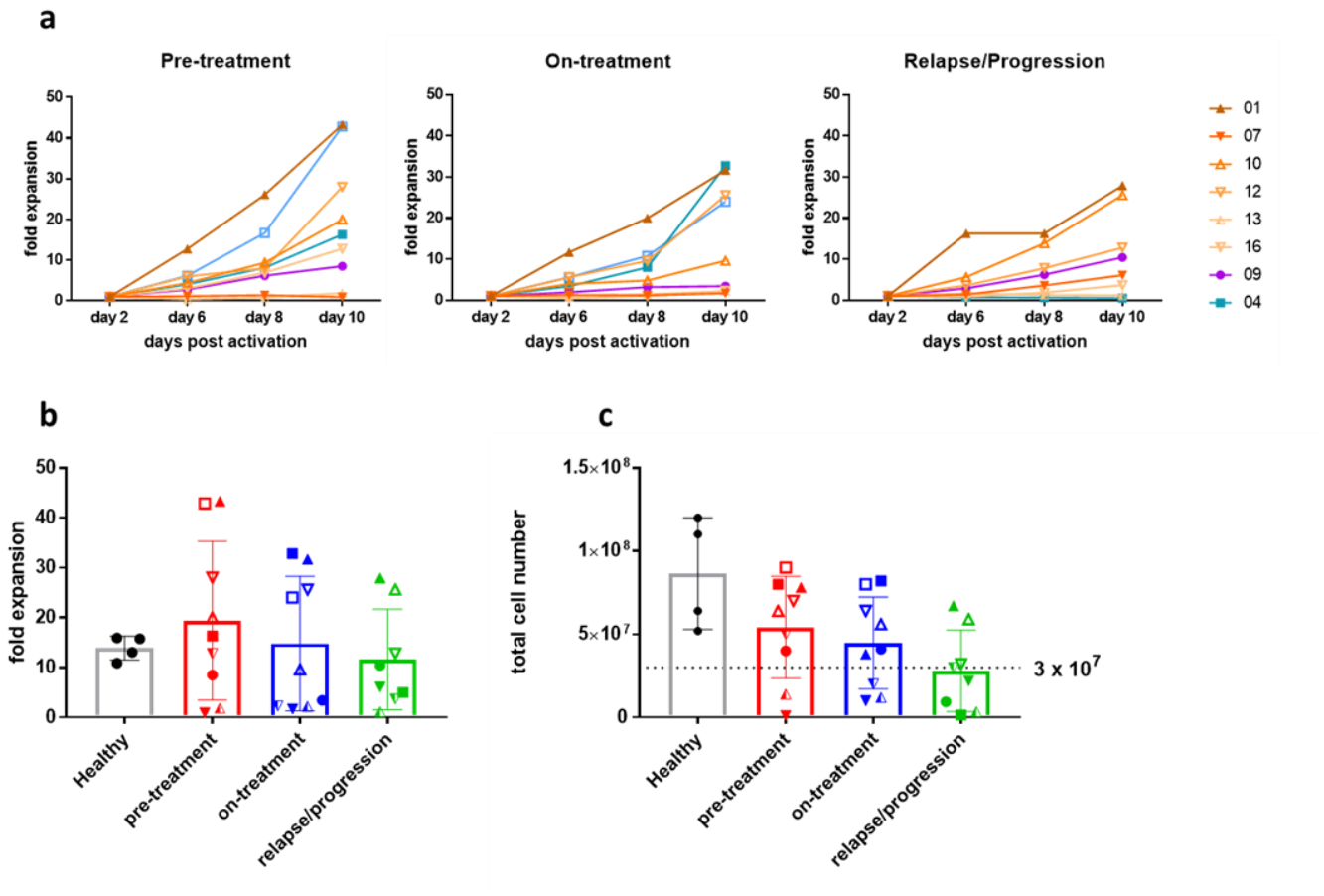


Figure 4.1: Expansion of T cells during the CAR T cell manufacturing process. Activated PBMCs were transduced with GD-2-CAR encoded retrovirus on day 2. Cells were counted every two days using a haemocytometer and Trypan blue dye. Fold expansion is expressed relative to viable cell number on day 2. **(a)** Fold expansion of CAR T cell products generated from PBMC collected at the three different time points. Data from each patient was assigned a specific symbol. Orange/brown symbols represent colorectal cancer patients, turquoise symbols indicate pancreatic cancer patients, and purple symbols represent the single glioblastoma patient. Lines connect expansion data from different days. **(b)** Comparison of fold expansion on day 10 between patients and healthy donor CAR T cell products. Column represents mean and error bars represent SD. No significant difference by one-way ANOVA test was detected. **(c)** Total cell yield at the end of CAR T cell manufacturing. Dotted line represents the required minimum cell number for downstream functional assays.

4.3.2 Efficiency of viral transduction and CAR expression

The manufacture of CAR T cells from patients' PBMCs was feasible at all time points. **Figure 4.2b** shows the transduction efficiency (measured as percentage of T cells expressing the GD2-specific CAR molecule) within CAR T cell products manufactured from patient samples at the three time points, compared to healthy controls. There was no significant difference in the mean percentage of CAR^+ T cells in products manufactured from patients' PBMCs compared to those manufactured from healthy donors. Although samples derived from healthy donors showed consistent transduction efficiencies, viral transduction efficiencies using PBMCs from cancer patients varied more widely. The comparison of transduction efficiencies between cells at different phases of chemotherapy is shown in **Figure 4.2c**. The mean transduction efficiencies of CAR T cell products from pre-treatment, on-treatment, and relapse/progression samples were 13% (SD = 10), 17% (SD = 9), and 18% (SD = 15), respectively. There was a tendency toward increased efficiency of transduction of T cells obtained 4-8 weeks after the first cycle of chemotherapy (on-treatment), as shown in eight out of nine patients, but this difference was not statistically significant. No upward or downward trend in the rate of transduced T cells was identified in of relapse/progression samples. Also, it was noted that the patient who had the lowest transduction efficiency in the pre-treatment sample cohort also had the lowest transduction efficiency among on-treatment and relapse/progression samples. These results suggest that cancer patient- derived PBMCs intrinsically vary in their ability to be transduced rather than suggesting that chemotherapy itself has a negative effect on the transduction of PBMCs. Indeed, I do not find evidence that short-term anti-neoplastic treatment has a deleterious effect on the efficiency of viral transduction.

There were two patients in whom the pre-treatment and relapse/progression samples had a very low percentage of CAR positive T cells (less than 3%). These patients were diagnosed with glioblastoma (patient #09) and advanced pancreatic adenocarcinoma (patient #04). Interestingly, T cells from patients which showed slower expansion rates (mentioned in part 4.3.1) achieved average to high-efficiency transduction, especially at the on-treatment and relapse/progression time points. These data suggest that the inherent

proliferative capacity (represented by fold expansion) did not determine viral transduction efficiency.

In summary, I was able to generate CAR T cells from patient blood samples, but it was not successful for every patient at every timepoint with low transduction efficiency observed in several samples. There was a trend toward increased transduction efficiency in the on-treatment group, but there was no significant difference between products from the three different time points, or healthy controls.

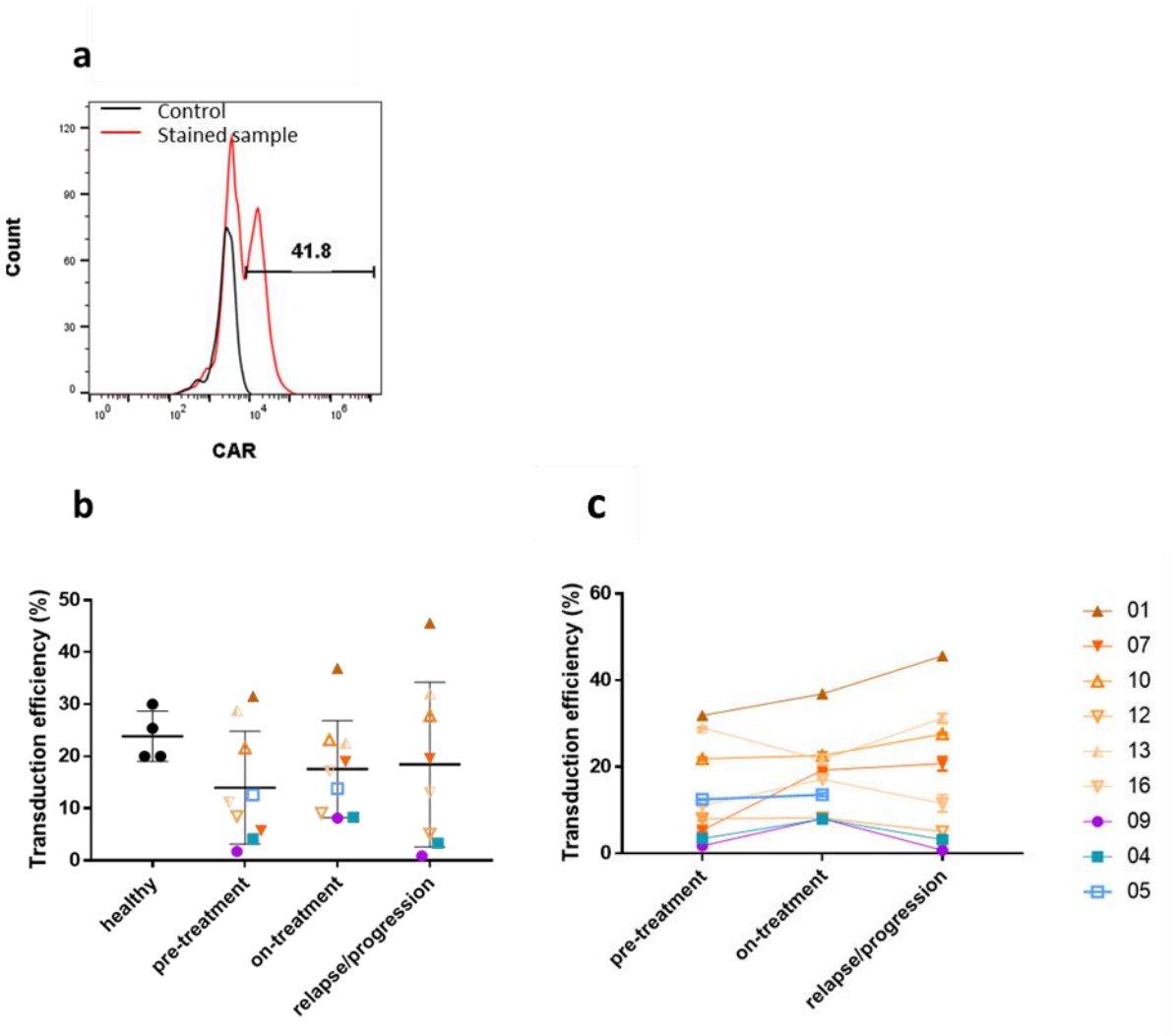


Figure 4.2: Transduction efficiency of CAR T cell products as determined by flow cytometry on day 6 post activation (4 days after transduction). $1x10^5$ cells from day 6 cultures were stained using the anti-idiotypic 1A7 antibody to detect CAR expression and analysed by flow cytometry. Non-transduced cells were used as controls. **(a)** Histogram showing CAR expression on $CD3^+$ T cells on day 6 of expansion. Black line represents non-transduced population, red line represents CAR T cell product on day 6. **(b)** Transduction efficiency of all samples on day 6 post activation. Line represents mean and error bars represent SD. **(c)** Comparison of transduction efficiency between CAR T cell products of each individual. Orange/brown symbols represent colorectal cancer patients, turquoise symbols indicate pancreatic cancer patients, and purple symbols represent the single glioblastoma patient. (*n=9*; no significant difference by ANOVA one-way was detected in all tests,)

4.3.3 Immunophenotypes of CAR T cells

In this section, immunophenotyping results for CAR T cell products were compared amongst pre-treatment, on-treatment, and relapse/progression time points. The four main subsets of CAR^+ T cells are: (i) naïve-like T cells (this phenotype is further explained in this section) that express both CD45RA and CCR7 markers; (ii) central memory T cells which have a $CD45RA^-$ $CCR7^+$ phenotype; (iii) effector memory T cells double negative for CD45RA and CCR7; (iv) and terminal effector T cells which are $CD45RA^+$ $CCR7^-$. Senescent cells are determined by the expression of CD57.

The phenotype of CAR T cell products from the nine patients were evaluated by determining the CD4/CD8 ratio, the relative frequencies of the four main subsets, and the frequency of senescent T cells using a 12-colour flow cytometry panel. The gating strategy and representative plots are shown in **Figure 4.3**. First dead cells and residual $CD14^+$/$CD19^+$/$CD56^+$ cells (which were less than 4%) were excluded and CD3 positive cells expressing CAR molecules were gated, such that all downstream analyses were focused on the CAR-expressing T cell population. $CD4^+$ and $CD8^+$ T cell populations were gated next, followed by analysis of CD45RA vs CCR7 staining to identify the naïve-like, central memory, effector memory, and terminal effector subsets, similar to **Figure 3.4** in Chapter 3.

The final CAR-T cell products displayed a predominantly $CD8^+$ CAR^+ T cell phenotype, with a mean of 59% (SD = 15), 62% (SD = 17) and 58% (SD = 18) $CD8^+$ cells respectively in pre-treatment, on-treatment and relapse/progression samples (**Figure 4.4c**). The differences between the mean proportion of $CD8^+$ CAR^+ T cells between groups of treatment were not statistically significant (**Figure 4.4a**). The graph in **Figure 4.4b** shows the ratio of CD4/CD8 CAR^+ T cells, which was reversed compared to the initial PBMC population (part 3.3.2). Whereas the CD4/CD8 ratio in the PBMC starting population was larger than 2, this ratio was less than 1 in final CAR T cell populations. It is interesting to note the consistently high frequency of $CD8^+$ CAR T cells in the end products, suggesting these cells are better supported by the culture conditions.

T cells of the naïve ($CD45RA^+$ $CCR7^+$) subset that express the memory marker CD95 are considered to be naïve-like or stem cell-like memory T cells (Gattinoni et al. 2011).

After 10 days of expansion using TexMACs medium supplemented with IL-7 and IL-15, almost 100% of $CD8^+$ and $CD4^+$ CAR^+ T cells uniformly expressed CD95 marker (data not shown). Therefore, I considered that CAR T cells expressed a 'naïve-like' phenotype ($CD45RA^+$ $CCR7^+$ $CD95^+$) rather than a true naïve ($CD45RA^+$ $CCR7^+$ $CD95^-$) phenotype as was seen in the original PBMC samples.

Figure 4.5 shows the proportion of naive-like, central memory, effector memory and terminal effector phenotypes of $CD8^+$ CAR^+ T cells. The mean percentage of naïve-like CAR^+ T cells was 27% (SD = 27) pre-treatment, 26% (SD = 22) on-treatment, and reducing to 19% (SD = 19) at relapse/progression. On-treatment products had the highest mean proportion of central memory T cells (mean = 11%; SD = 9) at any of the treatment time points. Relapse/progression products contained the highest mean percentage of effector memory (mean = 47%; SD = 24) T cells. However, despite these observed trends, there was no significant difference in mean proportions of each subset between any time points. Likewise, all pre-treatment, on-treatment, and relapse/progression products had similar mean proportions of terminal effector T cells (mean = 26%; SD= 18), (mean = 27%; SD= 18), mean = 24%; SD = 13), respectively. The proportions of $CD8^+$ naïve-like and central memory T cells in our products were lower than those reported in other studies using a similar manufacturing process, probably because of different starting populations (PBMCs versus sorted $CD4^+$ and $CD8^+$ cells, respectively) (Blaeschke, F. et al. 2018; Gargett et al. 2019). Another reason could be that different combinations of markers were used to determine memory subsets. CCR7 was chosen in this study while CD62L was used in others (Blaeschke, F. et al. 2018).

Next, the level of CD57 expression on $CD8^+$ CAR^+ T cells between groups was examined. Pre-treatment and on-treatment CAR^+ T cells showed a low level of CD57 expression on $CD8^+$ CAR T cells, with means of 32% (SD = 23) and 31% (SD = 20), respectively, in comparison to 42% (SD= 23) in relapse/progression samples, although this difference did not achieve statistical significance. Reciprocal to the expression of CD57, the proportion of $CD27^+$ cells in $CD8^+$ CAR^+ T cell population in the relapse/progression group was the lowest compared to pre-treated and on-treatment groups. Although this reduction was not statistically significant in this small cohort, it nevertheless suggests that self-

renewal capacity may be reduced in CAR T cells manufactured at the relapse/progression time point.

Within the $CD4^+$ CAR^+ T cell population, the proportion of these four major phenotypes (naïve-like, central memory, effector memory, and terminal effector) and the proportions of cells expressing CD27 or CD57 were compared among different time points **(Figure 4.6)**. Pre-treatment and on-treatment $CD4^+$ CAR^+ T cells had similar mean proportions of naïve-like and terminal effector phenotypes, respectively. In the on-treatment group, the percentages of $CD4^+$ CAR^+ T cells of central memory phenotype and of effector memory phenotype were the highest and lowest, respectively, compared to pre-treatment and relapse/progression groups. However, these distinctions were not statistically significant **(Figure 4.6a).** Interestingly, the proportion of $CD4^+$ CAR^+ T cells with central memory phenotype was greater than those with a naïve-like phenotype, which is opposite to that observed for $CD8^+$ CAR^+ T cells. Effector memory subsets formed the largest proportion in the $CD4^+$ T cell compartment compared to other phenotypes, which was similar to the observation made for the $CD8^+$ T cell population (**Figure 4.6b**). However, the terminal effector phenotype only contributed to a small proportion of $CD4^+$ CAR^+ T cells, which was contrary to the observed proportion for $CD8^+$ CAR^+ T cells. Expression of the senescence marker CD57 on $CD4^+$ CAR^+ T cells was similar between different groups, and the mean proportions of the senescent subset in $CD4^+$ T cells at pre-treatment, on-treatment, and relapse/progression time points were lower than those of the respective groups of $CD8^+$ CAR^+ T cells. It was observed that samples of $CD4^+$ CAR^+ T cells with high CD27 expression also had low CD57 expression. For example, $CD4^+$ CAR^+ T cells in patient #04 had a remarkably high percentage of $CD57^+$ cells compared to other patients, while the percentage of $CD27^+$ $CD4^+$ CAR T cells was correspondingly low at all time points for this patient, lending support to our use of these markers to represent different T cell subsets, with CD27 expression representing 'younger' cells with proliferative potential and CD57 expression representing 'older' senescent cells.

In summary, $CD8^+$ CAR T cells were predominant compared to $CD4^+$ CAR T cells in the final CAR T products at all time points. The CD95 marker was uniformly expressed on all CAR T cells, so cells of the $CD45RA^+$ $CCR7^+$ $CD95^+$ were classified as naïve-like in the final

products. Effector memory T cells made up a large proportion of both $CD8^+$ and $CD4^+$ CAR T cells at all time points. On-treatment CAR^+ T cells trended towards higher proportions of naïve-like and central memory phenotypes within both $CD8^+$ and $CD4^+$ T cell subsets compared to CAR^+ T cells in the pre-treatment and relapse/progression samples. However, these differences did not reach statistical significance.

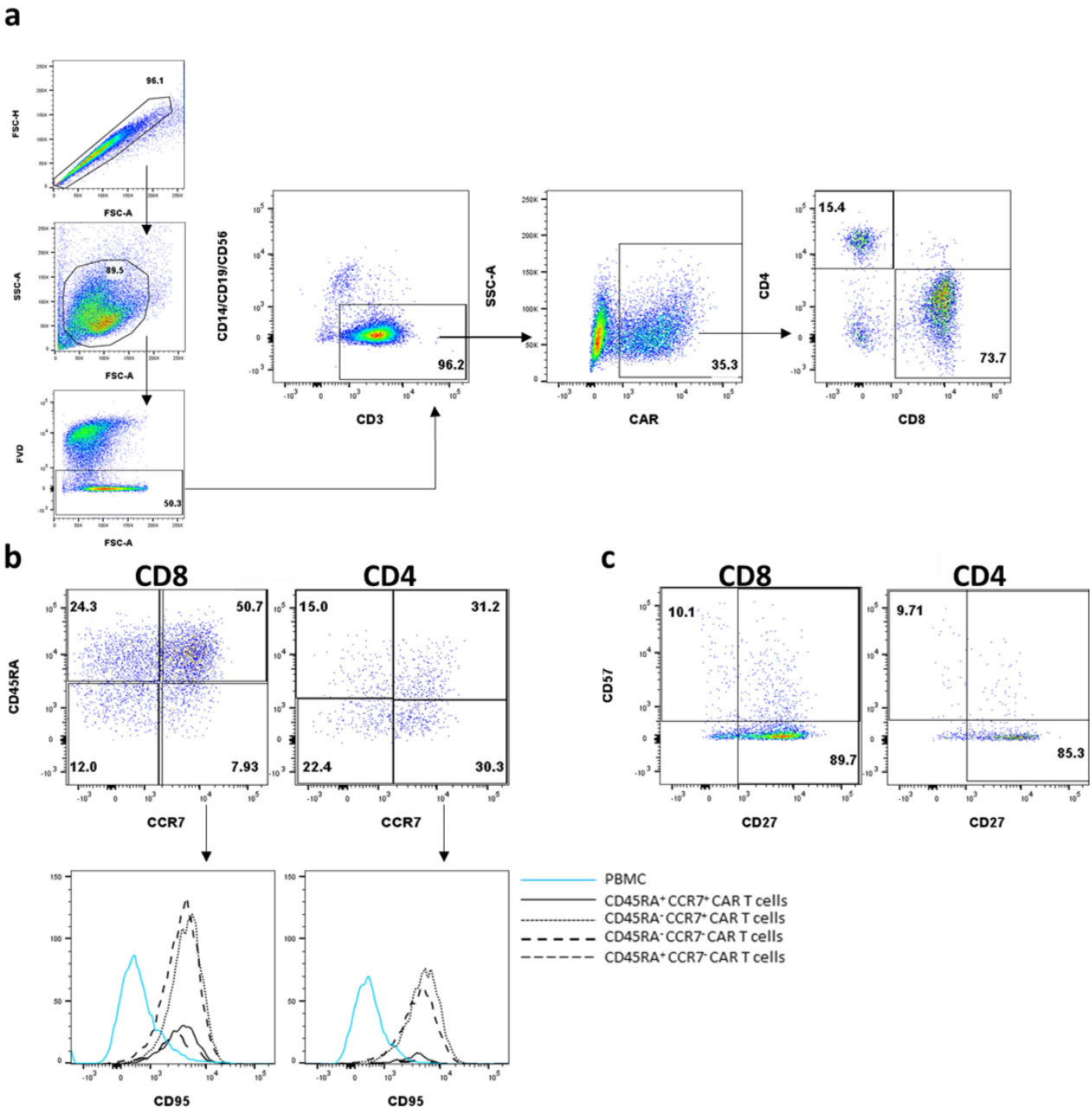


Figure 4.3: Gating strategy used for 12-colour flow cytometric analysis of CAR T cell products. Cryopreserved CAR T cell products were thawed and rested overnight. 2 x 10^5 cells were stained for flow cytometric analysis using a 12-colour panel (CD3-BV510, CD4-PE-Cy7, CD8-APC-H7, FVD-AF700, CD14/CD19/CD56-PerCP-Cy5.5, CD45RA-BUV395, CCR7-APC, CD27-CC515, CD57-BV421, CD95-BUV737, PD-1-BV786, CAR-primary 1A7-secondary PE). **(a)** $CD3^+$ T cells were gated based on live cells. Gated CAR^+ T cells were then further gated on CD4 vs CD8 markers . **(b)** Cells in CD4 and CD8 populations were identified as T-naïve-like ($CD45RA^+$ $CCR7^+$), central memory (T_{CM} : $CD45RA^-$ $CCR7^+$), effector memory (T_{EM}: $CD45RA^-$ $CCR7^-$), and terminal effector (T_{EMRA}: CD45RA+$CCR7^-$) based on CCR7-APC and CD45RA-BUV395 markers. $T_{naive\text{-}like}$, T_{CM}, T_{EM}, T_{EMRA} were further gated for CD95-BUV737 histograms. **(c)** The proportion of $CD27^+$ and $CD57^+$ cells in the CD8 or CD4 population.

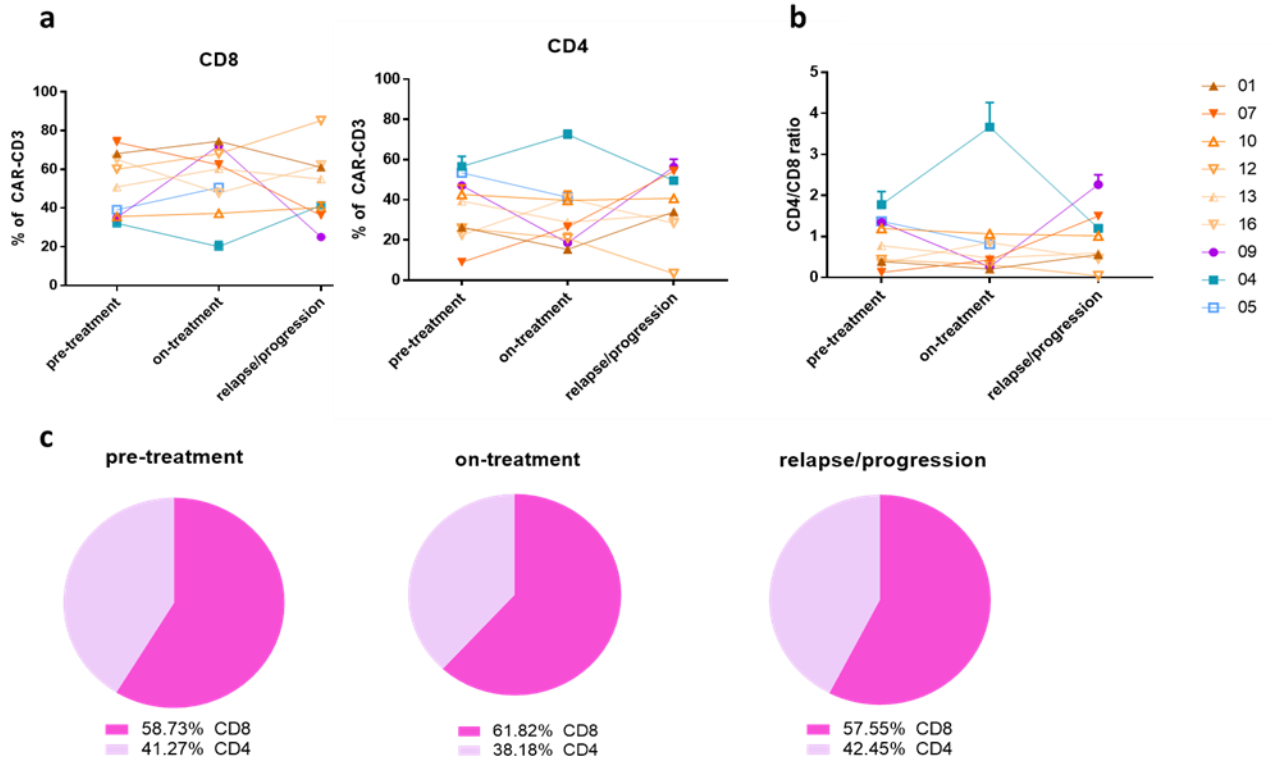


Figure 4.4: The proportion of CD4⁺ and CD8⁺ in CAR T cell population. (a) Frequencies of CD4⁺ and CD8⁺ cells within CAR⁺ T cells manufactured from PBMCs taken either pre-treatment, on-treatment or relapse/progression. Orange/brown symbols represent colorectal cancer patients, turquoise symbols indicate pancreatic cancer patients, and purple symbols represent the single glioblastoma patient. **(b)** CD4/CD8 ratio in CAR⁺ T cell population. **(c)** the mean proportion of CD4 and CD8 CAR T cells derived from PBMCs collected at different time points. (*n=9*, differences were not significant by one-way ANOVA test)

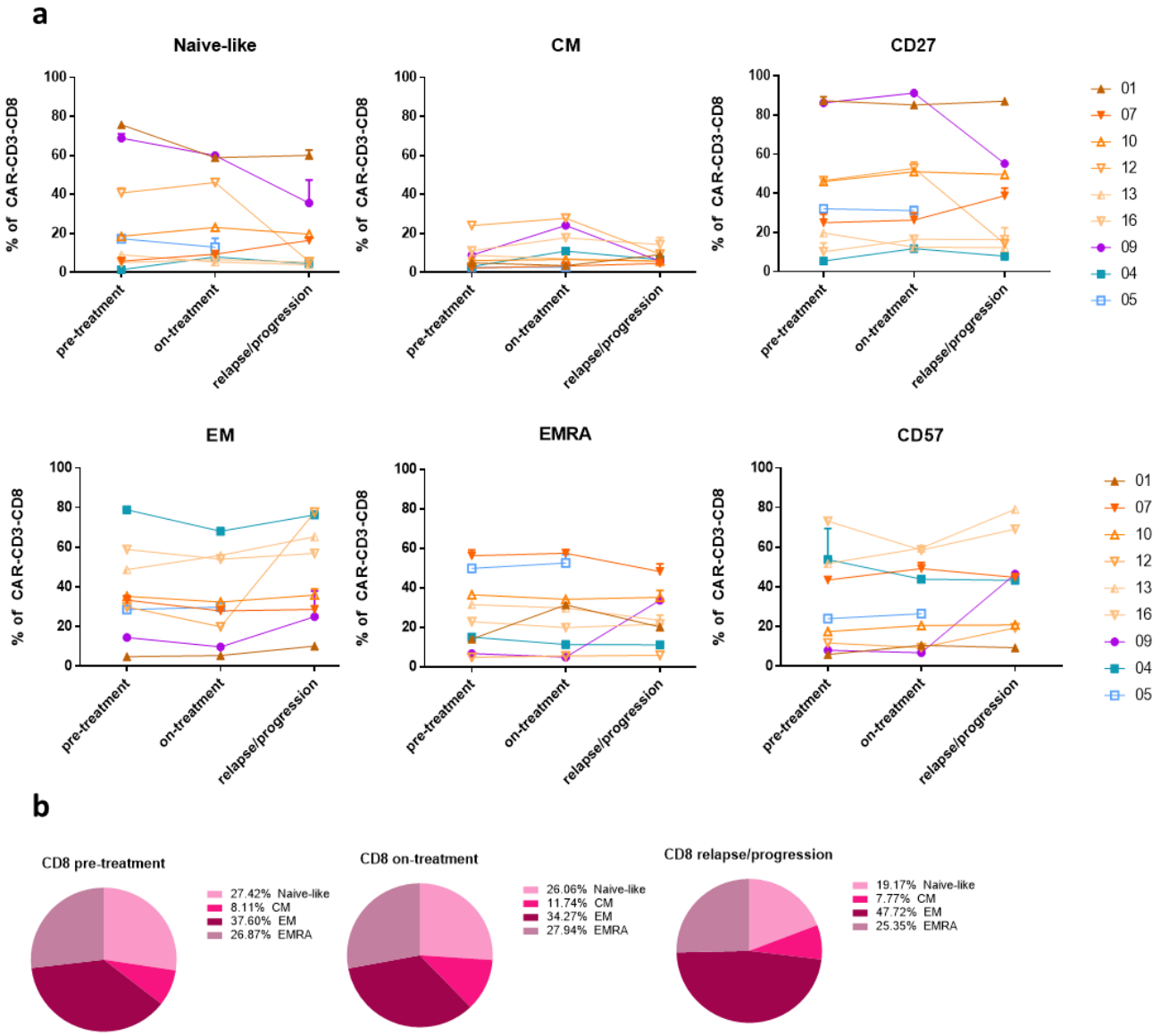


Figure 4.5: Major CD8⁺ CAR T cell subsets do not change in proportion regardless of stages of chemotherapeutic treatment. The frequency of each subset ($T_{Naive-like}$, T_{CM}, T_{EM}, T_{EMRA}, CD27⁺ and CD57⁺ within CD8⁺ CAR⁺ T cells) was obtained from 12 colour flow cytometry plots. Orange/brown symbols represent colorectal cancer patients, turquoise symbols indicate pancreatic cancer patients, and purple symbols represent the single glioblastoma patient. **(a)** Data for each patient over time. **(b)** Pie charts summarising the mean proportion of four main subsets ($T_{Naive-like}$, T_{CM}, T_{EM}, T_{EMRA}) of CD8⁺ T cells at different time points of treatment. (n = 9, no significant difference by one-way ANOVA was detected in all tests

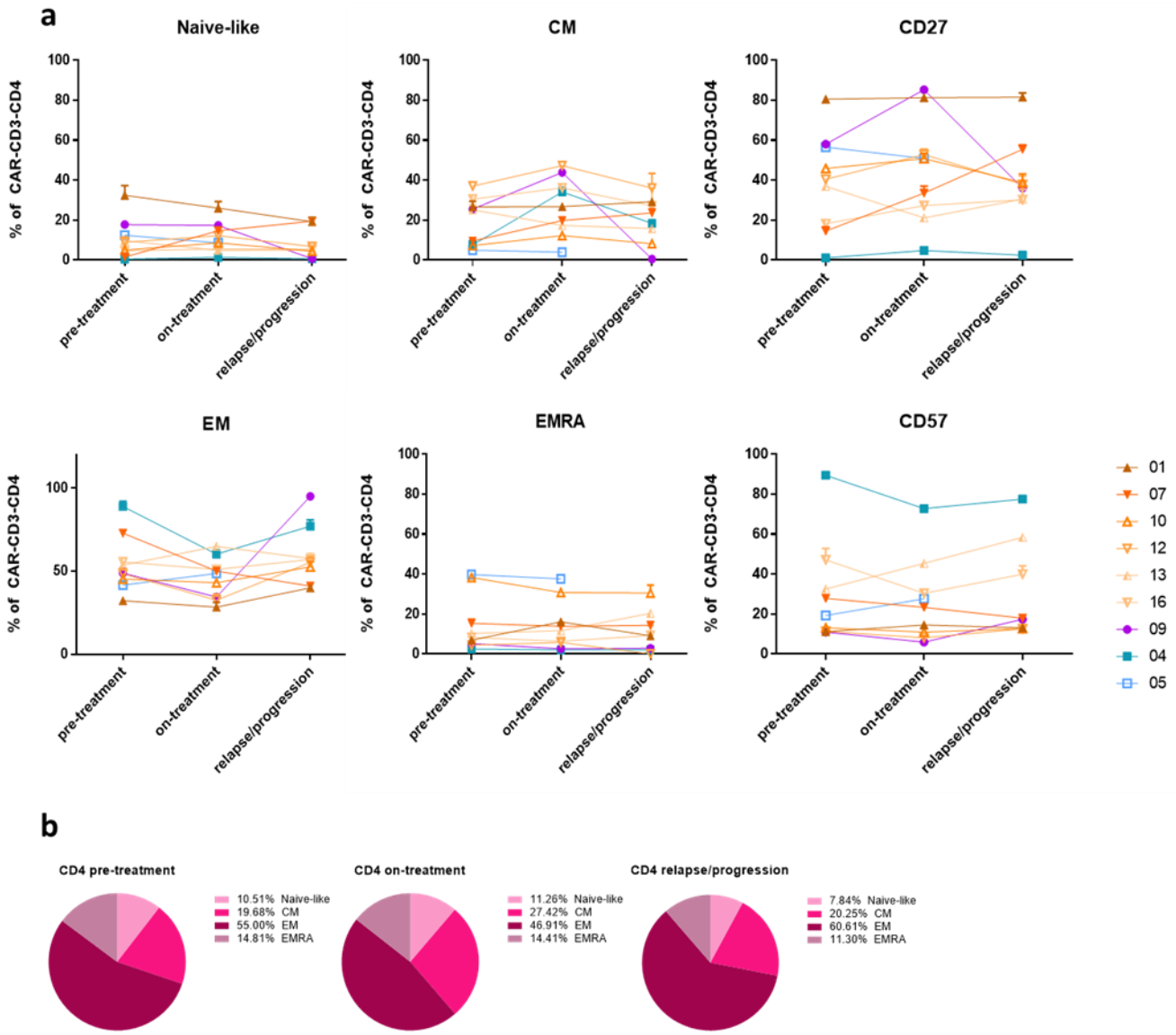


Figure 4.6: Major CD4⁺ CAR T cell subsets do not change in proportion regardless of stages of chemotherapeutic treatment. The frequency of each subset ($T_{Naive-like}$, T_{CM}, T_{EM}, T_{EMRA}, CD27⁺ and CD57⁺ within CD4⁺ CAR⁺ T cells) was obtained from 12 colour flow cytometry plots. Orange/brown symbols represent colorectal cancer patients, turquoise symbols indicate pancreatic cancer patients, and purple symbols represent the single glioblastoma patient. **(a)** Data for each patient over time. **(b)** Pie charts summarising the mean proportion of four main subsets ($T_{Naive-like}$, T_{CM}, T_{EM}, T_{EMRA}) of CD4⁺ T cells at different time points of treatment. (n = 9, no significant difference by one-way ANOVA was detected in all tests)

4.3.4 Changes in subset frequency between initial PBMC populations and final CAR T cell products

Next, a comparison of the immunophenotype of input PBMCs and final CAR T cell products was used to examine the alteration of T cell subpopulations after manufacturing. The gating strategy to determine subsets of T cells is shown in **Figure 4.7**. Here, I compared the proportion of total $CD3^+$ $CD8^+$ cells, as well as the subsets of naïve/naïve-like ($CD45RA^+$ $CCR7^+$), central memory ($CD45RA^-$ $CCR7^+$), effector memory ($CD45RA^-$ $CCR7^-$), and terminal effector ($CD45RA^+$ $CCR7^-$) between input PBMCs and the final CAR T cell product. Similar comparisons were performed for $CD4^+$ T cells and its four main immunophenotypes. Differences in the proportions of $CD8^+$ and $CD4^+$ T cells expressing CD27 and CD57 between starting populations and end products was also examined. These analyses reveal the effects of activation and culturing on the immunophenotype of the all T cells, rather than focusing on the CAR^+ population as for the preceding analyses.

The proportions of $CD4^+$ and $CD8^+$ T cells in the final products were significantly different compared to the input PBMC populations. Whereas $CD4^+$ T cells were predominant in PBMCs, $CD8^+$ T cells were the major phenotype in CAR T cell products (**Figure 4.8**). That led to a reversal of CD4: CD8 ratios, which was not observed in other studies using similar manufacturing protocols (Blaeschke, F. et al. 2018; Gargett et al. 2019).

The subset composition of $CD8^+$ and $CD4^+$ T cells was compared between the starting PBMC population and the final products (**Figure 4.9 and 4.10**). No significantly increased expansion of naïve/naïve-like or central memory cells was detected in the $CD8^+$ T cell population of CAR T cell products, although each individual sample showed alterations in their proportions during culture. Nonetheless, there was an increase in the mean proportion of effector memory $CD8^+$ T cells in the relapse/progression final products when compared to starting PBMCs. The opposite results were observed for the terminal effector $CD8^+$ T cell subset, which was reduced in all samples. Of note, relapse/progression CAR T cells showed the most striking change, which suggests that long-term chemotherapy and/or progressive disease may strongly contribute to effector phenotype-driven T cell

differentiation. Although expression of the senescence marker CD57 on $CD8^+$ T cells tended to reduce after the culture of CAR T cells, there was no statistically significant difference compared to the original PBMC population. Similar observations were made with respect to the CD27-expressing population.

Significant alterations in $CD4^+$ T cell phenotypes following activation and expansion were also observed. The proportion of naïve/naïve-like $CD4^+$ T cells and cells expressing CD27 significantly dropped in CAR T cell products compared to starting populations. In contrast, a significant enrichment of the effector memory phenotype was observed in $CD4^+$ T cells of all final products compared to input PBMC materials. A trend toward a decreased proportion of the central memory phenotype was also noted, although the difference between starting populations and the end products was not statistically significant at all time points. Interestingly, the mean percentages of $CD4^+$ terminal effector T cells and $CD4^+$ cells expressing CD57 in final products were higher than in initial PBMCs, although the difference was not statistically significant. This suggests that $CD4^+$ T cells might slowly differentiate into their exhausted/terminal stages after 10 days expansion in IL-7/IL-15 supplemented TexMACs media, and that this culture condition may not represent the optimal support for the $CD4^+$ T cell subset.

In short, the proportions of some $CD8^+$ and $CD4^+$ subsets were altered in final CAR T cell products compared to their corresponding input PBMCs, with most differences observed within the $CD4^+$ population. The CD4/CD8 ratios observed in the starting PBMC population were not maintained in the final products. The CAR T cell manufacturing procedure resulted in a significant expansion in both $CD8^+$ and $CD4^+$ T cells of effector memory phenotype, a decrease in the proportion of naïve-like and CD27-expressing $CD4^+$ T cells, and a trend toward an increased proportion of CD57-expressing terminal effector and senescent $CD4^+$ T cells in the final product. The expansion protocol also resulted in a considerable drop in the frequency of terminal effector $CD8^+$ T cells. Interestingly, the proportions of "young" (naïve/naïve-like, central memory, and $CD27^+$ cells) $CD8^+$ T cells were preserved in the final products and were at levels similar to those observed for input PBMCs.

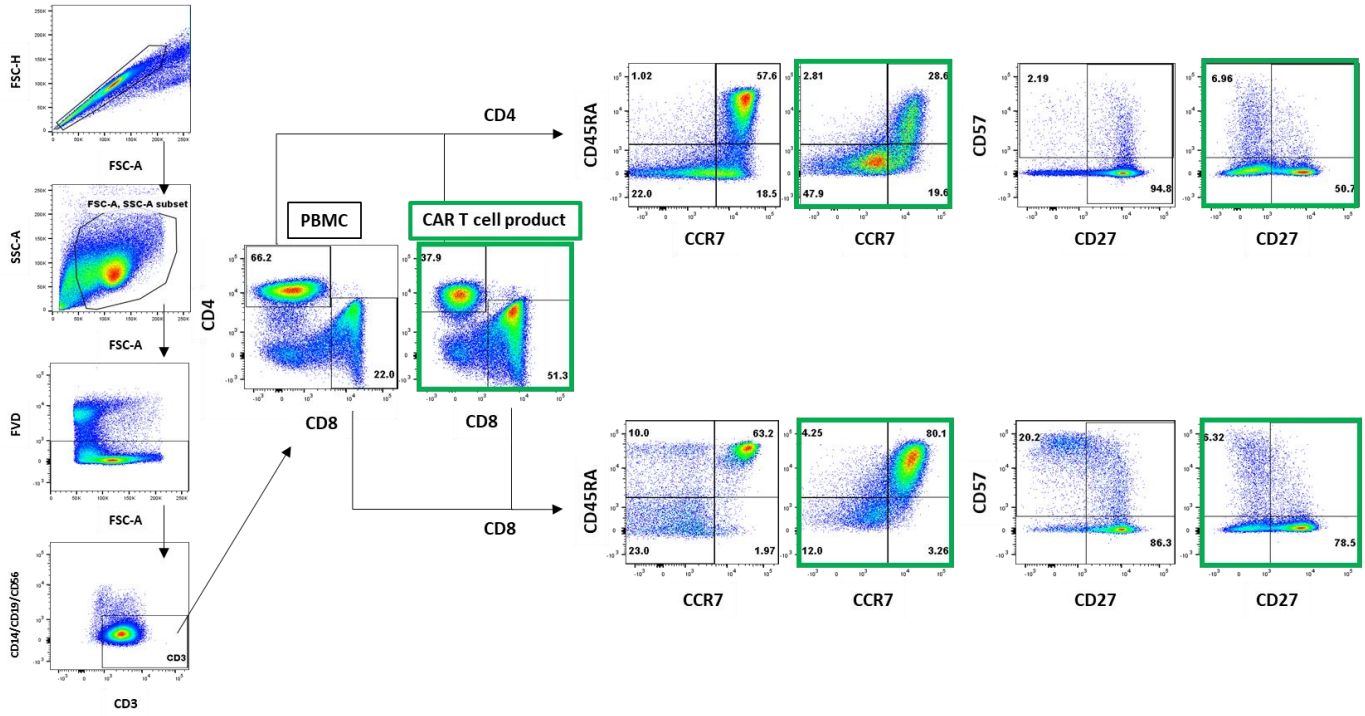


Figure 4.7: Gating strategy and representative plots of phenotypes of initial PBMCs and CAR T cell product. PBMC plots are outlined in black. CAR T cell product plots are outlined in green. This gating strategy was applied for data analyses in **Figure 4.8**, **Figure 4.9**, and **Figure 4.10**

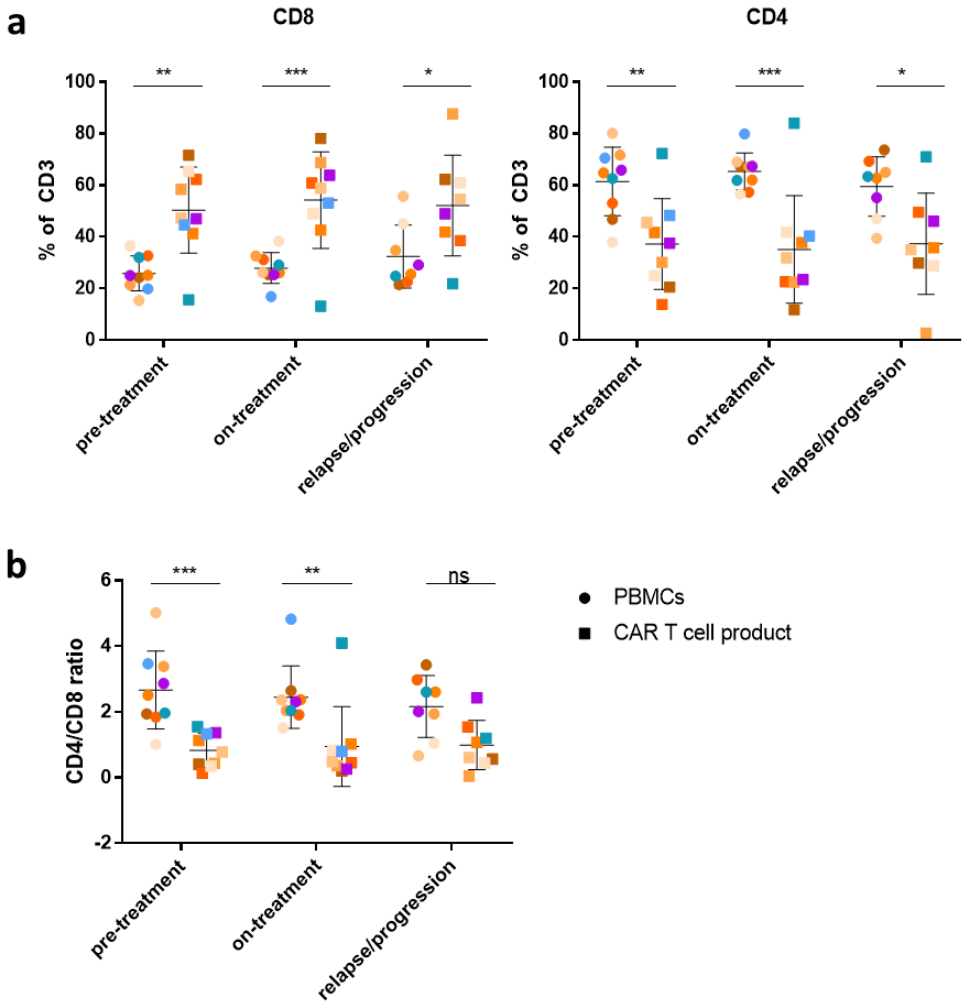


Figure 4.8: Alteration in CD8⁺ and CD4⁺ T cell frequencies in final products compared to original PBMC population. T cell phenotypes were determined based on flow cytometric results. **(a)** Data of CD8 and CD4 population for each patient. **(b)** CD4/CD8 ratio . Orange/brown symbols represent colorectal cancer patients, turquoise symbols indicate pancreatic cancer patients, and purple symbols represent the single glioblastoma patient. (n=9, line represents mean, error bars represent SD, ANOVA two-way test, *p<0.05, **p<0.005, ***p<0.0005, ns: not significant)

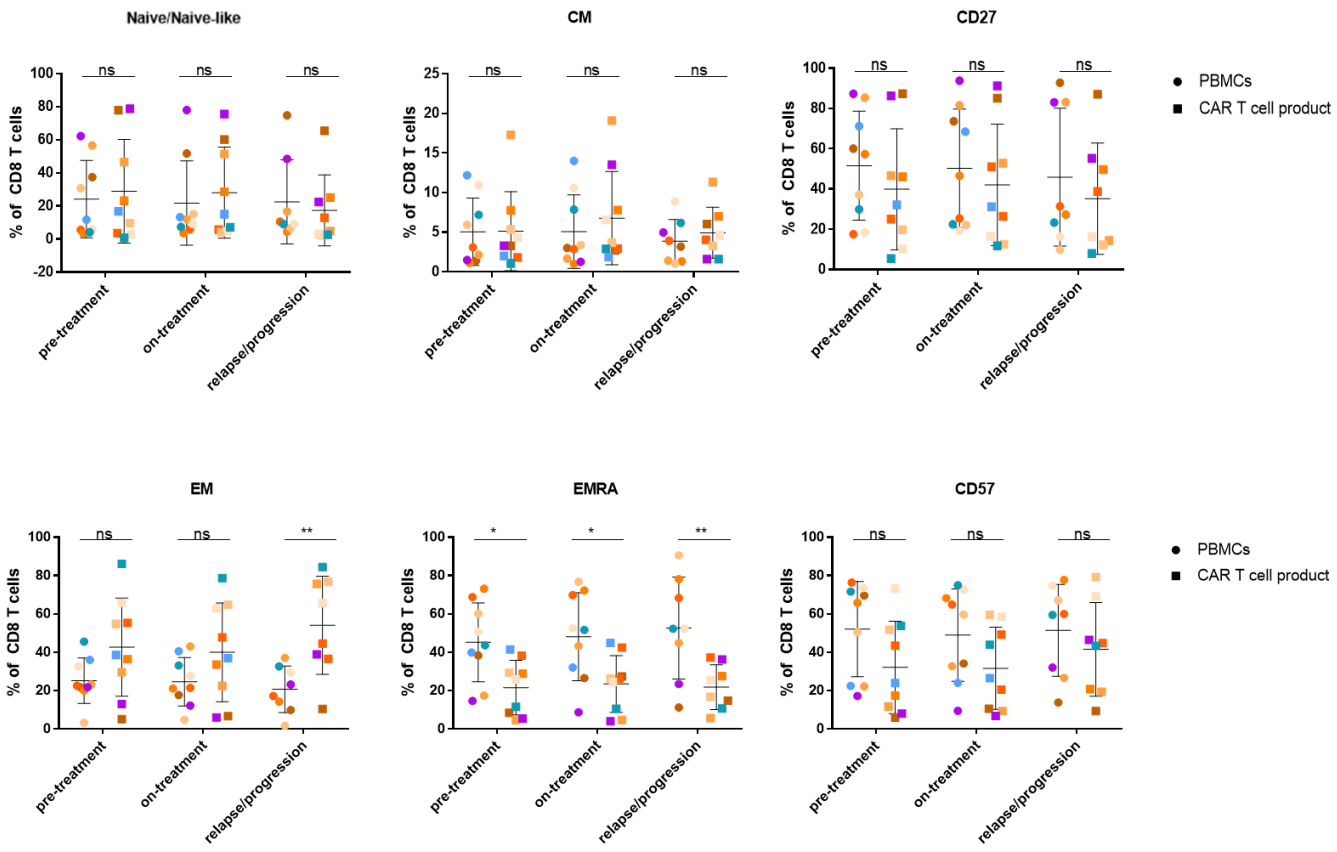


Figure 4.9: Alteration in major CD8⁺ T cell subset frequencies in final products compared to original PBMC population. T cell subset phenotypes (naïve T cells, central memory T cells, effector memory T cells, terminal effector T cells, $CD27^+$ and $CD57^+$ within $CD8^+$ T cells) were determined based on flow cytometric results. Subset phenotypes were determined as follows: naïve T cells ($CD45RA^+$ $CCR7^+$), central memory T cells ($CD45RA^-$ $CCR7^+$), effector memory T cells ($CD45RA^-$ $CCR7^-$), terminal effector T cells ($CD45RA^+$ $CCR7^-$). Orange/brown symbols represent colorectal cancer patients, turquoise symbols indicate pancreatic cancer patients, and purple symbols represent the single glioblastoma patient. (n=9, line represents mean, error bars represent SD, ANOVA two-way test, *p<0.05, **p<0.005, ns: not significant)

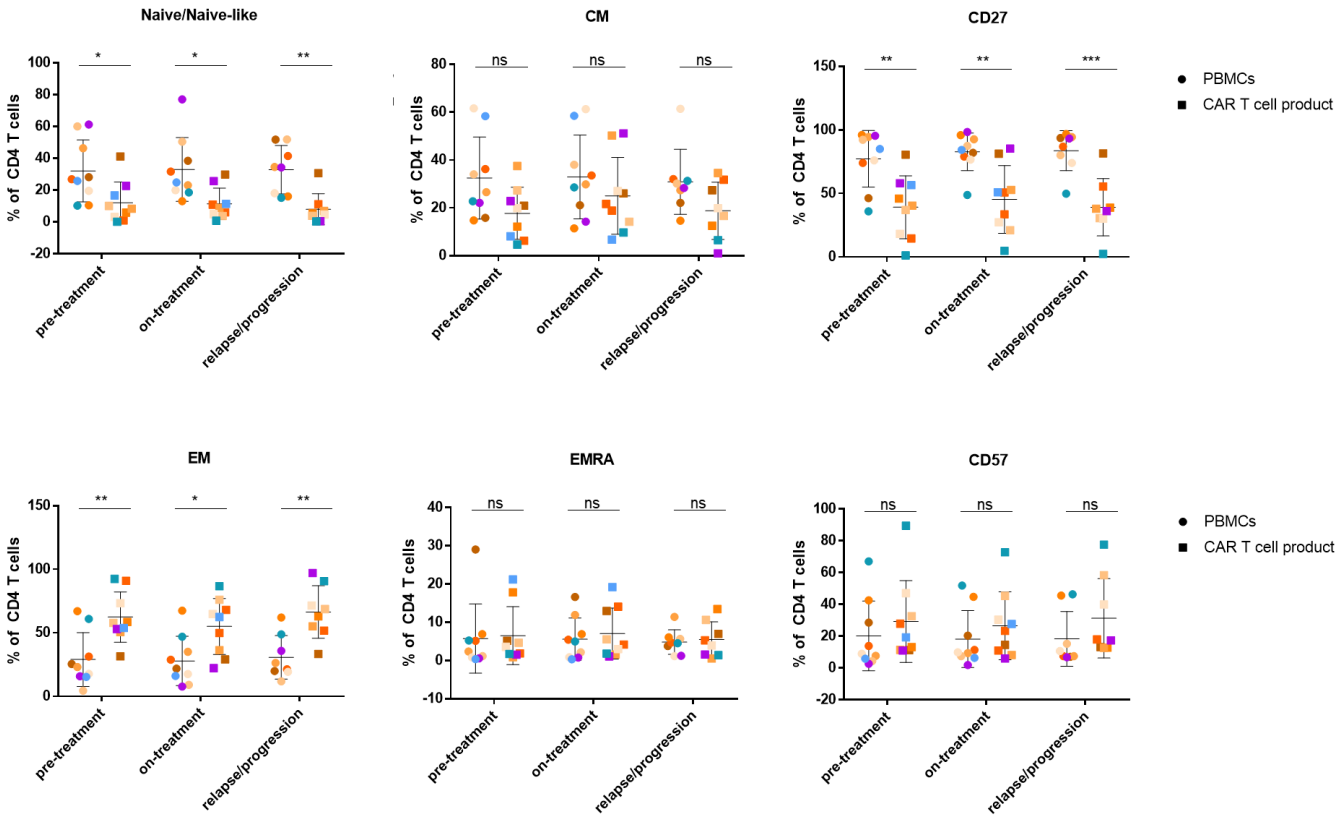


Figure 4.10: Alteration in major CD4⁺ T cell subset frequencies in final products compared to original PBMC population. T cell subset phenotypes (naïve T cells, central memory T cells, effector memory T cells, terminal effector T cells, CD27⁺ and CD57⁺ within CD4⁺ T cells) were determined based on flow cytometric results. Subset phenotypes were determined as follows: naïve T cells(CD45RA⁺ CCR7⁺), central memory T cells (CD45RA⁻ CCR7⁺), effector memory T cells (CD45RA⁻ CCR7⁻), terminal effector T cells (CD45RA⁺ CCR7⁻). Orange/brown symbols represent colorectal cancer patients, turquoise symbols indicate pancreatic cancer patients, and purple symbols represent the single glioblastoma patient. (n=9, line represents mean, error bars represent SD, ANOVA two-way test, * p<0.05, **p<0.005, ***p<0.0001, ns: not significant)

4.4 Conclusion

I have shown that, in general, manufacturing CAR T cells from cancer patients' PBMCs collected at different treatment time points is feasible, however I did not successfully manufacture CAR T cells at every time point for every patient. Transduction rates and fold expansion of transduced T cells showed no statistically significant differences among PBMCs collected at different time points. Despite a normal range of CD4/CD8 ratios observed in the initial PBMCs, the final CAR T cell products showed a predominance of $CD8^+$ T cells, especially at the on-treatment time point, which was not expected using our protocol (Gargett et al. 2019). No significant differences in the composition of T cell naïve/memory phenotypes were observed between products at any time points. By comparing the final CAR T cell products to their corresponding input PBMC populations, the proportions of $CD8^+$ T cells at different stages of differentiation were preserved with no significant changes observed in proportions of naïve/central memory cells or terminal/senescent cells. In contrast, CD4 T cells might be driven more toward a terminal effector/senescent stage of differentiation after expansion.

Chapter 5

Functions of CAR T cells manufactured from PBMCs collected at different time points

5.1 Overview

In this chapter, the function of CAR T cells was investigated. Several approaches such as the real time cytotoxicity (xCELLigence) assay, AICD assay, and multi-colour flow cytometry were used to compare the phenotype and function of CAR T cells derived from PBMCs at different treatment time points: pre-(chemotherapy) treatment, on-treatment, and at relapse/progression. I determined that the intrinsic fitness of T cells at the time of manufacturing may be a critical factor that affects CAR T cell function.

5.2 Introduction

The most important goal of CAR T cell therapy is to reconstitute in cancer patient an effective anti-cancer cellular immune response, which includes persisting populations of memory T cells (Xu, X-J, Zhao & Tang 2013). Adoptive CAR T cell therapy in selected haematological cancers induces sustained anti-cancer effects but using these genetically modified autologous T cells to treat solid cancers has not been as successful (Kochenderfer & Rosenberg 2013; Lamers et al. 2013). Several factors that contribute to the failure of CAR T cell therapy in solid tumours have been suggested. Among them, short lifespan and limited expansion of CAR T cells post infusion were determined to relate directly to negative clinical outcomes (Fraietta et al. 2018; Louis, CU et al. 2011). Strong cytotoxic effector functions of CAR T cells are also important for successful cellular immunotherapy. Therefore, increasing cell persistence and expansion post infusion is essential for fully executing antigen-specific engineered T cell effector functions and here I have sought to profile markers associated with T cell persistence and a high level of function of our CAR T cell products.

The short-term persistence of CAR T cells has been attributed to several factors. ACID due to the binding of the IgG region of the spacer element of CAR molecules to Fc receptors on other immune cells was reported in several studies (Hudecek et al. 2015; Künkele et al. 2015; Long, A. H. et al. 2015). Re-engineering CAR structures with modified spacer elements could help to resolve this issue. AICD may also be initiated by antigen-specific activation of CAR T cells. In addition, the engagement of programmed cell death protein 1 (PD-1) or Fas expressed on the T cell surface with their ligands (PD-L1/PD-L2 and FasL) on tumour cells can suppress the CAR T cell response and stop cells from proliferating after antigen encounter (Gargett et al. 2016; Künkele et al. 2015; Latchman et al. 2001). Our phase 1 clinical trial of GD2-CAR T cells in melanoma patients has revealed limited cell expansion *in vivo*, a decrease in viability and an increase in PD-1 expression on transduced T cells after antigen-specific activation *in vitro* (Gargett et al. 2016). Importantly, we also showed that blocking PD-1 on CAR T cells can protect them from AICD, which may result in greater persistence of CAR T cells post infusion (Gargett et al. 2016).

Interestingly, PD-1 blockade not only improves cell viability but also can potently enhance T cell cytotoxicity, and the addition of PD-1 inhibitor (pembrolizumab) to co-cultures of CAR T cells and target cells could increase CAR-T cell cytotoxic activity (Gargett et al. 2016; John et al. 2013). This finding was supported by a recent study on response and resistance to CD19-CAR T cell therapy in chronic lymphocytic leukemia. The study showed that the percentage of $CD8^+$ CAR T cells expressing the exhaustion marker PD-1 in patients who had a complete response was significantly lower than what was seen for patients with a partial response and in non-responders (Fraietta et al. 2018). Results of these studies suggest that CAR T cell products containing a limited proportion of $PD\text{-}1^+$ CAR^+ T cells might be the most effective preparation to increase anti-tumour effectiveness in solid cancers.

Proliferative capacity strongly correlates with anti-tumour potency of CAR T cells (Fraietta et al. 2018). Several cytokines are released by activated lymphocytes and promote T cell proliferation and acquisition of cytotoxic function (Boyman, O, Le´tourneau, S., Krieg, C., & Sprent, J. 2009; O'Shea, Gadina & Siegel 2019). It is well-known that interleukin (IL)-2 is a T cell growth factor which is produced mostly by activated T cells. It acts in an autocrine manner to maintain the activation state and proliferation of $CD4^+$ and $CD8^+$ T cells (Cheng et al. 2002). Therefore, a CAR T cell product intrinsically producing a high concentration of IL-2 may have a strong expansion capacity *in vivo.*

CAR T cells promote anti-tumour effects via a combination of mechanisms (Benmebarek et al. 2019). Direct, antigen-specific CAR T cell and tumour cell interaction can result in perforin and granzyme secretion (Maher et al. 2002), and cytotoxic cytokines released by activated CAR T cells can indirectly destroy tumour and stromal cells (Textor et al. 2014). Interferon gamma (IFN-γ) and tumour necrosis factor alpha (TNF) are mainly produced by activated T cells (Kearney et al. 2018; Textor et al. 2014). Furthermore, the anti-tumour capabilities of other native T cells are supported by cytokine-mediated recruitment of dendritic cells and macrophages into tumour sites (Shi et al. 2006). These professional antigen presenting cells respond to granulocyte-macrophage colony-stimulating factor (GM-CSF) and IFN-α, which are also released by activated CAR T cells (Ferrantini, Capone & Belardelli 2007; Shi et al. 2006). Therefore, analysing cytokine

release post CAR T cell re-activation gives an insight into their proliferative capacity and anti-tumour functionality.

To evaluate CAR T cell function and possible persistence *in vivo* in this study, a real-time cytotoxicity assay, multiplex cytokine analysis, quantification of exhaustion/senescence markers on activated CAR T cells, and assessments of CAR T cell viability post activation have been employed. The xCELLigence real-time cytotoxicity monitors the killing effect mediated by each CAR T cell product in real time (Cerignoli et al. 2018). The principle of this assay is based on measuring electrical impedance through gold microelectrodes embedded at bottom of microtiter wells, with adherent target cells as insulators. The impedance signals are automatically measured at a certain frequency over time. The read-out provides a sensitive assessment (cell index) of viable cell number, which can be converted to percentage cytolysis and other relevant kinetic parameters such as time to achieve 30% or 50% of killing effect (KT_{30} or KT_{50}) (Cerignoli et al. 2018). This powerful assay can be performed at a low effector: target cell ratio, which is physiologically relevant, and provides kinetic information on CAR T cell cytotoxic activity among different groups of samples.

A MACSPlex Cytokine 12 kit (Miltenyi Biotec) was used for measuring concentrations of various cytokines released by activated CAR T cells, in particular IFN-γ and TNF, which are associated with CAR T cell cytotoxic functions, and IL-2 which is a hallmark of T cell self-renewal and proliferation (Shen et al. 2018; Spolski, Lin & Leonard 2014) . Expression of the PD-1 exhaustion marker and the CD57 terminal differentiation marker on activated CAR T cells was also analysed using multicolour flow cytometry, to serve as indicators for the likely proliferative potential of these cells (Brenchley et al. 2003a; Okazaki & Honjo 2006). The expression of exhaustion/senescence markers and cytokine production capacity, as well as the viability of CAR T cells post CAR stimulation, were compared between CAR T cells produced from blood collected at the three different time points. These results allowed identification of the intrinsic fitness of CAR T cells manufactured from PBMCs at different treatment time points, and thus helped understanding of the influence of chemotherapy on functional capacity of the final CAR T cell product. In this section individual patients are represented by a constant symbol in the

data (e.g. patient #01 filled triangle, patient #04 filled square), allowing the reader to directly compare the functionality of a particular patient product between assays.

5.3 Results

5.3.1 CAR T cells derived at different phases of cancer chemotherapy were competent at killing target cancer cells

To examine whether the input cells used for CAR T cell manufacturing result in differences in the cytotoxicity of the final product, I conducted a real time cytotoxicity xCELLigence assay with different effector: target cell ratios (5:1 and 2:1) (Cerignoli et al. 2018). LAN-1 cells, a neuroblastoma cell line expressing the GD2 molecule at high level, were used as target cells, and CAR T cells or non-transduced control T cells were used as effector cells. The E:T ratios examined represent the ratio between the number of total T cells in final products (not CAR^+ T cells) and the number of target cells. The assay was designed to run for a minimum of 72 hours (three days) to more than 120 hours (five days). This allowed us to observe the temporal difference in the killing effects mediated by CAR T cells derived at different treatment time points.

As shown in **Figure 5.1a**, the addition of CAR T cells to LAN-1 cells gave rise to a time-dependent drop in cell index values. There was no reduction of cell index after adding non-transduced T cells or media to target cells. The observed reduction in cell index represents a loss in target cell viability and can be converted to percent cytolysis values via a mathematical formula that compares cell index values of test wells to values in control wells containing target cells alone (Cerignoli et al. 2018). As seen in the **Figure 5.1b**, the percentage of LAN-1 lysis increases in a time- and E:T ratio-dependent manner and varies according to the CAR T cell population used. Cytotoxicity curves of CAR T cells derived from patient #16 (colorectal cancer) and patient #09 (glioblastoma) are shown in these figures to illustrate the inter-patient and inter-CAR T cell product variability. On-treatment CAR T cells from these two patients were able to kill 30% of target cells within 10 hours (5:1 E:T ratio) while CAR T cells at other time points required longer time (patient #16 pre-treatment and relapse/progressive) or were unable (patient #09 pre-treatment) to reach 30% of target cell killing. CAR T cells at lower E:T ratios (2:1) required double the time

compared to that at the 5:1 E:T ratio to achieve 30% target cell killing. There was no cytotoxic activity observed in using non-transduced T cells as the controls. For several of the patient-derived CAR T cells tested pre-treatment and at relapse/progression (patients #04, #09 and #12), CAR T cells failed to reach 30% cytolysis after 60 hours, indicating a dysfunctional CAR-T cell product (**Figure 5.1c**). Interestingly, on-treatment CAR T cell products showed an extremely strong cytotoxic effect. These products still killed most target cells at the 5:1 ratio even though only 8% of T cells expressed the CAR. This ratio would equate to an actual ratio of about 2.5 tumour cells to each CAR^+ T cells. Remarkably, the mean percentage of cell killing of on-treatment CAR T products appeared higher than that of other products at all given time points (**Figure 5.1d**), although this trend was not statistically significant.

In summary, the real-time cytotoxicity assay allowed us to measure the cytotoxicity of all CAR T cells over time, revealing that the on-treatment CAR T cells demonstrated robust killing of antigen-positive tumour cells. In fact, on-treatment CAR T cells trended toward higher levels of cytotoxicity compared to CAR T cells manufactured at pre-treatment and relapse/progression time points, although further patient samples are required to confirm this preliminary observation.

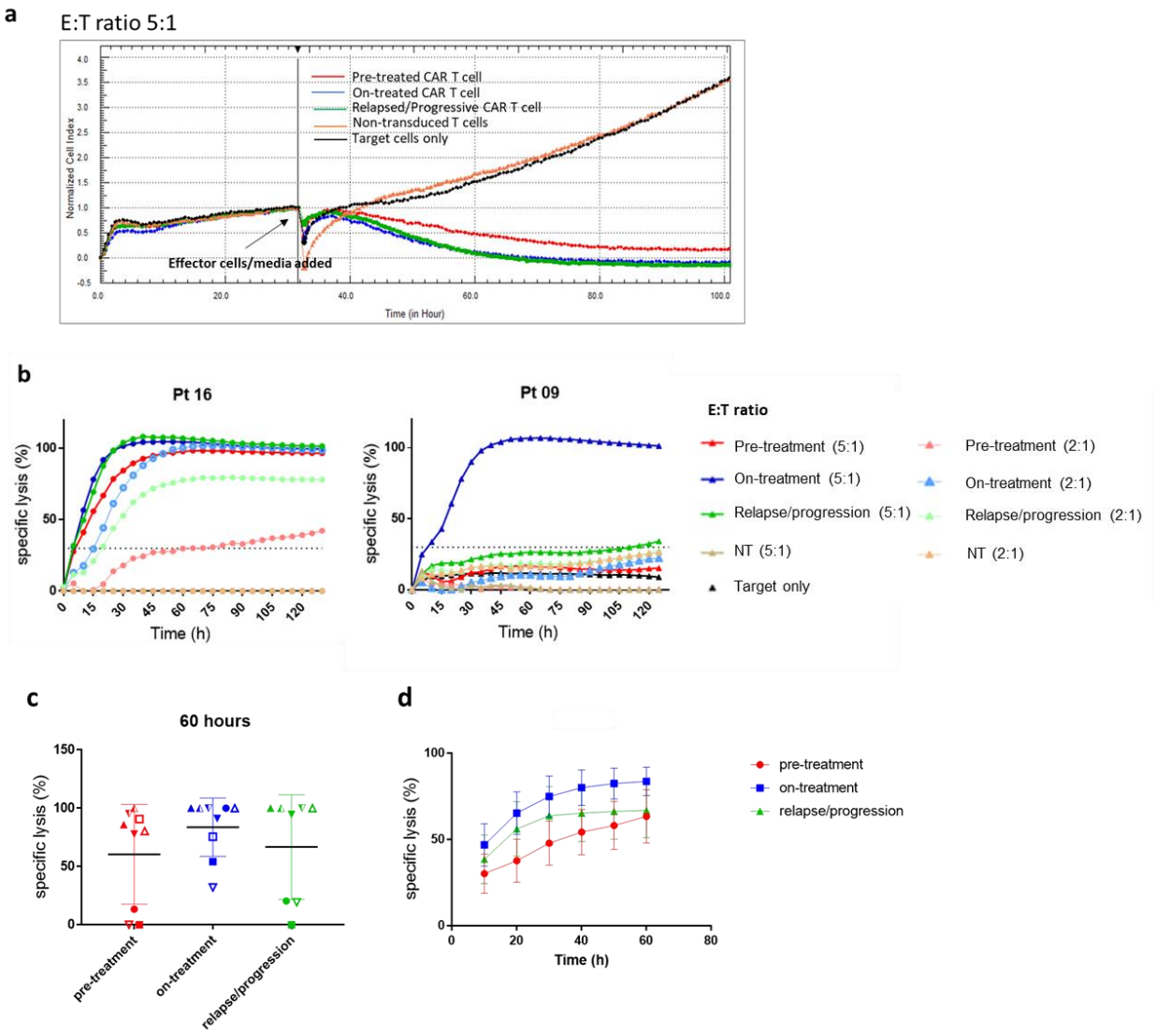


Figure 5.1: Killing of LAN-1 tumour cells by different CAR-T cell populations. (a) Representative Normalised Cell Index plot for GD2-expressing LAN-1 target cells treated with 5:1 ratio of different types of CAR T cells/non-transduced T cells/medium only. Raw Cell Index values were internally normalised relative to the measurement immediately prior to effector cell/medium addition. **(b)** Representative cytolysis plots for two patients, comparing cytotoxic effect of CAR T cells prepared from blood collected at different time points and tested at effector:target ratios of 5:1 or 2:1. Specific lysis (%) was calculated using cell index data from test wells relative to wells containing target cells alone, according to the formula presented in Methods, and is presented as the mean of duplicate wells. Time 0 represents the time of effector cells/ media addition. Dotted line marks the 30% killing threshold. **(c)** % cytolysis measured at 60 hours after adding effector cells/ medium at the 5:1 E:T ratio. Line represents mean and error bars represent SD. No significant difference by one-way ANOVA was detected. **(d)** % cytolysis for CAR T cells (at the 5:1 E:T ratio) prepared from all 9 patients using blood collected at the 3 different time points. Values represent mean and SEM. No significant difference by two-way ANOVA was detected in all tests (n= 9, NT: non-transduced T cells)

5.3.2 CAR T cells manufactured from on-treatment blood samples are less sensitive to AICD

CAR T cell persistence and survival is significantly affected by AICD and programmed cell death (PCD), which have been studied in both pre-clinical and clinical settings (Gargett et al. 2016; Tschumi et al. 2018b). AICD is attributable to excessive T cell stimulation while PCD is associated with the upregulation of Fas (CD95)/FasL expression (Tschumi et al. 2018b). To test the sensitivity of CAR T cells manufactured from pre-treatment, on-treatment, and relapse/progression patient blood samples, the percentage of viable CAR T cells was compared between different products to analyse the viability of CAR T cells after CAR stimulation using the anti-idiotypic antibody CAR-specific, 1A7, or in the absence of activation. Final products were activated in fully supplemented medium for 3 days using plate-bound CAR-specific antibody or not. Activated and non-activated cells were collected for subsequent flow cytometry to check cell viability. BD Horizon fixable viability stain 700 (FVS700) was used together with other antibodies in the 12- colour flow cytometry panel for the discrimination of viable from non-viable cells. Representative data are shown in **Figure 5.2a**. As shown in **Figure 5.2b**, on-treatment CAR T cell products were the least susceptible to cell death, while relapse/progression CAR T cell products were the most sensitive. Differences in cell viability of on-treatment CAR T cell products were statistically significant compared to pre-treatment and relapse/progression products in the resting state (mean = 66%; SD = 19), (mean = 54%; SD = 22), (mean= 46%; SD =25), respectively. In particular, on-treatment CAR T cells showed remarkable preservation of viability compared to relapse/progression CAR T cell products after antigen-specific stimulation (mean= 62%; SD = 19) and (mean = 40%; SD = 21), respectively. As analysed in the previous chapter, CD95 expression on CAR T cells, was uniformly positive at all time points. Similar results were observed in activated CAR T cells (**Figure S1**). CD95 (Fas molecule) was determined to mediate PCD in T cells via interaction with FasL expressed on target cells or other T cells (Brunner et al. 1995; Mak & Saunders 2006; Tschumi et al. 2018b). In addition, all CAR T cells expressed the CAR molecule at equivalent levels. So, the observed increase in cell death for the CAR T cells at relapse/progression is unlikely to result from the level of CD95 or CAR expression but may instead indicate a lower intrinsic fitness of the T cells.

In summary, on-treatment CAR T cells had improved survival compared to CAR T cells of other groups. Moreover, this difference was observed under conditions of both rest and stimulation.

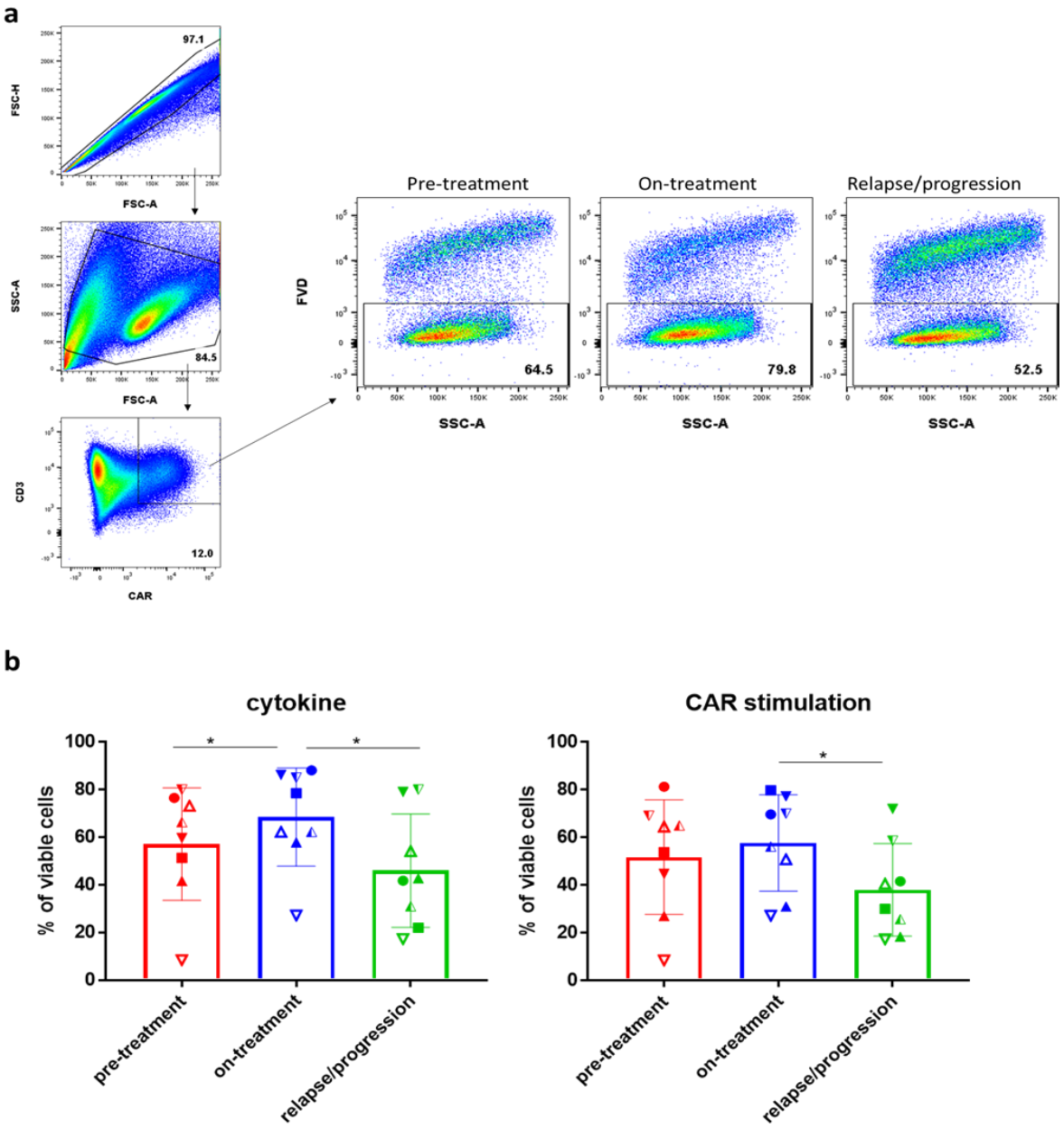


Figure 5.2: Differences in cell death occurring spontaneously or after specific CAR stimulation. CAR T cells were either resting in supplemented TeXMACs media or activated using plate-bound specific antibody for three days. Then, all samples were stained with antibodies of a 12-colour panel and analysed by flow cytometry to determine viability and detect different T cell subsets. **(a)** The gating strategy to detect the viability of CAR^{+}T cells is shown. All events from the scatter gate (excluding small debris) were assessed for expression of CD3 and CAR molecules, and double positive events were gated for further analysis. Fixable Viability Stain 700 was used to discriminate viable from non-viable cells. **(b)** CAR T cell viability after three days cultured in cytokines alone or after CAR stimulation. Columns represent mean and error bars represent SD. (n=9, ANOVA one-way test, * $p<0.05$)

5.3.3 Change of exhausted markers on T cell and CAR T cells in the final transgenic T cell products

To further assess how exhausted and/or senescent CAR T cells were after activation, post-activation T cell expression of PD-1, CD27 and CD57 was analysed after use of either anti-CD3 and anti-CD28 antibodies for universal activation or the 1A7 antibody for activation via the CAR. The mean percentage of PD-1 expressing cells was ~20% for both $CD8^+$ and $CD4^+$ CAR T cells under resting conditions. Post activation, the mean proportion of PD-1^+ $CD8^+$ CAR T cells in all three groups was mostly unchanged, whereas PD-1 expressing $CD4^+$ CAR T cells increased up to ~30% (pre-treatment and on-treatment) and ~40% (relapse/progression) (**Figure 5.3a – 5.3b**). In short, stimulation of CAR T cells caused a significant increase in PD-1 expression in the $CD4^+$ population, whereas stimulated $CD8^+$ CAR T cells showed a similar level of PD-1 expression compared to non-stimulated cells, and there were no striking differences in PD-1 expression among treatment groups.

Similar to PD-1, the expression pattern of CD27 on $CD8^+$ and $CD4^+$ CAR T cells was consistent among CAR T cells at different phases of chemotherapy (**Figure 5.3c-5.3d**). The level of CD27 expression varied considerably from patient to patient and was not significantly altered following activation via the CAR. The percentage of $CD27^+$ cells ranged from 10% to 80% between phase of chemotherapy and activation conditions. These data suggest that each CAR T cell product has a distinct and cell autonomous pattern of CD27 expression that was not substantially affected by phase of chemotherapy or activation conditions. However, there was a trend toward reduction in the proportion of $CD27^+$ $CD4^+$ CAR T cells observed following universal activation of relapse/progression CAR T cell products (**Figure 5.3d**), which may indicate that these products are no longer "young" or more likely to become terminally differentiated after stimulation.

The immunosenescent marker CD57 showed a similar pattern of expression to CD27, in that no major differences by phase of chemotherapy or activation conditions were observed. However, there was considerable variation among individuals, and the

percentage of $CD57^+$ cells ranged from 4% to 60% (**Figure 5.3e and 5.3f**). The proportion of $CD57^+$ cells among $CD8^+$ CAR T cells was more varied compared to $CD4^+$ CAR T cells. Most $CD4^+$ CAR T cells had a consistently low level of CD57 expression, except for samples from patient #04. CAR T cells manufactured from PBMCs of patient #04 significantly upregulated CD57 expression in all $CD4^+$ T cell populations (pre-treatment, on-treatment, and relapse/progression) in resting condition and after activation (**Figure 4.6a**). The striking CD57 upregulation was not seen in CAR T cells of the $CD8^+$ subset, although this sample had a high proportion of $CD57^+$ $CD8^+$ CAR T cells compared to other products.

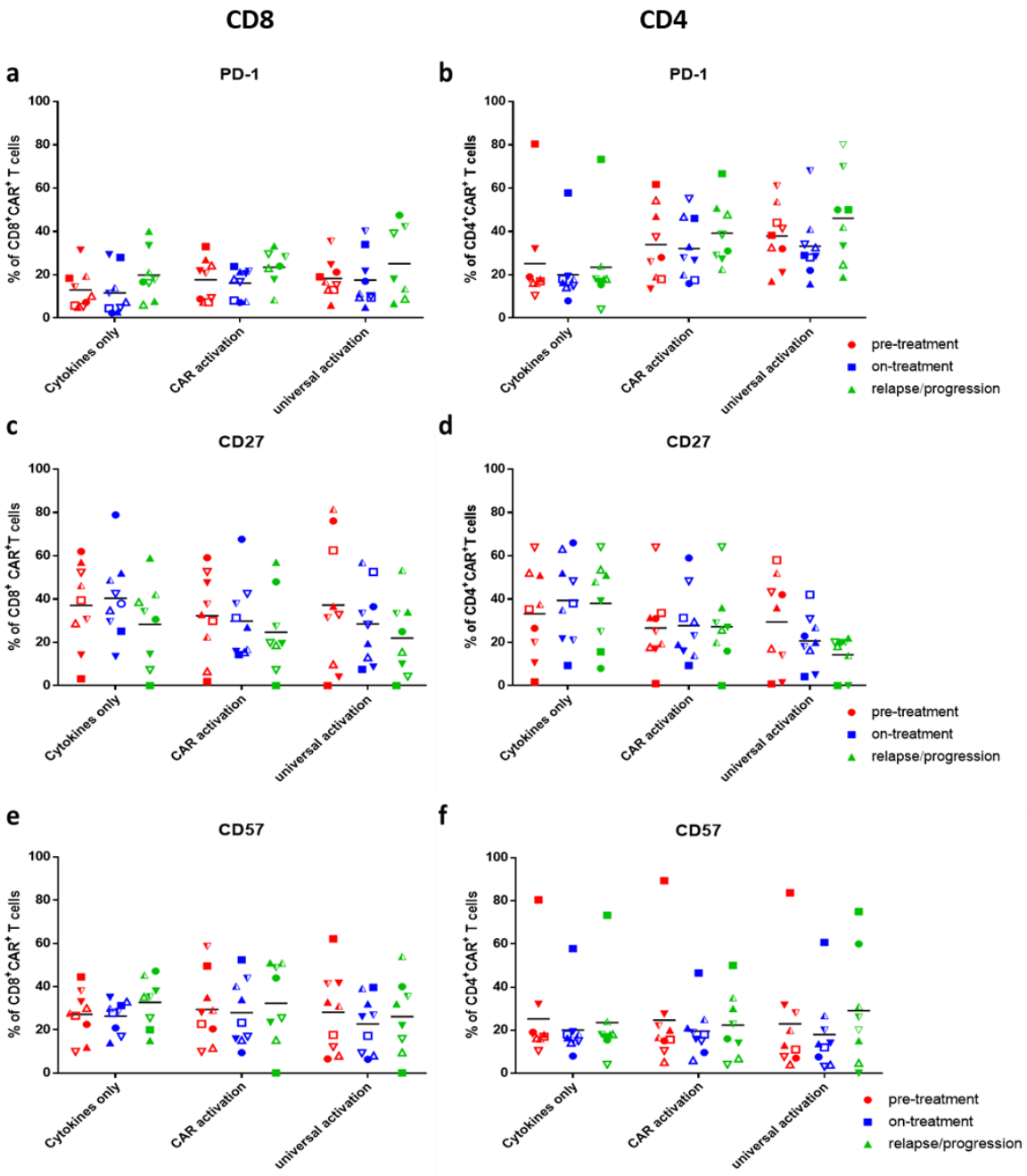


Figure 5.3: Expression of exhaustion and senescence markers by CAR T cells following stimulation. CAR T cells were either left in TexMACS medium supplemented with IL-7/IL-15 (cytokine only) or activated using plate-bound specific antibody (CAR activation) or CD3/CD28 antibodies (universal activation). After three days, cells were stained and analysed by flow cytometry to identify T cell subsets and assess expression of PD-1, CD27 and CD57. **(a)** PD-1 expression on $CD8^+$ CAR^+ T cells, **(b)** PD-1 expression on $CD4^+$ CAR^+ T cells. **(c)** CD27 expression on $CD8^+$ CAR^+ T cells. **(d)** CD27 expression on $CD4^+$ CAR^+ T cells. **(e)** CD57 expression on $CD8^+$ CAR^+ T cells. **(f)** CD57 expression on $CD4^+$ CAR^+ T cells. (n=9, line represents mean, no significant difference by two-way ANOVA was detected in all tests.)

5.3.4 Cytokine profile of CAR T cell products after activation

To address whether the cytokine profile was altered between CAR T cell products manufactured at different phases of chemotherapy, I used a MACSPlex Cytokine 12 kit for detecting and measuring cytokine concentrations. As shown in **Figure 5.4**, seven out of nine patients had their CAR T cell products being able to produce INF-γ, TNF and IL-2 above resting levels. Notably, activating CAR T cells via the CAR caused a significantly lower IFN-γ and TNF release compared to cells activated through CD3/CD28 molecules. Pre-treatment and relapse/progression CAR T cells manufactured from patients #04, #09 and #12 secreted only low levels of IFN-γ and TNF after activation. CAR T cells generated from patient #01 released the highest level of IL-2 following activation, suggesting high proliferative capability. Consistent with this, T cells derived from this patient also showed strong proliferation during the CAR T cell manufacturing process (**Figure 4.1a**). These observations may suggest that activation-induced release of IL-2 mainly depends on the intrinsic fitness of T cells.

All activated CAR T cell products produced GM-CSF at a concentration six times higher than resting cells (**Figure S2**). IL-6, another cytokine related to cytokine release syndrome, a CAR T cell therapy-related toxicity (Santomasso et al. 2019), did not show a significant increase in cytokine concentration in the supernatant of T cells activated via the CAR molecule or via CD3 and CD28 molecules (**Figure S2**). **Table S2** indicates the mean concentration of the other cytokines that were measured. Concentrations of IL-10, which is a suppressive cytokine, and IL-17, which is related to tumour-associated inflammation, were present at very low levels and did not increase after CAR-specific or universal activation.

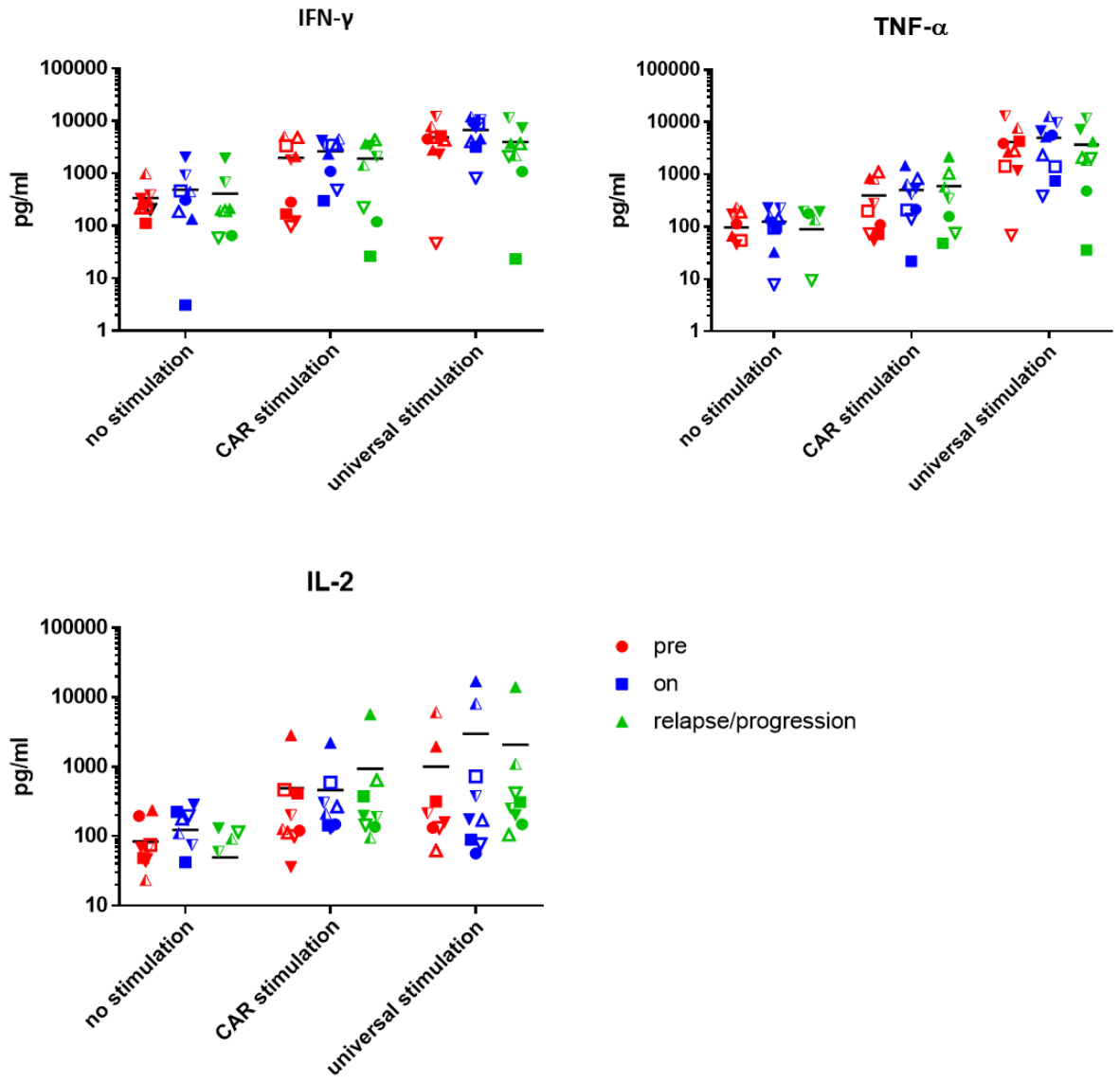


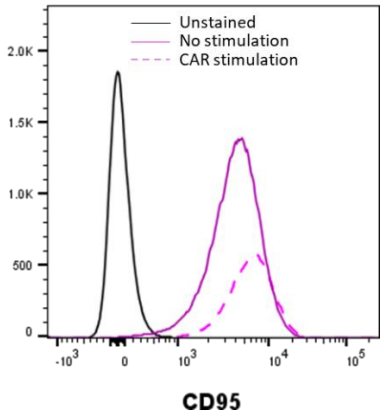
Figure 5.4: CAR T cells at different treatment time points exhibit similar cytokine release profiles upon activation. CAR T cells were either left in TexMACS medium supplemented with IL-7/IL-15 (cytokine only) or activated using plate-bound specific antibody (CAR activation) or CD3/CD28 antibodies (universal activation). Supernatant was collected after three days culture for cytokine release assays using MACSPlex 12 cytokine kit (n=9, line represents mean, no significant difference by two-way ANOVA was detected in all tests)

5.4 Conclusions

CAR T cells generated from PBMCs collected during chemotherapy (on-treatment) had consistent cytotoxic effects and were more resistant to cell death compared to the other groups. Although CAR T cells manufactured from PBMCs at the relapse/progression time point were more prone to AICD/PCD, they still demonstrated an equivalent cytotoxic effect to pre-treatment CAR T cells. No major differences were observed in the proportions of PD-1^{+}, CD27^{+} and CD57^{+} CAR T cells between groups. Most CAR T cell products were capable of making INF-γ, TNF and IL-2 following stimulation, with no major differences between groups. Products generated from patients #04, #09 and #12 that could not kill target cells in the cytotoxicity assay were also deficient in producing IFN-γ and TNF, suggesting an intrinsic defect in their function.

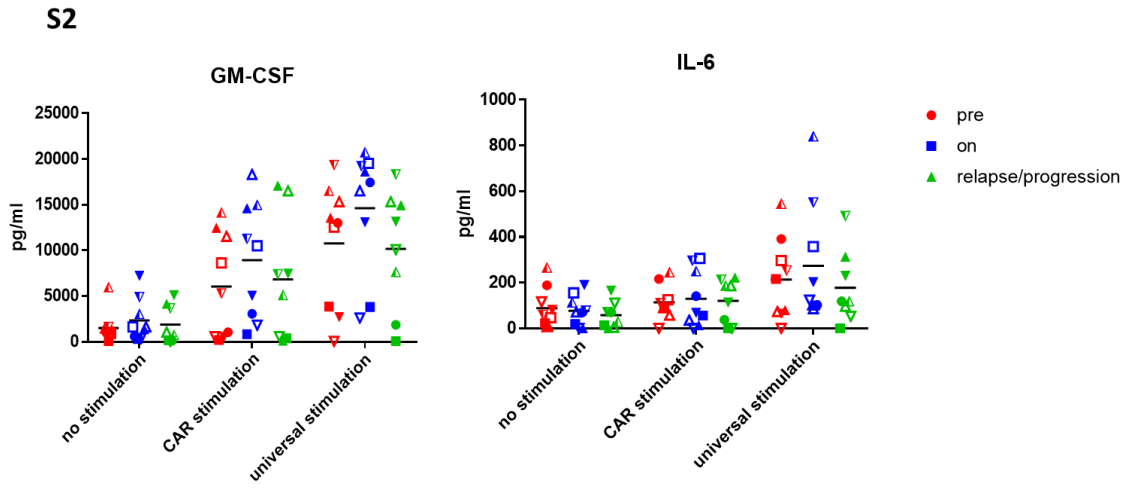
Supplementary data

S1



Supplementary figure S1: CD95 expression on $CD3^+CAR^+$ T cells following CAR stimulation or resting in supplemented medium.

S2



Supplementary figure S2: Concentration of GM-CSF and IL-6 in supernatant of resting or CAR-stimulated T cells or universally stimulated CAR T cells.

Table S2: Mean concentration of cytokines released by CAR T cells of all patients at different time points

	Media only			CAR stimulation			CD3/CD28 stimulation		
	Pre-treatment	On-treatment	Relapse	Pre-treatment	On-treatment	Relapse	Pre-treatment	On-treatment	Relapse
IL-4	32.8	78.3	57.1	86.1	73.6	69.7	25	197	100.45
IL-5	582	610	452	840	1539	1841.5	7855	6593	7297.5
IL-6	59.5	72	50.05	94	68.9	150.5	216	124	119
IL-9	67.3	70.4	66.55	110	216	402	3508	2230	2480.5
IL-10	235	230	203	248	216	250	211	242	217
IL-12	190	230	236	209	203	226	245	203	213.5
IL-17	224	103	167.5	178	238	240	211	224	163.5

Chapter 6
Discussion and conclusions

6.1 Discussion

Immunotherapy has emerged as a new and efficient treatment in haematological and solid cancers (Neelapu et al. 2017). Currently, common and well-studied immunotherapeutic modalities for cancer include vaccines, monoclonal antibody therapy, immune-checkpoint inhibitors, and adoptive T cell therapy including autologous genetically engineered chimeric antigen receptor T cells (CAR T cells) (NCI 2019). In this project, an *in vitro* study of therapeutic CAR T cells was conducted.

CAR T cell therapy has shown success in relapsed/refractory B-cell malignancies (Porter et al. 2011). KYMRIAH® (Tisagenlecleucel) is the first CAR T cell therapy, which has been approved by the US FDA for paediatric B-cell acute lymphoblastic leukaemia (B-ALL) and adult diffuse large B-cell lymphoma (NCI 2017). It is an individualised therapy using a patient's own T cells reprogrammed to express CD19-specific chimeric receptors (Porter et al. 2011). In previous clinical trials for B-ALL, CAR T cell therapy was associated with a high remission rate (90%) and a 24-month durable remission (Maude et al. 2014). In contrast, CAR T cells targeting IL-13Rα2 in glioblastoma, CAIX in renal cell carcinoma, mesothelin in pleural mesothelioma and metastatic lung cancers (Adusumilli et al. 2019; Brown et al. 2016a; Lamers et al. 2013) have shown limited clinical effects in phase I/II clinical trials. Short term persistence of CAR T cells in the circulation after infusion may be an important factor contributing to treatment failure (Xu, X-J, Zhao & Tang 2013).

Therefore, optimising CAR T cell manufacturing to promote *in vivo* persistence has been approached from several angles such as substitution of co-stimulatory signals in the structure of the CAR and selection or enrichment of specific T cell subsets in the starting cell population for manufacture (Abate-Daga & Davila 2016; Blaeschke, F. et al. 2018). Naïve, stem cell-like and central memory T cells have an increased capacity for self-renewal (Sallusto, Geginat & Lanzavecchia 2004), and CAR T cells enriched with these phenotypes are reported to be associated with improved clinical effectiveness (Xu, X-J, Zhao & Tang 2013).

There is increasing evidence that antineoplastic chemotherapy agents can have positive immunomodulatory effects and result in remarkable increases in the proportions of $CD8^+$ cytotoxic T cells and those with a memory phenotype (Plate et al. 2005; Verma et al. 2016). Post-chemotherapy blood samples have shown sustained depletion of immunosuppressive regulatory T cells and MDSCs, releasing the brake on the anti-tumour immune response (Eriksson et al. 2016). This finding raises the question of whether chemotherapeutic drugs could have a positive effect on the quantity and quality of PBMCs used for CAR T cell generation. Of note, the majority of subjects recruited in recent clinical trials for CAR T cell therapy were at a relapsed or refractory stage of their disease in the setting of a post-chemotherapy immune reconstitution (Brown & Mackall 2019; Kershaw et al. 2006). Taking these insights into account, I have hypothesised that PBMCs post-chemotherapy might be an appropriate and clinically relevant starting population for the optimal generation of highly functional CAR T cells.

In this study, CAR T cells from bulk PBMCs collected at different time points during chemotherapy treatment were manufactured. Then these three groups of CAR T cells were compared with respect to their immunophenotype, cell viability after specific CAR activation, differentiation stage, cytolytic capacity and cytokine secretion profiles. Results were integrated and discussed to give an overview of the feasibility of manufacturing CAR T cells using PBMCs pre-, during or post chemotherapy. In this study, GD2-specific CAR T cells were successfully generated from PBMCs collected at the three different time points. In instances where manufacturing failed, the results were attributed to cancer progression, or other host intrinsic factors, rather than the antineoplastic treatment itself.

The proliferation of T cells after activation and transduction is a requirement for manufacturing a sufficient yield of CAR-T cells. In this study, the input PBMCs expanded up to 43-fold. Compared to other reported expansion protocols in which T cells were activated by TransAct and cultured in IL-7/IL-15-supplemented medium, T cells from pre-treatment, on-treatment, and relapse/progression groups showed a similar or slightly lower proliferation rate, suggesting that T cells collected post-chemotherapy could expand during CAR T cell manufacturing (Blaeschke, F. et al. 2018; Gargett et al. 2019).

Generating sufficient numbers of clinical CAR T cells is a critical factor for successful CAR T cell manufacturing. KYMRIAH®'s doses for adult relapse or refractory diffuse large B cell lymphoma are 0.6-6 x 10^8 CAR^+ T cells/kg (*tisagenlecleucel (Rx)*). In clinical trials on solid cancers, total T cells required for each infusion are from 1 x 10^8 to 5 x 10^9 cells (1 x 10^6 -10 x 10^6 CAR^+ T cells/kg) (NCT03851146, NCT03013712, NCT03198052). These final cell doses could be obtained from 100-120 ml of blood which yields an estimated starting population of 1 x 10^8 PBMCs (Blaeschke, F. et al. 2018; Boyum 1968). In this study, a cell yield threshold value of 3 x 10^7 cells produced from a starting population of 1 x 10^7 PBMCs was established, to define samples that showed sufficient expansion of transduced T cells to perform downstream assays (**Table 6.1**). CAR T cell products meeting this threshold would also be sufficient for the lowest dose of our current clinical trial of GD2 CAR T cell therapy in solid cancer patients (ACTRN12613000198729), suggesting the clinical relevance of this threshold value. In another study, sufficient numbers of CAR T cells to generate clinical CAR T cell products could not be expanded for two out of 32 patients (Turtle et al. 2016b). Low cell yield in final products can result from slow cell expansion, an insufficient cell input number, or both.

Seven samples that failed to meet the yield cut off were from three elderly patients: #07, #13, and #16 aged 88, 82 and 81 years, respectively, for whom the transduced T cells proliferated less well compared to others. The pre-treatment and on-treatment CAR T cell products from patient #07 did not expand after a 10-day culture. The relapse/progression CAR T cell product of patient #13 had less than a two-fold increase in cell number compared to starting population number. Similarly, the on-treatment samples of patient #16 only doubled in cell number after expansion. Lack of sufficient T cell expansion in

these patients' samples is consistent with previous findings related to an aged immune system (Weyand & Goronzy 2016). A failure of cell expansion limits the final CAR T cell yield available for subsequent *in vitro* assays and therapy and may require a greater input number of PBMCs or different culture conditions in the case of elderly donors.

One blood sample that failed to meet the threshold was derived from a patient with progressive pancreatic cancer (patient #04, 67 years), who did not have lymphopenia. Transduced T cells derived from this patient divided slowly (three-fold) during the CAR T cell manufacturing process. The patient's disease progressed soon after initiating chemotherapy (13 weeks) and NLR increased from 1 to 3.7, perhaps suggesting the presence of global immunosuppression associated with an advanced cancer stage (Grivennikov, Greten & Karin 2010). Progressive disease therefore might also constrain T cell function including replicative ability (Gonzalez, Hagerling & Werb 2018; Grivennikov, Greten & Karin 2010). This explanation is supported by the rapid proliferation of T cells in pre-treatment and on-treatment samples (16-fold and 33-fold, respectively) from the same patient, suggesting that intrinsic defects in T cell fitness were not present at these time points. In contrast, other patients' relapse/progression samples (collected after initiating chemotherapy at an average of 46 weeks) (patient #01, #10) showed robust expansion comparable to that of the pre-treatment samples. These patients had unchanged and decreased NLR values, respectively, at the relapse/progression time point compared to the pre-treatment time point. These results may indicate that disease relapse after a chemotherapy-induced partial remission may not compromise T cell expansion.

The last sample below the required yield of CAR T cells was generated from a patient (#09) with lymphopenia (less than 500 cells per microlitre of whole blood) at the time of disease progression. Although T cells of this patient proliferated sufficiently (10-fold) during the expansion phase, the final cell yield of the CAR T cell product did not meet the threshold value. I noted that patient #09 received temozolomide-based chemoradiation, which has been associated with severe lymphopenia (Byun et al. 2019). Cumulative radiation dose may also impair T cell replication and explain the low cell yield in the final product.

Thus, aging may reduce the proliferative ability of PBMCs at all treatment time points and certain treatment modalities constrain the final cell yield during CAR T cell manufacturing.

Table 6.1: Cell yield of CAR T cell products did not meet the threshold value of 3 x10^7 cells after expansion

	Cell yield threshold 3 x 10^7 cells		
	Pre-treatment	**On-treatment**	**Relapse**
#01	✓	✓	✓
#07	✗	✗	✗
#10	✓	✓	✓
#12	✓	✓	✓
#13	✗	✗	✗
#16	✓	✗	✓
#09	✓	✓	✗^
#04	✓	✓	✗
#05	✓	✓	
Total	7/9 (78%)	6/9 (67%)	4/8 (50%)

The cut off threshold was set at 3x10^7 which is sufficient for the first CAR-T cell dose level in our current trial protocol. ✓ success, ✗ proposed failure due to progressive disease, ✗ proposed failure due to effects of old-age on T cell expansion, ^: lymphopenia

The efficiency of T cell transduction is also important for the success of CAR T cell therapy (Abate-Daga & Davila 2016). The mean transduction efficiency achieved in this study was 16% which is lower than results from other studies using similar CAR T cell manufacturing protocols (Blaeschke, F. et al. 2018) and same viral vector encoding the GD2-specific CAR (Gargett et al. 2019). Here, I excluded technical factors because healthy volunteer samples, which were simultaneously produced contained much higher proportion of CAR-positive T cells (30% to 40%). Three patients diagnosed with progressive colorectal cancer (patient #12), pancreatic carcinoma (patient #04) and glioblastoma (patient #09) had medium-low transduction efficiencies (1%-8%), with

extremely low (≤5%) CAR expression observed in pre-treatment and relapse/progression CAR T cell samples (**Table 6.2**). Possible explanations include the cancer type, disease progression and cancer treatment modality. The effect of antineoplastic treatment was excluded because extremely low transduction efficiency also occurred in pre-treatment products and with different cancer treatment modalities. In addition, although on-treatment CAR T cells of these three patients had a low percentage of CAR-expressing T cells, this rate is still significantly higher than the mean transduction efficiency of pre-treatment and relapse/progression CAR T cell products that were close to zero. This is of interest as it suggests that those T cells that have survived exposure to a cytotoxic agent may have better capacity for viral transduction. This trend of improved transduction efficiency for on-treatment samples was also observed in all samples from this cohort, but the mean difference between time points did not reach statistical significance. Another factor that may affect T cell transduction efficiency is cancer type. I observed a trend toward higher transduction efficiency for all colorectal cancer samples compared to pancreatic cancer and glioblastoma samples. However, I would need more samples in the pancreatic cancer and glioblastoma groups to better support this idea. Since CAR T cell products with low transduction efficiency were noted in specific patients and not clearly related to any of the factors discussed above (cancer type, cancer treatment modality and treatment phase), it is hypothesised that the intrinsic fitness of an individual's T cells explains the low transduction efficiency. Interestingly, T cells derived from samples with low transduction efficiency still displayed strong proliferation and a positive correlation between transduction efficiency and fold expansion was not found. In fact, samples from elderly patients (#13 and #07) with a slower expansion rate had a medium-high transduction efficiency (19%-32%). This result suggests that an unknown mechanism not related to the post-activation proliferative ability T cells exerts an influence on transduction efficiency.

Table 6.2: Low transduction efficiency (≤ 5%) is shown in red.

	Transduction efficiency (%)		
	Pre-treatment	**On-treatment**	**Relapse**
#01	32	37	46
#07	5.5	19	20
#10	22	23	28
#12	8	8	5
#13	29	22	32
#16	11	17	13
#09	2	8	2
#04	3	8	3
#05	12	14	

Repopulation of lymphocyte subsets following chemotherapy has been widely investigated (Hakim et al. 1997; Kubota et al. 2001; Plate et al. 2005; Verma et al. 2016). Several papers have reported that the proportion of $CD4^+$ T cells significantly decreases in the two weeks after initiating cytotoxic treatment and slowly increases but does not return the baseline level until after 9 months (Hakim et al. 1997; Verma et al. 2016). The frequency of the $CD8^+$ T cell population also drops within the first month after treatment but can rebound to pre-treatment levels within 9 months (Mackall, CL 2000; Verma et al. 2016). In contrast, other literature indicates that gemcitabine and paclitaxel do not supress the proportions of either $CD4^+$ or $CD8^+$ T cells after the first cycle of chemotherapy (Javeed et al. 2009; Plate et al. 2005).

In this study, no significant changes were shown in the mean proportions of $CD8^+$ and $CD4^+$ T cells post-chemotherapy. Also, there were no differences in the mean proportions of naïve, central memory, effector memory and terminal effector subsets of T cells at pre-treatment, on-treatment (at week 4), and relapse/progression (after week 8) time points. Although the results of the current study were not consistent with

observations from other studies revealing significant post-chemotherapy increases in the percentages of memory T cells ($CD45RA^{-}CD45RO^{+}$) (Mackall, CL 2000; Plate et al. 2005; Verma et al. 2016), its small sample size is not sufficient to support a robust conclusion. In addition, the three different types of cancers and distinct treatment modalities included in the current study could produce diverse outcomes in lymphocyte subset numbers and, indeed, significant alterations in T cell subsets were not observed.

In addition to assessing total cell yield and CAR expression, characterisation of CAR-T cell immunophenotype has been major element in this study. Previously, efforts in my laboratory have been directed toward promoting a central memory phenotype of CAR-T cell products so that *in vivo* persistence might be enhanced (Gargett & Brown 2015; Gargett et al. 2019). The combination of IL-7 and IL-15 has been demonstrated to promote a naïve-like or central memory phenotype during the production of CAR T cells (Gargett & Brown 2015; Gargett et al. 2019; Xu, Y et al. 2014). In several studies, a central memory phenotype of $CD8^{+}$ CAR T cells dominated after IL-7/IL-15-based expansion (Blaeschke, F. et al. 2018; Gargett et al. 2019). In contrast in this study, it was found that the effector memory phenotype described the largest proportion of $CD8^{+}$ CAR T cells. Interestingly, similar findings were also reported in a study that compared IL-2- versus IL-7/IL-5-based expansion for CAR T cells (Xu, Y et al. 2014). However, the results herein also showed that a naïve/central memory phenotype was favoured in some samples. For several samples, the frequency of naïve and central memory $CD8^{+}$ T cells increased up to 5 to 7-fold during the 10-day expansion period (**Figure 4.9**). Although this subset of $CD8^{+}$ T cells expanded preferentially in these samples, it did not come to dominate the $CD8^{+}$ CAR T cell population because naïve and central memory cells comprised a small fraction (6% to 7%) of the input T cell population. Although the combination of IL-7/IL-15 cytokines in culture medium has been previously shown to promote a "young" phenotype compared to IL-2-based medium, the relative proportions of naïve-like ($CD45RA^{+}$ $CCR7^{+}$ or $CD45RA^{+}$ $CCR7^{+}$ $CD62L^{+}$ $CD95^{+}$) and central memory ($CD45RA^{-}$ $CCR7^{+}$ $CD62L^{+}$ $CD95^{+}$) phenotype T cells in the starting PBMCs and CAR T cell products were not disclosed in these publications (Blaeschke, F. et al. 2018; Gargett et al. 2019). Here, it was found that the *ex vivo* expansion conditions favoured preservation of the proportions of the naïve-like and central memory phenotype

cell in the $CD8^+$ CAR T cell population, especially in pre-treatment and on-treatment groups. Preservation of these phenotypes in $CD8^+$ CAR T cells was in agreement with results of other studies (Xu, Y et al. 2014).

In all, results of this study supported earlier findings that expanding cultured T cells with IL-7/IL-15 promotes the generation of the $CCR7^+$ phenotype (Boyman, O et al. 2008; Gargett & Brown 2015). It also suggests that the proportion of naïve/central memory cells among the starting cells also contributes to their final fraction in CAR T cell products. To obtain the highest yield of the desired T cell subsets, methods to enrich cells in the starting population with naïve/central memory subsets may be an additional consideration.

T cells undergoing multiple rounds of replication acquire senescent characteristics, marked by expression of the CD57 molecule (Kern et al. 1996). Senescent T cells are characterised by the inability to proliferate in response to antigen encounter and have increased sensitivity to antigen-induced apoptosis, which both result in failure of cell expansion (Brenchley et al. 2003a; Kasakovski, Xu & Li 2018). The ability of CAR T cells to expand is strongly associated with the effectiveness of adoptive cell therapy for cancer (Xu, X-J, Zhao & Tang 2013). Limiting the proportion of senescent CAR T cells in a product, therefore, should improve expansion of CAR T cells *in vivo*. I found that both $CD4^+$ and $CD8^+$ CAR T cells did not differentiate to a terminally differentiated or senescent stage after *in vitro* expansion. All CAR T cell products derived at different treatment time points showed similarly subtle differences in the proportion of CD57-expressing cells compared to the input PBMCs, indicating that this phenotype was not affected by chemotherapy exposure. Hence, the optimised expansion protocol defined in our previous study (Gargett et al. 2019) and used in the present work limits the development of terminally differentiated senescent cells, and the fraction of senescent $CD57^+$ cells remains stable during CAR T cell expansion.

AICD results in a reduction in CAR T cell numbers after infusion, and was another parameter investigated in this study. CAR T cells expressing CD95 have previously been demonstrated to progress to cell death with or without further activation (Mak & Saunders 2006; Tschumi et al. 2018a). It is noted that almost 100% of transduced T cells in the

present study expressed CD95. If the sensitivity of CD95-expressing CAR T cells to AICD can be reduced, then CAR T cells may be rescued from apoptosis and consequently have prolonged survival. CAR T cell products manufactured at relapse/progression were found to be the most susceptible to AICD. In contrast, the viability of on-treatment CAR T cell products under both resting and CAR-activated conditions was significantly higher than products generated from pre-treatment samples. However, this result derives from a short-term *in vitro* assay. I did not re-stimulate CAR T cells to analyse the effects of prolonged or repeated activation on cell viability, which more accurately reflects AICD (Künkele et al. 2015). Therefore, as a preliminary finding, on-treatment CAR T cells had superior resistance to AICD following a first round of stimulation. By this parameter, CAR T cells manufactured at the relapse/progression time point may be a less appropriate candidate therapy than cells manufactured at pre-treatment or on-treatment time points.

A final critical parameter in assessing CAR T cell products is their cytotoxic function. Importantly, all on-treatment CAR T cell products could exert cytolytic activity against antigen-positive tumour target cells, while only 67% of pre-treatment and 63% of relapse/progression CAR T cell products could kill target cells (**Table 6.3**). On-treatment CAR T cells demonstrated high cytotoxic potency and achieved a 30% killing effect after 60 hours at 5:1 E:T cell ratio, compared to products derived at other time points.

Table 6.3: All on-treatment CAR T cell products reached a threshold of 30% target cell killing . ✓ achieving, ✗ not achieving.

Cytotoxic function cut off at 30% of killing effect			
	Pre-treatment	**On-treatment**	**Relapse**
#01	✓	✓	✓
#07	✓	✓	✓
#10	✓	✓	✓
#12	✗	✓	✗
#13	✓	✓	✓
#16	✓	✓	✓
#09	✗	✓	✗
#04	✗	✓	✗
#05	✓	✓	
Total	6/9 (67%)	9/9 (100%)	5/8 (63%)

A failure to kill tumour target cells may arise from too few antigen-specific CAR T cells in the products, from suboptimal cytotoxic function of CAR T cells or low CAR T cell viability. In an attempt to understand why some CAR T cell products failed to kill tumour targets, the functional characteristics of these products were assessed using other approaches. All CAR T cells showed upregulated production of IFN-γ and TNF after CAR-stimulation and universal stimulation, so that complete loss of T cell function was highly unlikely. CAR T cell products that failed to kill target cells *in vitro* had low transduction efficiency (1%-7%). However, three on-treatment products, that contained similar proportions of CAR T cells from the same patients (#04, #09, #12), exhibited high rates of cytolysis in the cytotoxicity assay. This indicated that low transduction efficiency does not preclude the production of a CAR T cell product with strong tumour cell killing activity. Interestingly, these three patients did not respond to chemotherapy. Moreover, the CAR T cells derived from PBMCs at pre-treatment or relapse/progression time points in patients whose disease had progressed during treatment failed to achieve a positive result in the cytotoxicity assay. Indeed, the high observed rates of AICD among these pre-treatment and

relapse/progression products, which was discussed in the previous paragraph, may limit CAR T cell function and their serial killing of multiple target cells *in vitro*, thereby minimising their cytotoxic effectiveness. This explanation suggests the interesting possibility of an association between CAR T cell survival and function *in vitro* and clinically effective therapy (Xu, X-J, Zhao & Tang 2013).

Host intrinsic factors such as global immunosuppression may contribute to failure of chemotherapy and CAR T cell therapy. In a preliminary analysis, I investigated whether the NLR obtained from routine complete blood examinations was associated with the success of CAR-T cell manufacturing. NLR has been found to be a powerful clinical prognostic factor but showed no association with CAR T cell potency in this study. NLR at baseline and post-chemotherapy were high (>4) in several patients but CAR T cells derived from their PBMCs still displayed high cytotoxic functions. However, this observation needs to be confirmed by results from a larger patient cohort.

This study has several limitations. The cohort of patients for this study was rather small and limits interpretation of the data. Although phases of chemotherapy were proposed to affect T cell number and function, no statistically significant differences among samples at the different treatment time points provide support for this notion. The lack of statistically significant results in this study may also result from the inherent variability of individual patients who have particular types of cancer and experience different chemotherapy regimens. The small sample size might also lead to an overestimate of the association between the on-treatment CAR T cell products and the higher functional capacity of these CAR T cells. Further studies with a larger number of patients who were diagnosed with different cancer types and received different types of treatment are required to confirm or refute these findings herein and to continue the search for clinical and laboratory factors by which the successful manufacture of a high yield of long-lived and highly functional CAR T cells can be predicted. Also, choosing pre-selected $CD4^+$ and $CD8^+$ T cells and/or enriched $CD62L^+$ T cells rather bulk PBMCs for CAR T cell generation should be considered to augment the proportion of naïve-like and central memory CAR^+ T cells/ all T cells in final products (Gargett et al. 2019; Priesner et al. 2016). Removing immunoinhibitory cell types such as Tregs and MDSCs in input populations for CAR T cell

production or lymphodepletion using fludarabine and cyclophosphamide before adoptive transfer of CAR T cells may be other methods for improving the effectiveness of CAR T cell therapy (Long, Adrienne H. et al. 2016; Turtle et al. 2015).

6.2 Conclusions

Adoptive cell therapy with CAR T cells is a new and exciting anti-cancer strategy. Many studies have been conducted with the aim of improving the effectiveness of CAR T cells and thus enhancing the clinical utility of CAR T cell therapy for solid cancer patients. Here, CAR T cells generated from PBMCs of patients with advanced cancer showed similar proliferative ability and transduction efficiency as those made from non-cancer patients. Using PBMCs collected before the second cycle of chemotherapy as input cells for an IL-7/IL-15-based expansion protocol may yield long lived and highly functional CAR T cell products for solid cancer therapy. This protocol gave rise to similar immunophenotype of CAR positive T cells and all T cells in final products after expansion. This study also confirms that PBMCs collected at cancer relapse can be used to manufacture potent CAR T cells.

References

Abate-Daga, D & Davila, ML 2016, 'CAR models: next-generation CAR modifications for enhanced T-cell function', *Molecular Therapy - Oncolytics,* vol. 3, no. Supplement C, 2016/01/01/, p. 16014.

Abken, H 2017, 'Driving CARs on the Highway to Solid Cancer: Some Considerations on the Adoptive Therapy with CAR T Cells', *Human gene therapy,* vol. 28, no. 11, Nov, pp. 1047-60.

ACS 2016, *Chemotherapy side effects*, American Cancer Society, viewed 30 August 2019, <https://www.cancer.org/treatment/treatments-and-side-effects/treatment-types/chemotherapy/chemotherapy-side-effects.html>.

Adusumilli, PS, Zauderer, MG, Rusch, VW, Cearbhaill, RE, Zhu, A, Ngai, DA, McGee, E, Chintala, NK, Messinger, JC, Vincent, A, Halton, EF, Diamonte, C, Pineda, J, Modi, S, Solomon, SB, Jones, DR, Brentjens, RJ, Rivière, I & Sadelain, M 2019, 'Abstract CT036: A phase I clinical trial of malignant pleural disease treated with regionally delivered autologous mesothelin-targeted CAR T cells: Safety and efficacy', *Cancer Research,* vol. 79, no. 13 Supplement, p. CT036.

Ahmed, N, Brawley, V, Hegde, M & et al. 2017, 'Her2-specific chimeric antigen receptor–modified virus-specific t cells for progressive glioblastoma: A phase 1 dose-escalation trial', *JAMA Oncology,* vol. 3, no. 8, pp. 1094-101.

AIHW 2019, *Cancer data in Australia*, Australian Institute of Health and Welfare, viewed 30 August 2019, <https://www.aihw.gov.au/reports/cancer/cancer-data-in-australia/acim-books-acd-pivot-table>.

Ashe, JM, Wiest, DL, Abe, R & Singer, A 1999, 'ZAP-70 Protein Promotes Tyrosine Phosphorylation of T Cell Receptor Signaling Motifs (ITAMs) in Immature $CD4^{+}CD8^{+}$ Thymocytes with Limiting p56 lck', *The Journal of experimental medicine,* vol. 189, no. 7, pp. 1163-68.

Battula, VL, Shi, Y, Evans, KW, Wang, R-Y, Spaeth, EL, Jacamo, RO, Guerra, R, Sahin, AA, Marini, FC, Hortobagyi, G, Mani, SA & Andreeff, M 2012, 'Ganglioside GD2 identifies breast cancer stem cells and promotes tumorigenesis', *The Journal of clinical investigation,* vol. 122, no. 6, 06/01/, pp. 2066-78.

Bellone, G, Novarino, A., Vizio, B., Brondino, G., Addeo, A., Prati, A., Giacobino, A., Campra, D., Fronda, G. R., Ciuffreda, L. 2009, 'Impact of surgery and chemotherapy on cellular immunity in pancreatic carcinoma patients in view of an integration of standard cancer treatment with immunotherapy', *International Journal of Oncology* vol. 34, no. 6, pp. 1701-15.

Benmebarek, M-R, Karches, CH, Cadilha, BL, Lesch, S, Endres, S & Kobold, S 2019, 'Killing Mechanisms of Chimeric Antigen Receptor (CAR) T Cells', *International journal of molecular sciences,* vol. 20, no. 6, p. 1283.

Bilchik, A, Miyashiro, M, Kelley, M, Kuo, C, Fujiwara, Y, Nakamori, S, Monden, M & Hoon, DSB 2000, 'Molecular detection of metastatic pancreastic carcinoma cells using a multimarker reverse transcriptase-polymerase chain reaction assay', *Cancer,* vol. 88, no. 5, p. 14.

Blaeschke, F, Kaeuferle, T, Feucht, J, Weber, D, Lotfi, R, Kaiser, A, Assenmacher, M, Doering, M & Feuchtinger, T 2016, 'Defined Central Memory and Stem Memory T Cell Phenotype of CD4 and CD8 CAR T Cells for the Treatment of CD19+ Acute Lymphoblastic Leukemia in an Automated Closed System', *Blood,* vol. 128, no. 22, p. 4558.

Blaeschke, F, Stenger, D, Kaeuferle, T, Willier, S, Lotfi, R, Kaiser, AD, Assenmacher, M, Doring, M, Feucht, J & Feuchtinger, T 2018, 'Induction of a central memory and stem cell memory phenotype in functionally active CD4(+) and CD8(+) CAR T cells produced in an automated good manufacturing practice system for the treatment of CD19(+) acute lymphoblastic leukemia', *Cancer immunology, immunotherapy : CII,* vol. 67, no. 7, Jul, pp. 1053-66.

Bofill, M, Janossy, G, Lee, CA, MacDonald-Burns, D, Phillips, AN, Sabin, C, Timms, A, Johnson, MA & Kernoff, PB 1992, 'Laboratory control values for CD4 and CD8 T lymphocytes. Implications for HIV-1 diagnosis', *Clinical and experimental immunology,* vol. 88, no. 2, pp. 243-52.

Boomer, JS & Green, JM 2010, 'An Enigmatic Tail of CD28 Signaling', *Cold Spring Harbor Perspectives in Biology,* vol. 2, no. 8, August 1, 2010.

Boyman, O, Ramsey, C, Kim, DM, Sprent, J & Surh, CD 2008, 'IL-7/Anti-IL-7 mAb Complexes Restore T Cell Development and Induce Homeostatic T Cell Expansion without Lymphopenia', *The Journal of Immunology,* vol. 180, no. 11, p. 7265.

Boyman, O, Le´tourneau, S., Krieg, C., & Sprent, J. 2009, 'Homeostatic proliferation and survival of Naive and memory T cells', *European Journal of Immunology,* vol. 39, pp. 2088–94.

Boyum, A 1968, 'Isolation of mononuclear cells and granulocytes from human blood. Isolation of monuclear cells by one centrifugation, and of granulocytes by combining centrifugation and sedimentation at 1 g', *Scand J Clin Lab Invest Suppl,* vol. 97, pp. 77-89.

Brenchley, JM, Karandikar, NJ, Betts, MR, Ambrozak, DR, Hill, BJ, Crotty, LE, Casazza, JP, Kuruppu, J, Migueles, SA, Connors, M, Roederer, M, Douek, DC & Koup, RA 2003a, 'Expression of CD57 defines replicative senescence and antigen-induced apoptotic death of CD8+T cells', *Blood,* vol. 101, no. 7, p. 2711.

Brenchley, JM, Karandikar, NJ, Betts, MR, Ambrozak, DR, Hill, BJ, Crotty, LE, Casazza, JP, Kuruppu, J, Migueles, SA, Connors, M, Roederer, M, Douek, DC & Koup, RA 2003b, 'Expression of CD57 defines replicative senescence and antigen-induced apoptotic death of $CD8^+$ T cells', *Blood,* vol. 101, no. 7, p. 2711.

Brentjens, R, Yeh, R, Bernal, Y, Riviere, I & Sadelain, M 2010, 'Treatment of Chronic Lymphocytic Leukemia With Genetically Targeted Autologous T Cells: Case Report of an Unforeseen Adverse Event in a Phase I Clinical Trial', *Molecular Therapy,* vol. 18, no. 4, 04/01, pp. 666-68.

Brentjens, RJ, Rivière, I, Park, JH, Davila, ML, Wang, X, Stefanski, J, Taylor, C, Yeh, R, Bartido, S, Borquez-Ojeda, O, Olszewska, M, Bernal, Y, Pegram, H, Przybylowski, M, Hollyman, D, Usachenko, Y, Pirraglia, D, Hosey, J, Santos, E, Halton, E, Maslak, P, Scheinberg, D, Jurcic, J, Heaney, M, Heller, G, Frattini, M & Sadelain, M 2011, 'Safety and persistence of adoptively transferred autologous CD19-targeted T cells in patients with relapsed or chemotherapy refractory B-cell leukemias', *Blood,* vol. 118, no. 18, pp. 4817-28.

Bridgeman, JS, Hawkins, RE, Bagley, S, Blaylock, M, Holland, M & Gilham, DE 2010, 'The Optimal Antigen Response of Chimeric Antigen Receptors Harboring the CD3ζ Transmembrane Domain Is Dependent upon Incorporation of the Receptor into the Endogenous TCR/CD3 Complex', *The Journal of Immunology,* vol. 184, no. 12, p. 6938.

Brode, S, Raine, T, Zaccone, P & Cooke, A 2006, 'Cyclophosphamide-Induced Type-1 Diabetes in the NOD Mouse Is Associated with a Reduction of CD4+CD25+Foxp3+Regulatory T Cells', *The Journal of Immunology,* vol. 177, no. 10, p. 6603.

Broere, F, Apasov, SG, Sitkovsky, MV & van Eden, W 2011, 'A2 T cell subsets and T cell-mediated immunity', in FP Nijkamp & MJ Parnham (eds), *Principles of Immunopharmacology: 3rd revised and extended edition*, Birkhäuser Basel, Basel, pp. 15-27.

Brown, CE, Alizadeh, D, Starr, R, Weng, L, Wagner, JR, Naranjo, A, Ostberg, JR, Blanchard, MS, Kilpatrick, J, Simpson, J, Kurien, A, Priceman, SJ, Wang, X, Harshbarger, TL, D'Apuzzo, M, Ressler, JA, Jensen, MC, Barish, ME, Chen, M, Portnow, J, Forman, SJ & Badie, B 2016a, 'Regression of Glioblastoma after Chimeric Antigen Receptor T-Cell Therapy', *The New England journal of medicine,* vol. 375, no. 26, pp. 2561-69.

Brown, CE, Alizadeh, D, Starr, R, Weng, L, Wagner, JR, Naranjo, A, Ostberg, JR, Blanchard, MS, Kilpatrick, J, Simpson, J, Kurien, A, Priceman, SJ, Wang, X, Harshbarger, TL, D'Apuzzo, M, Ressler, JA, Jensen, MC, Barish, ME, Chen, M, Portnow, J, Forman, SJ & Badie, B 2016b, 'Regression of Glioblastoma after Chimeric Antigen Receptor T-Cell Therapy', *New England Journal of Medicine,* vol. 375, no. 26, pp. 2561-69.

Brown, CE & Mackall, CL 2019, 'CAR T cell therapy: inroads to response and resistance', *Nature Reviews Immunology,* vol. 19, no. 2, 2019/02/01, pp. 73-74.

Brunner, T, Mogil, RJ, LaFace, D, Yoo, NJ, Mahboubi, A, Echeverri, F, Martin, SJ, Force, WR, Lynch, DH, Ware, CF & Green, DR 1995, 'Cell-autonomous Fas (CD95)/Fas-ligand interaction mediates activation-induced apoptosis in T-cell hybridomas', *Nature,* vol. 373, no. 6513, 02/02/print, pp. 441-44.

Byun, HK, Kim, N, Yoon, HI, Kang, S-G, Kim, SH, Cho, J, Baek, JG, Chang, JH & Suh, C-O 2019, 'Clinical predictors of radiation-induced lymphopenia in patients receiving chemoradiation for glioblastoma: clinical usefulness of intensity-modulated radiotherapy in the immuno-oncology era', *Radiation Oncology,* vol. 14, no. 1, 2019/03/27, p. 51.

Cancer-Australia 2019a, *Bowel cancer (colorectal cancer) in Australia statistics*, Australia Government Cancer Australia, viewed 30 August 2019, <https://bowel-cancer.canceraustralia.gov.au/statistics>.

Cancer-Australia 2019b, *Pancreatic cancer*, Australian Government Cancer Australia, viewed 30 August 2019, <https://pancreatic-cancer.canceraustralia.gov.au/statistics>.

Cancer-Australia 2019c, *Brain cancer in Australia statistics*, Australian Government Cancer Australia, viewed 30 August 2019, <https://brain-cancer.canceraustralia.gov.au/statistics>.

Cerignoli, F, Abassi, YA, Lamarche, BJ, Guenther, G, Santa Ana, D, Guimet, D, Zhang, W, Zhang, J & Xi, B 2018, 'In vitro immunotherapy potency assays using real-time cell analysis', *PloS one,* vol. 13, no. 3, pp. e0193498-e98.

Cheng, LE, Öhlén, C, Nelson, BH & Greenberg, PD 2002, 'Enhanced signaling through the IL-2 receptor in CD8⁺ T cells regulated by antigen recognition results in preferential proliferation and expansion of responding CD8⁺ T cells rather than promotion of cell death', *Proceedings of the National Academy of Sciences,* vol. 99, no. 5, p. 3001.

Coleman, S, Clayton, A, Mason, MD, Jasani, B, Adams, M & Tabi, Z 2005a, 'Recovery of CD8+ T-Cell Function During Systemic Chemotherapy in Advanced Ovarian Cancer', *Cancer Research,* vol. 65, no. 15, p. 7000.

Coleman, S, Clayton, A, Mason, MD, Jasani, B, Adams, M & Tabi, Z 2005b, 'Recovery of CD8+T-Cell Function During Systemic Chemotherapy in Advanced Ovarian Cancer', *Cancer research,* vol. 65, no. 15, p. 7000.

Conroy, T, Desseigne, F, Ychou, M, Bouché, O, Guimbaud, R, Bécouarn, Y, Adenis, A, Raoul, J-L, Gourgou-Bourgade, S, de la Fouchardière, C, Bennouna, J, Bachet, J-B, Khemissa-Akouz, F, Péré-Vergé, D, Delbaldo, C, Assenat, E, Chauffert, B, Michel, P, Montoto-Grillot, C & Ducreux, M 2011, 'FOLFIRINOX versus Gemcitabine for Metastatic Pancreatic Cancer', *New England Journal of Medicine,* vol. 364, no. 19, pp. 1817-25.

Cordoba, S-P, Choudhuri, K, Zhang, H, Bridge, M, Basat, AB, Dustin, ML & van der Merwe, PA 2013, 'The large ectodomains of CD45 and CD148 regulate their segregation from and inhibition of ligated T-cell receptor', *Blood,* vol. 121, no. 21, p. 4295.

Coussens, LM & Werb, Z 2002, 'Inflammation and cancer', *Nature,* vol. 420, no. 6917, pp. 860-67.

Croft, M 2003, 'Costimulation of T cells by OX40, 4-1BB, and CD27', *Cytokine & Growth Factor Reviews,* vol. 14, no. 3, 2003/06/01/, pp. 265-73.

Diehn, M, Alizadeh, A, Rando, O, Liu, C, Stankunas, K, Botstein, D & Crabtree, G 2002, 'Genomic expression programs and the integration of the CD28 costimulatory signal in T cell activation', *Science's STKE,* vol. 99, 10/01, p. 11796.

Eriksson, E, Wenthe, J, Irenaeus, S, Loskog, A & Ullenhag, G 2016, 'Gemcitabine reduces MDSCs, tregs and TGFβ-1 while restoring the teff/treg ratio in patients with pancreatic cancer', *Journal of Translational Medicine,* vol. 14, no. 1, 2016/09/29, p. 282.

ESMO clinical practice guidelines news, viewed 31 June 2019, <https://www.esmo.org/Guidelines/Guidelines-News>.

Fadul, CE, Fisher, JL, Gui, J, Hampton, TH, Côté, AL & Ernstoff, MS 2011, 'Immune modulation effects of concomitant temozolomide and radiation therapy on peripheral blood mononuclear cells in patients with glioblastoma multiforme', *Neuro-oncology,* vol. 13, no. 4, pp. 393-400.

Fagnoni, FF, Lozza, L, Zibera, C, Zambelli, A, Ponchio, L, Gibelli, N, Oliviero, B, Pavesi, L, Gennari, R, Vescovini, R, Sansoni, P, Da Prada, G & Robustelli Della Cuna, G 2002, 'T-cell dynamics after high-dose chemotherapy in adults: elucidation of the elusive CD8+ subset reveals multiple homeostatic T-cell compartments with distinct implications for immune competence', *Immunology,* vol. 106, no. 1, pp. 27-37.

Ferrantini, M, Capone, I & Belardelli, F 2007, 'Interferon-α and cancer: Mechanisms of action and new perspectives of clinical use', *Biochimie,* vol. 89, no. 6, 2007/06/01/, pp. 884-93.

Ferrari, V, Rodrigues Cacere, C, Machado, CM, Pannuti, CS, Dulley, FL, Barros, JCA, da Silva Duarte, AJ & Benard, G 2006, 'Distinct patterns of regeneration of central memory, effector memory and effector TCD8+ cell subsets after different hematopoietic cell transplant types: Possible influence in the recovery of anti-cytomegalovirus immune response and risk for its reactivation', *Clinical Immunology,* vol. 119, no. 3, 2006/06/01/, pp. 261-71.

Fesnak, AD, June, CH & Levine, BL 2016, 'Engineered T cells: the promise and challenges of cancer immunotherapy', *Nat Rev Cancer,* vol. 16, no. 9, 09//print, pp. 566-81.

Fitzer-Attas, CJ, Schindler, DG, Waks, T & Eshhar, Z 1998, 'Harnessing Syk Family Tyrosine Kinases as Signaling Domains for Chimeric Single Chain of the Variable Domain Receptors: Optimal Design for T Cell Activation', *The Journal of Immunology,* vol. 160, no. 1, p. 145.

Fontenot, JD, Gavin, MA & Rudensky, AY 2003, 'Foxp3 programs the development and function of CD4+CD25+ regulatory T cells', *Nature Immunology,* vol. 4, no. 4, 2003/04/01, pp. 330-36.

Fraietta, JA, Lacey, SF, Orlando, EJ, Pruteanu-Malinici, I, Gohil, M, Lundh, S, Boesteanu, AC, Wang, Y, O'Connor, RS, Hwang, W-T, Pequignot, E, Ambrose, DE, Zhang, C, Wilcox, N, Bedoya, F, Dorfmeier, C, Chen, F, Tian, L, Parakandi, H, Gupta, M, Young, RM, Johnson, FB, Kulikovskaya, I, Liu, L, Xu, J, Kassim, SH, Davis, MM, Levine, BL, Frey, NV, Siegel, DL, Huang, AC, Wherry, EJ, Bitter, H, Brogdon, JL, Porter, DL, June, CH & Melenhorst, JJ 2018, 'Determinants of response and resistance to CD19 chimeric antigen receptor (CAR) T cell therapy of chronic lymphocytic leukemia', *Nature medicine,* vol. 24, no. 5, 2018/05/01, pp. 563-71.

Galluzzi, L, Buqué, A, Kepp, O, Zitvogel, L & Kroemer, G 2015, 'Immunological Effects of Conventional Chemotherapy and Targeted Anticancer Agents', *Cancer Cell,* vol. 28, no. 6, 2015/12/14/, pp. 690-714.

Galsky, MD, Wang, H, Hahn, NM, Twardowski, P, Pal, SK, Albany, C, Fleming, MT, Starodub, A, Hauke, RJ, Yu, M, Zhao, Q, Sonpavde, G, Donovan, MJ, Patel, VG, Sfakianos, JP, Domingo-Domenech, J, Oh, WK, Akers, N, Losic, B, Gnjatic, S, Schadt, EE, Chen, R, Kim-Schulze, S, Bhardwaj, N & Uzilov, AV 2018, 'Phase 2 Trial of Gemcitabine, Cisplatin, plus Ipilimumab in Patients with Metastatic Urothelial Cancer and Impact of DNA Damage Response Gene Mutations on Outcomes', *European Urology,* vol. 73, no. 5, 2018/05/01/, pp. 751-59.

Gargett, T & Brown, MP 2015, 'Different cytokine and stimulation conditions influence the expansion and immune phenotype of third-generation chimeric antigen receptor T cells specific for tumor antigen GD2', *Cytotherapy,* vol. 17, no. 4, 2015/04/01/, pp. 487-95.

Gargett, T, Yu, W, Dotti, G, Yvon, ES, Christo, SN, Hayball, JD, Lewis, ID, Brenner, MK & Brown, MP 2016, 'GD2-specific CAR T Cells Undergo Potent Activation and Deletion Following Antigen Encounter but can be Protected From Activation-induced Cell Death by PD-1 Blockade', *Molecular Therapy,* vol. 24, no. 6, pp. 1135-49.

Gargett, T, Truong, NGA, Ebert, LM, Yu, W & Brown, MP 2019, 'Optimization of manufacturing conditions for chimeric antigen receptor T cells to favor cells with a central memory phenotype', *Cytotherapy,* vol. 21, no. 6, 2019/06/01/, pp. 593-602.

Gattinoni, L, Lugli, E, Ji, Y, Pos, Z, Paulos, CM, Quigley, MF, Almeida, JR, Gostick, E, Yu, Z, Carpenito, C, Wang, E, Douek, DC, Price, DA, June, CH, Marincola, FM, Roederer, M & Restifo, NP 2011, 'A human

memory T-cell subset with stem cell-like properties', *Nature medicine,* vol. 17, no. 10, 09/18, pp. 1290-97.

Ghiringhelli, F, Larmonier, N, Schmitt, E, Parcellier, A, Cathelin, D, Garrido, C, Chauffert, B, Solary, E, Bonnotte, B & Martin, F 2004, 'CD4+CD25+ regulatory T cells suppress tumor immunity but are sensitive to cyclophosphamide which allows immunotherapy of established tumors to be curative', *European Journal of Immunology,* vol. 34, no. 2, 2004/02/01, pp. 336-44.

Giakoustidis, A, Neofytou, K, Costa Neves, M, Giakoustidis, D, Louri, E, Cunningham, D & Mudan, S 2018, 'Identifying the role of neutrophil-to-lymphocyte ratio and platelets-to-lymphocyte ratio as prognostic markers in patients undergoing resection of pancreatic ductal adenocarcinoma', *Annals of hepato-biliary-pancreatic surgery,* vol. 22, no. 3, pp. 197-207.

Gonzalez, H, Hagerling, C & Werb, Z 2018, 'Roles of the immune system in cancer: from tumor initiation to metastatic progression', *Genes & Development,* vol. 32, no. 19-20, pp. 1267-84.

Gravestein, LA, Amsen, D, Boes, M, Calvo, CR, Kruisbeek, AM & Borst, J 1998, 'The TNF receptor family member CD27 signals to Jun N-terminal kinase via Traf-2', *European Journal of Immunology,* vol. 28, no. 7, 1998/07/01, pp. 2208-16.

Grivennikov, SI, Greten, FR & Karin, M 2010, 'Immunity, Inflammation, and Cancer', *Cell,* vol. 140, no. 6, 2010/03/19/, pp. 883-99.

Guest, RD, Hawkins, RE, Kirillova, N, Cheadle, EJ, Arnold, J, O'Neill, A, Irlam, J, Chester, KA, Kemshead, JT, Shaw, DM, Embleton, MJ, Stern, PL & Gilham, DE 2005, 'The Role of Extracellular Spacer Regions in the Optimal Design of Chimeric Immune Receptors: Evaluation of Four Different scFvs and Antigens', *Journal of Immunotherapy,* vol. 28, no. 3, pp. 203-11.

Gui, J, Mustachio, LM, Su, D-M & Craig, RW 2012, 'Thymus Size and Age-related Thymic Involution: Early Programming, Sexual Dimorphism, Progenitors and Stroma', *Aging and disease,* vol. 3, no. 3, pp. 280-90.

Hakim, FT, Cepeda, R, Kaimei, S, Mackall, CL, McAtee, N, Zujewski, J, Cowan, K & Gress, RE 1997, 'Constraints on CD4 Recovery Postchemotherapy in Adults: Thymic Insufficiency and Apoptotic Decline of Expanded Peripheral CD4 Cells', *Blood,* vol. 90, no. 9, p. 3789.

Hamann, D, Baars, PA, Rep, MH, Hooibrink, B, Kerkhof-Garde, SR, Klein, MR & van Lier, RA 1997, 'Phenotypic and functional separation of memory and effector human CD8+ T cells', *The Journal of experimental medicine,* vol. 186, no. 9, pp. 1407-18.

He, Q, Li, G, Ji, X, Ma, L, Wang, X, Li, Y & Fan, C 2017, 'Impact of the immune cell population in peripheral blood on response and survival in patients receiving neoadjuvant chemotherapy for advanced gastric cancer', *Tumor Biology,* vol. 39, no. 5, 2017/05/01, p. 1010428317697571.

Hendriks, J, Gravestein, LA, Tesselaar, K, van Lier, RAW, Schumacher, TNM & Borst, J 2000, 'CD27 is required for generation and long-term maintenance of T cell immunity', *Nature Immunology,* vol. 1, no. 5, 2000/11/01, pp. 433-40.

Hettmer, S, Ladisch, S & Kaucic, K 2005, 'Low complex ganglioside expression characterizes human neuroblastoma cell lines', *Cancer letters,* vol. 225, no. 1, pp. 141-49.

Hinrichs, CS, Borman, ZA, Gattinoni, L, Yu, Z, Burns, WR, Huang, J, Klebanoff, CA, Johnson, LA, Kerkar, SP, Yang, S, Muranski, P, Palmer, DC, Scott, CD, Morgan, RA, Robbins, PF, Rosenberg, SA & Restifo, NP 2011, 'Human effector $CD8^{+}$T cells derived from naive rather than memory subsets possess superior traits for adoptive immunotherapy', *Blood,* vol. 117, no. 3, p. 808.

Hudecek, M, Sommermeyer, D, Kosasih, PL, Silva-Benedict, A, Liu, L, Rader, C, Jensen, MC & Riddell, SR 2015, 'The nonsignaling extracellular spacer domain of chimeric antigen receptors is decisive for in vivo antitumor activity', *Cancer Immunology Research,* vol. 3, no. 2, pp. 125-35.

Hurwitz , H, Fehrenbacher , L, Novotny , W, Cartwright , T, Hainsworth , J, Heim , W, Berlin , J, Baron , A, Griffing , S, Holmgren , E, Ferrara , N, Fyfe , G, Rogers , B, Ross , R & Kabbinavar , F 2004, 'Bevacizumab plus Irinotecan, Fluorouracil, and Leucovorin for Metastatic Colorectal Cancer', *New England Journal of Medicine,* vol. 350, no. 23, pp. 2335-42.

Iacobuzio-Donahue, CA, Fu, B, Yachida, S, Luo, M, Abe, H, Henderson, CM, Vilardell, F, Wang, Z, Keller, JW, Banerjee, P, Herman, JM, Cameron, JL, Yeo, CJ, Halushka, MK, Eshleman, JR, Raben, M, Klein, AP, Hruban, RH, Hidalgo, M & Laheru, D 2009, 'DPC4 Gene Status of the Primary Carcinoma Correlates With Patterns of Failure in Patients With Pancreatic Cancer', *Journal of Clinical Oncology,* vol. 27, no. 11, 2009/04/10, pp. 1806-13.

Iida, M, Takayama, E, Naganawa, K, Mitsudo, K, Adachi, M, Baba, J-I, Fujimoto-Muto, M, Motohashi, M, Mizuno-Kamiya, M, Kawaki, H, Kioi, M, Ichinose, M, Sumitomo, S-I, Muramatsu, Y, Shikimori, M, Tohnai, I & Kondoh, N 2014, 'Increase of Peripheral Blood CD57+ T-Cells in Patients with Oral Squamous Cell Carcinoma', *Anticancer Research,* vol. 34, no. 10, pp. 5729-34.

Jacobson, CA, Farooq, U & Ghobadi, A 2019, 'Axicabtagene Ciloleucel, an Anti-CD19 Chimeric Antigen Receptor T-Cell Therapy for Relapsed or Refractory Large B-Cell Lymphoma: Practical Implications for the Community Oncologist', *The Oncologist*.

James, SE, Greenberg, PD, Jensen, MC, Lin, Y, Wang, J, Till, BG, Raubitschek, AA, Forman, SJ & Press, OW 2008, 'Antigen Sensitivity of CD22-Specific Chimeric TCR Is Modulated by Target Epitope Distance from the Cell Membrane', *The Journal of Immunology,* vol. 180, no. 10, p. 7028.

Javeed, A, Ashraf, M, Riaz, A, Ghafoor, A, Afzal, S & Mukhtar, MM 2009, 'Paclitaxel and immune system', *European Journal of Pharmaceutical Sciences,* vol. 38, no. 4, 2009/11/05/, pp. 283-90.

John, LB, Devaud, C, Duong, CPM, Yong, CS, Beavis, PA, Haynes, NM, Chow, MT, Smyth, MJ, Kershaw, MH & Darcy, PK 2013, 'Anti-PD-1 Antibody Therapy Potently Enhances the Eradication of Established Tumors By Gene-Modified T Cells', *Clinical Cancer Research,* vol. 19, no. 20, p. 5636.

Jonnalagadda, M, Mardiros, A, Urak, R, Wang, X, Hoffman, LJ, Bernanke, A, Chang, W-C, Bretzlaff, W, Starr, R, Priceman, S, Ostberg, JR, Forman, SJ & Brown, CE 2015, 'Chimeric Antigen Receptors With Mutated IgG4 Fc Spacer Avoid Fc Receptor Binding and Improve T Cell Persistence and Antitumor Efficacy', *Molecular Therapy,* vol. 23, no. 4, 02/17

11/15/received

10/17/accepted, pp. 757-68.

Kalos, M, Levine, BL, Porter, DL, Katz, S, Grupp, SA, Bagg, A & June, CH 2011, 'T Cells with Chimeric Antigen Receptors Have Potent Antitumor Effects and Can Establish Memory in Patients with Advanced Leukemia', *Science Translational Medicine,* vol. 3, no. 95, pp. 95ra73-95ra73.

Kared, H, Martelli, S, Ng, TP, Pender, SLF & Larbi, A 2016, 'CD57 in human natural killer cells and T-lymphocytes', *Cancer Immunology, Immunotherapy,* vol. 65, no. 4, 2016/04/01, pp. 441-52.

Kasakovski, D, Xu, L & Li, Y 2018, 'T cell senescence and CAR-T cell exhaustion in hematological malignancies', *Journal of Hematology & Oncology,* vol. 11, no. 1, 2018/07/04, p. 91.

Kearney, CJ, Vervoort, SJ, Hogg, SJ, Ramsbottom, KM, Freeman, AJ, Lalaoui, N, Pijpers, L, Michie, J, Brown, KK, Knight, DA, Sutton, V, Beavis, PA, Voskoboinik, I, Darcy, PK, Silke, J, Trapani, JA, Johnstone, RW & Oliaro, J 2018, 'Tumor immune evasion arises through loss of TNF sensitivity', *Science Immunology,* vol. 3, no. 23, p. eaar3451.

Kern, F, Ode-Hakim, S, Vogt, K, Hoflich, C, Reinke, P & Volk, HD 1996, 'The enigma of CD57+CD28- T cell expansion--anergy or activation?', *Clinical and experimental immunology,* vol. 104, no. 1, pp. 180-84.

Kershaw, MH, Westwood, JA, Parker, LL, Wang, G, Eshhar, Z, Mavroukakis, SA, White, DE, Wunderlich, JR, Canevari, S, Rogers-Freezer, L, Chen, CC, Yang, JC, Rosenberg, SA & Hwu, P 2006, 'A Phase I Study on Adoptive Immunotherapy Using Gene-Modified T Cells for Ovarian Cancer', *Clinical Cancer Research,* vol. 12, no. 20, pp. 6106-15.

Klastersky, J, on behalf of the, EGC, de Naurois, J, on behalf of the, EGC, Rolston, K, on behalf of the, EGC, Rapoport, B, on behalf of the, EGC, Maschmeyer, G, on behalf of the, EGC, Aapro, M, on behalf of the, EGC, Herrstedt, J & on behalf of the, EGC 2016, 'Management of febrile neutropaenia: ESMO Clinical Practice Guidelines†', *Annals of Oncology,* vol. 27, no. suppl_5, pp. v111-v18.

Klebanoff, CA, Gattinoni, L, Palmer, DC, Muranski, P, Ji, Y, Hinrichs, CS, Borman, ZA, Kerkar, SP, Scott, CD, Finkelstein, SE, Rosenberg, SA & Restifo, NP 2011, 'Determinants of Successful CD8+T-Cell Adoptive Immunotherapy for Large Established Tumors in Mice', *Clinical Cancer Research,* vol. 17, no. 16, p. 5343.

Kochenderfer, JN, Feldman, SA, Zhao, Y, Xu, H, Black, MA, Morgan, RA, Wilson, WH & Rosenberg, SA 2009, 'Construction and preclinical evaluation of an anti-CD19 chimeric antigen receptor', *Journal of immunotherapy (Hagerstown, Md. : 1997),* vol. 32, no. 7, pp. 689-702.

Kochenderfer, JN, Wilson, WH, Janik, JE, Dudley, ME, Stetler-Stevenson, M, Feldman, SA, Maric, I, Raffeld, M, Nathan, D-AN, Lanier, BJ, Morgan, RA & Rosenberg, SA 2010, 'Eradication of B-lineage cells and regression of lymphoma in a patient treated with autologous T cells genetically engineered to recognize CD19', *Blood,* vol. 116, no. 20, pp. 4099-102.

Kochenderfer, JN, Dudley, ME, Feldman, SA, Wilson, WH, Spaner, DE, Maric, I, Stetler-Stevenson, M, Phan, GQ, Hughes, MS, Sherry, RM, Yang, JC, Kammula, US, Devillier, L, Carpenter, R, Nathan, D-AN,

Morgan, RA, Laurencot, C & Rosenberg, SA 2012, 'B-cell depletion and remissions of malignancy along with cytokine-associated toxicity in a clinical trial of anti-CD19 chimeric-antigen-receptor–transduced T cells', *Blood,* vol. 119, no. 12, p. 2709.

Kochenderfer, JN & Rosenberg, SA 2013, 'Treating B-cell cancer with T cells expressing anti-CD19 chimeric antigen receptors', *Nat Rev Clin Oncol,* vol. 10, no. 5, 05//print, pp. 267-76.

Koinis, F, Vetsika, EK, Aggouraki, D, Skalidaki, E, Koutoulaki, A, Gkioulmpasani, M, Georgoulias, V & Kotsakis, A 2016, 'Effect of First-Line Treatment on Myeloid-Derived Suppressor Cells' Subpopulations in the Peripheral Blood of Patients with Non–Small Cell Lung Cancer', *Journal of Thoracic Oncology,* vol. 11, no. 8, 2016/08/01/, pp. 1263-72.

Kondelkova, K, Vokurkova, D, Krejsek, J, Borska, L, Fiala, Z & Ctirad, A 2010, 'Regulatory T cells (TREG) and their roles in immune system with respect to immunopathological disorders', *Acta Medica (Hradec Kralove),* vol. 53, no. 2, pp. 73-7.

Konig, R 2010, *Signal Transduction in T lymphocytes*, 2 edn, Elsevier Inc,

Kubota, Y, Ohji, H, Itoh, K, Sasagawa, I & Nakada, T 2001, 'Changes in cellular immunity during chemotherapy for testicular cancer', *International Journal of Urology,* vol. 8, no. 11, 2001/11/01, pp. 604-08.

Künkele, A, Johnson, AJ, Rolczynski, LS, Chang, CA, Hoglund, V, Kelly-Spratt, KS & Jensen, MC 2015, 'Functional Tuning of CARs Reveals Signaling Threshold above Which CD8⁺ CTL Antitumor Potency Is Attenuated due to Cell Fas–FasL-Dependent AICD', *Cancer Immunology Research,* vol. 3, no. 4, pp. 368-79.

Lamers, CHJ, Sleijfer, S, van Steenbergen, S, van Elzakker, P, van Krimpen, B, Groot, C, Vulto, A, den Bakker, M, Oosterwijk, E, Debets, R & Gratama, JW 2013, 'Treatment of Metastatic Renal Cell Carcinoma With CAIX CAR-engineered T cells: Clinical Evaluation and Management of On-target Toxicity', *Molecular Therapy,* vol. 21, no. 4, pp. 904-12.

Latchman, Y, Wood, CR, Chernova, T, Chaudhary, D, Borde, M, Chernova, I, Iwai, Y, Long, AJ, Brown, JA, Nunes, R, Greenfield, EA, Bourque, K, Boussiotis, VA, Carter, LL, Carreno, BM, Malenkovich, N, Nishimura, H, Okazaki, T, Honjo, T, Sharpe, AH & Freeman, GJ 2001, 'PD-L2 is a second ligand for PD-1 and inhibits T cell activation', *Nature Immunology,* vol. 2, no. 3, 2001/03/01, pp. 261-68.

Le Priol, Y, Puthier, D, Lécureuil, C, Combadière, C, Debré, P, Nguyen, C & Combadière, B 2006a, 'High Cytotoxic and Specific Migratory Potencies of Senescent CD8+CD57+ Cells in HIV-Infected and Uninfected Individuals', *The Journal of Immunology,* vol. 177, no. 8, p. 5145.

Le Priol, Y, Puthier, D, Lécureuil, C, Combadière, C, Debré, P, Nguyen, C & Combadière, B 2006b, 'High Cytotoxic and Specific Migratory Potencies of Senescent CD8+CD57+Cells in HIV-Infected and Uninfected Individuals', *The Journal of Immunology,* vol. 177, no. 8, p. 5145.

Lee, BM, Chung, SY, Chang, JS, Lee, KJ & Seong, J 2018, 'The Neutrophil-Lymphocyte Ratio and Platelet-Lymphocyte Ratio Are Prognostic Factors in Patients with Locally Advanced Pancreatic Cancer Treated with Chemoradiotherapy', *Gut and liver,* vol. 12, no. 3, pp. 342-52.

Li, J-Y, Duan, X-F, Wang, L-P, Xu, Y-J, Huang, L, Zhang, T-F, Liu, J-Y, Li, F, Zhang, Z, Yue, D-L, Wang, F, Zhang, B & Zhang, Y 2014, 'Selective Depletion of Regulatory T Cell Subsets by Docetaxel Treatment in Patients with Nonsmall Cell Lung Cancer', *Journal of Immunology Research,* vol. 2014, p. 10.

LLS 2009, *Chimaric antigen receptor (CAR) T cell therapy*, The Leukeamia and Lymphoma Society, viewed 20 July 2019, <https://www.lls.org/treatment/types-of-treatment/immunotherapy/chimeric-antigen-receptor-car-t-cell-therapy>.

Long, AH, Haso, WM, Shern, JF, Wanhainen, KM, Murgai, M, Ingaramo, M, Smith, JP, Walker, AJ, Kohler, ME, Venkateshwara, VR, Kaplan, RN, Patterson, GH, Fry, TJ, Orentas, RJ & Mackall, CL 2015, '4-1BB costimulation ameliorates T cell exhaustion induced by tonic signaling of chimeric antigen receptors', *Nat Med,* vol. 21, no. 6, Jun, pp. 581-90.

Long, AH, Highfill, SL, Cui, Y, Smith, JP, Walker, AJ, Ramakrishna, S, El-Etriby, R, Galli, S, Tsokos, MG, Orentas, RJ & Mackall, CL 2016, 'Reduction of MDSCs with All-trans Retinoic Acid Improves CAR Therapy Efficacy for Sarcomas', *Cancer Immunology Research,* vol. 4, no. 10, pp. 869-80.

Louis, CU, Savoldo, B, Dotti, G, Pule, M, Yvon, E, Myers, GD, Rossig, C, Russell, HV, Diouf, O, Liu, E, Liu, H, Wu, M-F, Gee, AP, Mei, Z, Rooney, CM, Heslop, HE & Brenner, MK 2011, 'Antitumor activity and long-term fate of chimeric antigen receptor–positive T cells in patients with neuroblastoma', *Blood,* vol. 118, no. 23, pp. 6050-56.

Louis, DN, Ohgaki, H, Wiestler, OD, Cavenee, WK, Burger, PC, Jouvet, A, Scheithauer, BW & Kleihues, P 2007, 'The 2007 WHO Classification of Tumours of the Central Nervous System', *Acta Neuropathologica,* vol. 114, no. 2, 07/06

05/21/received

05/21/accepted, pp. 97-109.

Luo, G, Guo, M, Liu, Z, Xiao, Z, Jin, K, Long, J, Liu, L, Liu, C, Xu, J, Ni, Q & Yu, X 2015, 'Blood Neutrophil–Lymphocyte Ratio Predicts Survival in Patients with Advanced Pancreatic Cancer Treated with Chemotherapy', *Annals of Surgical Oncology,* vol. 22, no. 2, 2015/02/01, pp. 670-76.

Lutsiak, MEC, Semnani, RT, De Pascalis, R, Kashmiri, SVS, Schlom, J & Sabzevari, H 2005, 'Inhibition of CD4+25+ T regulatory cell function implicated in enhanced immune response by low-dose cyclophosphamide', *Blood,* vol. 105, no. 7, pp. 2862-68.

Mackall, C, Fleisher, T, Brown, M, Magrath, I, Shad, A, Horowitz, M, Wexler, L, Adde, M, McClure, L & Gress, R 1994, 'Lymphocyte depletion during treatment with intensive chemotherapy for cancer', *Blood,* vol. 84, no. 7, pp. 2221-28.

Mackall, CL, Fleisher, TA, Brown, MR, Andrich, MP, Chen, CC, Feuerstein, IM, Magrath, IT, Wexler, LH, Dimitrov, DS & Gress, RE 1997a, 'Distinctions Between CD8+ and CD4+ T-Cell Regenerative Pathways Result in Prolonged T-Cell Subset Imbalance After Intensive Chemotherapy', *Blood,* vol. 89, no. 10, p. 3700.

Mackall, CL, Fleisher, TA, Brown, MR, Andrich, MP, Chen, CC, Feuerstein, IM, Magrath, IT, Wexler, LH, Dimitrov, DS & Gress, RE 1997b, 'Distinctions Between CD8⁺ and CD4⁺ T-Cell Regenerative Pathways Result in Prolonged T-Cell Subset Imbalance After Intensive Chemotherapy', *Blood,* vol. 89, no. 10, p. 3700.

Mackall, CL 2000, 'T-Cell Immunodeficiency Following Cytotoxic Antineoplastic Therapy: A Review', *STEM CELLS,* vol. 18, no. 1, pp. 10-18.

MAEDA, K, HAZAMA, S, TOKUNO, K, KAN, S, MAEDA, Y, WATANABE, Y, KAMEI, R, SHINDO, Y, MAEDA, N, YOSHIMURA, K, YOSHINO, S & OKA, M 2011, 'Impact of Chemotherapy for Colorectal Cancer on Regulatory T-Cells and Tumor Immunity', *Anticancer Research,* vol. 31, no. 12, December 1, 2011, pp. 4569-74.

Maher, J, Brentjens, RJ, Gunset, G, Rivière, I & Sadelain, M 2002, 'Human T-lymphocyte cytotoxicity and proliferation directed by a single chimeric TCRζ /CD28 receptor', *Nature Biotechnology,* vol. 20, no. 1, 2002/01/01, pp. 70-75.

Mak, TW & Saunders, ME 2006, '15 - T Cell Differentiation and Effector Function', in TW Mak & ME Saunders (eds), *The Immune Response*, Academic Press, Burlington, pp. 403-32.

Malmström, A, Grønberg, BH, Marosi, C, Stupp, R, Frappaz, D, Schultz, H, Abacioglu, U, Tavelin, B, Lhermitte, B, Hegi, ME, Rosell, J & Henriksson, R 2012, 'Temozolomide versus standard 6-week radiotherapy versus hypofractionated radiotherapy in patients older than 60 years with glioblastoma: the Nordic randomised, phase 3 trial', *The Lancet Oncology,* vol. 13, no. 9, pp. 916-26.

Mariani SM, KP 1998, 'Surface expression of TRAIL/Apo-2 ligand in activated mouse T and B cells', *European Journal of Immunology,* vol. 28, pp. 1492–98.

Martin, RG, Ii, Scoggins, CR, Egnatashvili, V, Staley, CA, McMasters, KM & Kooby, DA 2009, 'Arterial and venous resection for pancreatic adenocarcinoma: Operative and long-term outcomes', *Archives of Surgery,* vol. 144, no. 2, pp. 154-59.

Maude, SL, Frey, N, Shaw, PA, Aplenc, R, Barrett, DM, Bunin, NJ, Chew, A, Gonzalez, VE, Zheng, Z, Lacey, SF, Mahnke, YD, Melenhorst, JJ, Rheingold, SR, Shen, A, Teachey, DT, Levine, BL, June, CH, Porter, DL & Grupp, SA 2014, 'Chimeric Antigen Receptor T Cells for Sustained Remissions in Leukemia', *New England Journal of Medicine,* vol. 371, no. 16, pp. 1507-17.

Middleton, G, Greenhalf, W, Costello, E, Shaw, V, Cox, T, Ghaneh, P, Palmer, DH & Neoptolemos, JP 2016, 'Immunobiological effects of gemcitabine and capecitabine combination chemotherapy in advanced pancreatic ductal adenocarcinoma', *British journal of cancer,* vol. 114, no. 5, pp. 510-18.

Milone, MC, Fish, JD, Carpenito, C, Carroll, RG, Binder, GK, Teachey, D, Samanta, M, Lakhal, M, Gloss, B, Danet-Desnoyers, G, Campana, D, Riley, JL, Grupp, SA & June, CH 2009, 'Chimeric receptors containing CD137 signal transduction domains mediate enhanced survival of T cells and increased antileukemic efficacy in vivo', *Molecular therapy : the journal of the American Society of Gene Therapy,* vol. 17, no. 8, pp. 1453-64.

Mócsai, A, Ruland, J & Tybulewicz, VLJ 2010, 'The SYK tyrosine kinase: a crucial player in diverse biological functions', *Nature reviews. Immunology,* vol. 10, no. 6, pp. 387-402.

Morello, A, Sadelain, M & Adusumilli, PS 2016, 'Mesothelin-Targeted CARs: Driving T Cells to Solid Tumors', *Cancer Discovery,* vol. 6, no. 2, p. 133.

Morgan, RA, Yang, JC, Kitano, M, Dudley, ME, Laurencot, CM & Rosenberg, SA 2010, 'Case Report of a Serious Adverse Event Following the Administration of T Cells Transduced With a Chimeric Antigen Receptor Recognizing ERBB2', *Molecular Therapy,* vol. 18, no. 4, 02/23

01/14/received

01/22/accepted, pp. 843-51.

Morgan, RA, Johnson, LA, Davis, JL, Zheng, Z, Woolard, KD, Reap, EA, Feldman, SA, Chinnasamy, N, Kuan, C-T, Song, H, Zhang, W, Fine, HA & Rosenberg, SA 2012, 'Recognition of glioma stem cells by genetically modified T cells targeting EGFRvIII and development of adoptive cell therapy for glioma', *Human gene therapy,* vol. 23, no. 10, pp. 1043-53.

Motomura, T, Shirabe, K, Mano, Y, Muto, J, Toshima, T, Umemoto, Y, Fukuhara, T, Uchiyama, H, Ikegami, T, Yoshizumi, T, Soejima, Y & Maehara, Y 2013, 'Neutrophil–lymphocyte ratio reflects hepatocellular carcinoma recurrence after liver transplantation via inflammatory microenvironment', *Journal of Hepatology,* vol. 58, no. 1, 2013/01/01/, pp. 58-64.

NCCI 2019, *Relative survival by stage at diagnosis (colorectal cancer)*, National Cancer Control Indicators viewed 30 August 2019, <https://ncci.canceraustralia.gov.au/outcomes/relative-survival-rate/relative-survival-stage-diagnosis-colorectal-cancer>.

NCI 2017, *tisagenlecleucel*, National Cancer Institute, US department of Health and Human Services, viewed 30 August 2019, <https://www.cancer.gov/about-cancer/treatment/drugs/tisagenlecleucel>.

NCI 2018, *Cancer Statistics*, National Cancer Institute, US department of Health and Human Services

viewed 26 August 2019, <https://www.cancer.gov/about-cancer/understanding/statistics>.

NCI 2019, *Immunotherapy to Treat Cancer*, National Cancer Institute, US department of Health and Human Services, viewed 26 August 2019, <https://www.cancer.gov/about-cancer/treatment/types/immunotherapy>>.

Neelapu, SS, Locke, FL, Bartlett, NL, Lekakis, LJ, Miklos, DB, Jacobson, CA, Braunschweig, I, Oluwole, OO, Siddiqi, T, Lin, Y, Timmerman, JM, Stiff, PJ, Friedberg, JW, Flinn, IW, Goy, A, Hill, BT, Smith, MR, Deol, A, Farooq, U, McSweeney, P, Munoz, J, Avivi, I, Castro, JE, Westin, JR, Chavez, JC, Ghobadi, A, Komanduri, KV, Levy, R, Jacobsen, ED, Witzig, TE, Reagan, P, Bot, A, Rossi, J, Navale, L, Jiang, Y, Aycock, J, Elias, M, Chang, D, Wiezorek, J & Go, WY 2017, 'Axicabtagene Ciloleucel CAR T-Cell Therapy in Refractory Large B-Cell Lymphoma', *New England Journal of Medicine,* vol. 377, no. 26, 2017/12/28, pp. 2531-44.

O'Rourke, DM, Nasrallah, MP, Desai, A, Melenhorst, JJ, Mansfield, K, Morrissette, JJD, Martinez-Lage, M, Brem, S, Maloney, E, Shen, A, Isaacs, R, Mohan, S, Plesa, G, Lacey, SF, Navenot, J-M, Zheng, Z, Levine, BL, Okada, H, June, CH, Brogdon, JL & Maus, MV 2017, 'A single dose of peripherally infused EGFRvIII-directed CAR T cells mediates antigen loss and induces adaptive resistance in patients with recurrent glioblastoma', *Science Translational Medicine,* vol. 9, no. 399, p. eaaa0984.

O'Shea, JJ, Gadina, M & Siegel, RM 2019, '9 - Cytokines and Cytokine Receptors', in RR Rich et al (eds), *Clinical Immunology (Fifth Edition)*, Content Repository Only!, London, pp. 127-55.e1.

Ohta, A, Gorelik, E, Prasad, SJ, Ronchese, F, Lukashev, D, Wong, MKK, Huang, X, Caldwell, S, Liu, K, Smith, P, Chen, J-F, Jackson, EK, Apasov, S, Abrams, S & Sitkovsky, M 2006, 'A2A adenosine receptor protects tumors from antitumor T cells', *Proceedings of the National Academy of Sciences of the United States of America,* vol. 103, no. 35, pp. 13132-37.

Okazaki, T & Honjo, T 2006, 'The PD-1–PD-L pathway in immunological tolerance', *Trends in Immunology,* vol. 27, no. 4, 2006/04/01/, pp. 195-201.

Oken M, CR, Tormey D, Horton J, Davis TE, McFadden ET, Carbone PP 1982, 'Toxicity and response criteria of the Eastern Cooperative Oncology Group', *American Journal of Clinical Oncology,* vol. 5, pp. 649-55.

Onyema, OO, Decoster, L, Njemini, R, Forti, LN, Bautmans, I, De Waele, M & Mets, T 2015, 'Chemotherapy-induced Changes and Immunosenescence of CD8+ T-Cells in Patients with Breast Cancer', *Anticancer Research,* vol. 35, no. 3, pp. 1481-89.

Oren, R, Hod-Marco, M, Haus-Cohen, M, Thomas, S, Blat, D, Duvshani, N, Denkberg, G, Elbaz, Y, Benchetrit, F, Eshhar, Z, Stauss, H & Reiter, Y 2014, 'Functional Comparison of Engineered T Cells Carrying a Native TCR versus TCR-like Antibody–Based Chimeric Antigen Receptors Indicates Affinity/Avidity Thresholds', *The Journal of Immunology,* vol. 193, no. 11, pp. 5733-43.

Palmer, BE, Blyveis, N, Fontenot, AP & Wilson, CC 2005, 'Functional and Phenotypic Characterization of CD57+CD4+T Cells and Their Association with HIV-1-Induced T Cell Dysfunction', *The Journal of Immunology,* vol. 175, no. 12, p. 8415.

Plate, JMD, Plate, AE, Shott, S, Bograd, S & Harris, JE 2005, 'Effect of gemcitabine on immune cells in subjects with adenocarcinoma of the pancreas', *Cancer Immunology, Immunotherapy,* vol. 54, no. 9, 2005/09/01, pp. 915-25.

Porter, DL, Levine, BL, Kalos, M, Bagg, A & June, CH 2011, 'Chimeric Antigen Receptor–Modified T Cells in Chronic Lymphoid Leukemia', *New England Journal of Medicine,* vol. 365, no. 8, pp. 725-33.

Priesner, C, Aleksandrova, K, Esser, R, Mockel-Tenbrinck, N, Leise, J, Drechsel, K, Marburger, M, Quaiser, A, Goudeva, L, Arseniev, L, Kaiser, AD, Glienke, W & Koehl, U 2016, 'Automated Enrichment, Transduction, and Expansion of Clinical-Scale CD62L(+) T Cells for Manufacturing of Gene Therapy Medicinal Products', *Human gene therapy,* vol. 27, no. 10, pp. 860-69.

Reuschenbach, M, von Knebel Doeberitz, M & Wentzensen, N 2009, 'A systematic review of humoral immune responses against tumor antigens', *Cancer Immunology, Immunotherapy,* vol. 58, no. 10, 2009/06/28, p. 1535.

Rodríguez-Pinto, D 2005, 'B cells as antigen presenting cells', *Cellular Immunology,* vol. 238, no. 2, 2005/12/01/, pp. 67-75.

Roos, WP, Batista, LFZ, Naumann, SC, Wick, W, Weller, M, Menck, CFM & Kaina, B 2006, 'Apoptosis in malignant glioma cells triggered by the temozolomide-induced DNA lesion O6-methylguanine', *Oncogene,* vol. 26, no. 2, 07/03/online, pp. 186-97.

Rose, S 2018, 'Making Better CARs for Kids', *Cancer Discovery,* vol. 8, no. 5, p. 522.

Rosenberg, S & Dudley, M 2004, 'Cancer regression in patients with metastatic melanoma after the transfer of autologous antitumor lymphocytes', *Proceedings of the National Academy of Sciences,* vol. 101, no. suppl 2, October 5, 2004, pp. 14639-45.

Sadelain, M, Rivière, I & Brentjens, R 2003, 'Targeting tumours with genetically enhanced T lymphocytes', *Nat Rev Cancer,* vol. 3, no. 1, 01//print, pp. 35-45.

Sallusto, F, Lenig, D, Förster, R, Lipp, M & Lanzavecchia, A 1999, 'Two subsets of memory T lymphocytes with distinct homing potentials and effector functions', *Nature,* vol. 401, no. 6754, 1999/10/01, pp. 708-12.

Sallusto, F, Geginat, J & Lanzavecchia, A 2004, 'Central Memory and Effector Memory T Cell Subsets: Function, Generation, and Maintenance', *Annual Review of Immunology,* vol. 22, no. 1, pp. 745-63.

Santomasso, B, Bachier, C, Westin, J, Rezvani, K & Shpall, EJ 2019, 'The Other Side of CAR T-Cell Therapy: Cytokine Release Syndrome, Neurologic Toxicity, and Financial Burden', *American Society of Clinical Oncology Educational Book*, no. 39, 2019/05/01, pp. 433-44.

Schwartz, RH 2003, 'T Cell Anergy', *Annual Review of Immunology,* vol. 21, no. 1, 2003/04/01, pp. 305-34.

Scurr, M, Pembroke, T, Bloom, A, Roberts, D, Thomson, A, Smart, K, Bridgeman, H, Adams, R, Brewster, A, Jones, R, Gwynne, S, Blount, D, Harrop, R, Hills, R, Gallimore, A & Godkin, A 2017, 'Low-Dose Cyclophosphamide Induces Antitumor T-Cell Responses, which Associate with Survival in Metastatic Colorectal Cancer', *Clinical cancer research : an official journal of the American Association for Cancer Research,* vol. 23, no. 22, pp. 6771-80.

Shen, J, Xiao, Z, Zhao, Q, Li, M, Wu, X, Zhang, L, Hu, W & Cho, CH 2018, 'Anti-cancer therapy with TNFα and IFNγ: A comprehensive review', *Cell Proliferation,* vol. 51, no. 4, 2018/08/01, p. e12441.

Shi, Y, Liu, CH, Roberts, AI, Das, J, Xu, G, Ren, G, Zhang, Y, Zhang, L, Yuan, ZR, Tan, HSW, Das, G & Devadas, S 2006, 'Granulocyte-macrophage colony-stimulating factor (GM-CSF) and T-cell responses: what we do and don't know', *Cell Research,* vol. 16, no. 2, 2006/02/01, pp. 126-33.

Shimizu, J, Yamazaki, S & Sakaguchi, S 1999, 'Induction of Tumor Immunity by Removing $CD25^+CD4^+$ T Cells: A Common Basis Between Tumor Immunity and Autoimmunity', *The Journal of Immunology,* vol. 163, no. 10, p. 5211.

Shitara, K, Muro, K, Matsuo, K, Ura, T, Takahari, D, Yokota, T, Sawaki, A, Kawai, H, Ito, S, Munakata, M & Sakata, Y 2009, 'Chemotherapy for patients with advanced gastric cancer with performance status 2', *Gastrointestinal cancer research : GCR,* vol. 3, no. 6, pp. 220-24.

Singhal, N, Selva-Nayagam, S & Brown, MP 2007, 'Prolonged and severe myelosuppression in two patients after low-dose temozolomide treatment- case study and review of literature', *Journal of Neuro-Oncology,* vol. 85, no. 2, 2007/11/01, pp. 229-30.

Sommermeyer, D, Hudecek, M, Kosasih, PL, Gogishvili, T, Maloney, DG, Turtle, CJ & Riddell, SR 2015, 'Chimeric antigen receptor-modified T cells derived from defined CD8+ and CD4+ subsets confer superior antitumor reactivity in vivo', *Leukemia,* vol. 30, 09/15/online, p. 492.

Spolski, R, Lin, JX & Leonard, WJ 2014, 'The γc Family of Cytokines: A Pleiotropic Family That Controls Proliferation, Survival, and Differentiation', *Reference Module in Biomedical Sciences*, Elsevier.

Srivastava, S & Riddell, SR 2015, 'Engineering CAR-T cells: Design concepts', *Trends in immunology,* vol. 36, no. 8, pp. 494-502.

Steinberg, M, Adjali, O, Swainson, L, Merida, P, Bartolo, VD, Pelletier, L, Taylor, N & Noraz, N 2004, 'T-cell receptor–induced phosphorylation of the ζ chain is efficiently promoted by ZAP-70 but not Syk', *Blood,* vol. 104, no. 3, pp. 760-67.

Stupp, R, Brada, M, van den Bent, MJ, Tonn, JC & Pentheroudakis, G 2014, 'High-grade glioma: ESMO Clinical Practice Guidelines for diagnosis, treatment and follow-up†', *Annals of Oncology,* vol. 25, no. suppl_3, pp. iii93-iii101.

Suzuki, E, Kapoor, V, Jassar, AS, Kaiser, LR & Albelda, SM 2005, 'Gemcitabine Selectively Eliminates Splenic $Gr\text{-}1^+CD11b^+$ Myeloid Suppressor Cells in Tumor-Bearing Animals and Enhances Antitumor Immune Activity', *Clinical Cancer Research,* vol. 11, no. 18, p. 6713.

Talmadge JE, JJ, Kelsay L, Borgeson CD, Faltynek C, Perry GA 1993, 'T-cell reconstitution by molecular, phenotypic, and functional analysis in the thymus, bone marrow, spleen, and blood following split-dose polychemotherapy and therapeutic activity for metastatic breast cancer in mice.', *Journal of Immunotherapy with emphais on tumour immunology,* vol. 14, no. 4, pp. 258-68.

Textor, A, Listopad, JJ, Wührmann, LL, Perez, C, Kruschinski, A, Chmielewski, M, Abken, H, Blankenstein, T & Charo, J 2014, 'Efficacy of CAR T-cell Therapy in Large Tumors Relies upon Stromal Targeting by IFNγ', *Cancer Research,* vol. 74, no. 23, pp. 6796-805.

Thistlethwaite, FC, Gilham, DE, Guest, RD, Rothwell, DG, Pillai, M, Burt, DJ, Byatte, AJ, Kirillova, N, Valle, JW, Sharma, SK, Chester, KA, Westwood, NB, Halford, SER, Nabarro, S, Wan, S, Austin, E & Hawkins, RE 2017, 'The clinical efficacy of first-generation carcinoembryonic antigen (CEACAM5)-specific CAR T cells is limited by poor persistence and transient pre-conditioning-dependent respiratory toxicity', *Cancer immunology, immunotherapy : CII,* vol. 66, no. 11, pp. 1425-36.

tisagenlecleucel (Rx), Medscape, WebMD, viewed 30 August 2019, <https://reference.medscape.com/drug/kymriah-tisagenlecleucel-1000169>.

Tschumi, BO, Dumauthioz, N, Marti, B, Zhang, L, Lanitis, E, Irving, M, Schneider, P, Mach, J-P, Coukos, G, Romero, P & Donda, A 2018a, 'CART cells are prone to Fas- and DR5-mediated cell death', *Journal for ImmunoTherapy of Cancer,* vol. 6, no. 1, pp. 71-71.

Tschumi, BO, Dumauthioz, N, Marti, B, Zhang, L, Schneider, P, Mach, J-P, Romero, P & Donda, A 2018b, 'CART cells are prone to Fas- and DR5-mediated cell death', *Journal for ImmunoTherapy of Cancer,* vol. 6, no. 1, 2018/07/13, p. 71.

Turtle, CJ, Swanson, HM, Fujii, N, Estey, EH & Riddell, SR 2009, 'A distinct subset of self-renewing human memory CD8+ T cells survives cytotoxic chemotherapy', *Immunity,* vol. 31, no. 5, pp. 834-44.

Turtle, CJ, Berger, C, Sommermeyer, D, Hanafi, L-A, Pender, B, Robinson, EM, Melville, K, Budiarto, TM, Steevens, NN, Chaney, C, Cherian, S, Wood, BL, Soma, L, Chen, X, Heimfeld, S, Jensen, MC, Riddell, SR & Maloney, DG 2015, 'Anti-CD19 Chimeric Antigen Receptor-Modified T Cell Therapy for B Cell Non-Hodgkin Lymphoma and Chronic Lymphocytic Leukemia: Fludarabine and Cyclophosphamide Lymphodepletion Improves In Vivo Expansion and Persistence of CAR-T Cells and Clinical Outcomes', *Blood,* vol. 126, no. 23, pp. 184-84.

Turtle, CJ, Hanafi, L-A, Berger, C, Hudecek, M, Pender, B, Robinson, E, Hawkins, R, Chaney, C, Cherian, S, Chen, X, Soma, L, Wood, B, Li, D, Heimfeld, S, Riddell, SR & Maloney, DG 2016a, 'Immunotherapy of non-Hodgkin's lymphoma with a defined ratio of $CD8^+$ and $CD4^+$CD19-specific chimeric antigen receptor–modified T cells', *Science Translational Medicine,* vol. 8, no. 355, p. 355ra116.

Turtle, CJ, Hanafi, L-A, Berger, C, Hudecek, M, Pender, B, Robinson, E, Hawkins, R, Chaney, C, Cherian, S, Chen, X, Soma, L, Wood, B, Li, D, Heimfeld, S, Riddell, SR & Maloney, DG 2016b, 'Immunotherapy of non-Hodgkin's lymphoma with a defined ratio of $CD8^+$and $CD4^+$ CD19-specific chimeric antigen receptor–modified T cells', *Science Translational Medicine,* vol. 8, no. 355, p. 355ra116.

van der Stegen, SJC, Hamieh, M & Sadelain, M 2015, 'The pharmacology of second-generation chimeric antigen receptors', vol. 14, 07/01/online, p. 499.

Verma, R, Foster, RE, Horgan, K, Mounsey, K, Nixon, H, Smalle, N, Hughes, TA & Carter, CRD 2016, 'Lymphocyte depletion and repopulation after chemotherapy for primary breast cancer', *Breast Cancer Research,* vol. 18, no. 1, 2016/01/26, p. 10.

Vincent, J, Mignot, G, Chalmin, F, Ladoire, S, Bruchard, M, Chevriaux, A, Martin, F, Apetoh, L, Rébé, C & Ghiringhelli, F 2010, '5-Fluorouracil Selectively Kills Tumor-Associated Myeloid-Derived Suppressor Cells Resulting in Enhanced T Cell–Dependent Antitumor Immunity', *Cancer Research,* vol. 70, no. 8, p. 3052.

Von Hoff , DD, Ervin , T, Arena , FP, Chiorean , EG, Infante , J, Moore , M, Seay , T, Tjulandin , SA, Ma , WW, Saleh , MN, Harris , M, Reni , M, Dowden , S, Laheru , D, Bahary , N, Ramanathan , RK, Tabernero , J, Hidalgo , M, Goldstein , D, Van Cutsem , E, Wei , X, Iglesias , J & Renschler , MF 2013, 'Increased Survival in Pancreatic Cancer with nab-Paclitaxel plus Gemcitabine', *New England Journal of Medicine,* vol. 369, no. 18, pp. 1691-703.

Walsh, SR, Cook, EJ, Goulder, F, Justin, TA & Keeling, NJ 2005, 'Neutrophil-lymphocyte ratio as a prognostic factor in colorectal cancer', *Journal of Surgical Oncology,* vol. 91, no. 3, 2005/09/01, pp. 181-84.

Wang, L, Zhou, D, Ren, H & Chen, Y 2018, 'Effects of modified FOLFOX-6 chemotherapy on cellular immune function in patients with gastric cancer', *Oncology letters,* vol. 15, no. 6, pp. 8635-40.

Wang, S & El-Deiry, WS 2003, 'TRAIL and apoptosis induction by TNF-family death receptors', *Oncogene,* vol. 22, no. 53, 2003/11/01, pp. 8628-33.

Wang, X, Naranjo, A, Brown, CE, Bautista, C, Wong, CW, Chang, W-C, Aguilar, B, Ostberg, JR, Riddell, SR, Forman, SJ & Jensen, MC 2012, 'Phenotypic and functional attributes of lentivirus-modified CD19-specific human CD8+ central memory T cells manufactured at clinical scale', *Journal of immunotherapy (Hagerstown, Md. : 1997),* vol. 35, no. 9, Nov-Dec, pp. 689-701.

Watanabe, N, Bajgain, P, Sukumaran, S, Ansari, S, Heslop, HE, Rooney, CM, Brenner, MK, Leen, AM & Vera, JF 2016, 'Fine-tuning the CAR spacer improves T-cell potency', *Oncoimmunology,* vol. 5, no. 12, pp. e1253656-e56.

Weyand, CM & Goronzy, JJ 2016, 'Aging of the Immune System. Mechanisms and Therapeutic Targets', *Annals of the American Thoracic Society,* vol. 13, no. Supplement_5, 2016/12/01, pp. S422-S28.

Wherry, EJ & Kurachi, M 2015, 'Molecular and cellular insights into T cell exhaustion', *Nature reviews. Immunology,* vol. 15, no. 8, pp. 486-99.

WHO 2019, *Cancer*, World Health Organisation viewed 26 August 2019, <https://www.who.int/news-room/fact-sheets/detail/cancer>.

Wijayahadi, N, Haron, MR, Stanslas, J & Yusuf, Z 2007, 'Changes in Cellular Immunity during Chemotherapy for Primary Breast Cancer with Anthracycline Regimens', *Journal of Chemotherapy,* vol. 19, no. 6, 2007/12/01, pp. 716-23.

Wu, Z-L, Schwartz, E, Seeger, R & Ladisch, S 1986, 'Expression of GD2 Ganglioside by Untreated Primary Human Neuroblastomas', *Cancer Research,* vol. 46, no. 1, pp. 440-43.

Xu, X-J, Zhao, H-Z & Tang, Y-M 2013, 'Efficacy and safety of adoptive immunotherapy using anti-CD19 chimeric antigen receptor transduced T-cells: a systematic review of phase I clinical trials', *Leukemia & Lymphoma,* vol. 54, no. 2, 2013/02/01, pp. 255-60.

Xu, Y, Zhang, M, Ramos, CA, Durett, A, Liu, E, Dakhova, O, Liu, H, Creighton, CJ, Gee, AP, Heslop, HE, Rooney, CM, Savoldo, B & Dotti, G 2014, 'Closely related T-memory stem cells correlate with in vivo expansion of CAR.CD19-T cells and are preserved by IL-7 and IL-15', *Blood,* vol. 123, no. 24, p. 3750.

Yu, S, Li, A, Liu, Q, Li, T, Yuan, X, Han, X & Wu, K 2017, 'Chimeric antigen receptor T cells: a novel therapy for solid tumors', *Journal Of Hematology & Oncology,* vol. 10, no. 1.

Ziebart, A, Huber, U, Jeske, S, Laban, S, Doescher, J, Hoffmann, TK, Brunner, C, Jackson, EK & Schuler, PJ 2017, 'The influence of chemotherapy on adenosine-producing B cells in patients with head and neck squamous cell carcinoma', *Oncotarget,* vol. 9, no. 5, pp. 5834-47.

Zirakzadeh, AA, Kinn, J, Krantz, D, Rosenblatt, R, Winerdal, ME, Hu, J, Hartana, CA, Lundgren, C, Bergman, EA, Johansson, M, Holmström, B, Hansson, J, Sidikii, A, Vasko, J, Marits, P, Sherif, A & Winqvist, O 2017, 'Doxorubicin enhances the capacity of B cells to activate T cells in urothelial urinary bladder cancer', *Clinical Immunology,* vol. 176, 2017/03/01/, pp. 63-70.